duplicate

THE ENERGY BUDGET OF THE STRATOSPHERE DURING 1965

by

MERWIN EUGENE RICHARDS

B.S., University of Washington
1960

SUBMITTED IN PARTIAL FULFILLMENT
OF THE REQUIREMENT FOR THE
DEGREES OF MASTER OF
SCIENCE

at the

MASSACHUSETTS INSTITUTE OF TECHNOLOGY
August 21, 1967

Signature of Author .....
Departments of Aeronautics and Astronautics
and Meteorology, August, 1967.

Certified by .....
Thesis Supervisor

Accepted by .....
Chairman, Departmental Committee on Graduate Students

THE ENERGY BUDGET OF THE STRATOSPHERE DURING 1965

by

MERWIN EUGENE RICHARDS

Submitted to the Departments of Aeronautics and Astronautics and of Meteorology on August 21, 1967 in partial fulfillment of the requirements for the degrees of Master of Science.

ABSTRACT

A monthly statistical analysis was made of the effects of large scale horizontal eddy transport processes on the zonal momentum, heat and energy budgets for three layers of the 1965 stratosphere. Geostrophic wind components were computed from IQSY data at 100, 50, 30 and 10 mb for use in calculating the statistical quantities used in the analysis.

It was found that temporal and spatial variances and covariances computed from monthly means of temperature and geostrophic wind components give meaningful results when used in the computation of momentum, heat and energy balances. Monthly meridional distributions of eddy transports and energy conversions show large latitudinal and height variations. They also indicate a physically reasonable compatibility with month to month changes in zonal mean values of temperature, zonal wind and geopotential.

It was further determined that in the winter, the eddies in the middle stratosphere convert a self contained source of zonal available potential energy into eddy available potential energy. It is speculated that further conversion of this energy eventuates in its availability as a significant source for the mean zonal motions.

Thesis Supervisor: Reginald E. Newell

Title: Associate Professor of Meteorology

TABLE OF CONTENTS

LIST OF TABLES

LIST OF FIGURES

I. INTRODUCTION

The purpose of this study is to describe the effects of large scale horizontal eddy processes on the monthly zonal momentum, heat and energy budgets of three closed regions of the stratosphere during the last International Year of the Quiet Sun, viz. January through December 1965. The regions considered are three north polar caps bounded by a vertical surface at 20^{o} north latitude and by isobaric surfaces at 100, 50, 30 and 10 millibars.

The bases for this study are the physical laws of conservation of mass, momentum and energy combined with the methods of statistical analysis formulated by Priestly (1949) and further described by Starr and White (1952). In this method of analysis the meteorological variables, i.e. wind, temperature, pressure, etc., whose time dependence and three dimensional space distribution are defined by prolonged periods of daily or semidaily observation, are reduced to a two dimensional distribution of climatological variables by time and space averaging. Space averages are taken as zonal means around latitude circles, a procedure strongly commended by the observed zonal symmetry of wind and temperature on hemispheric weather charts, while time averages are taken over the particular time period of interest, one month in the case of this study.

Due to the non-linearity of the equations which govern the atmosphere and describe the necessity for its satisfaction of the conservation laws, correlations of the dependent atmospheric variables become

important in the evolution of their spatial distribution. When our system of averaging is applied to these equations the advection terms, which contain a horizontal or vertical wind component, e.g. V, plus some property Q of the air as dependent variables, are resolved into three distinct components representing the transport of Q. Two of these components result from the spatial and temporal correlations of V and Q and are commonly referred to as standing eddy and transient eddy fluxes respectively. The third component results from the product of the means of V and Q and is generally known as mean motion transport. These components are obtained by a resolution technique, first introduced by Reynolds (1894), whereby V and Q are expressed as

$$V = \bar{V} + V' \tag{1.1a}$$

$$Q = \bar{Q} + Q' \tag{1.1b}$$

where bar and prime operators denote time means and deviations from time means respectively. Time means are further decomposed into space means (averages around latitude circles) plus deviations from space means as follows

$$\bar{V} = [\bar{V}] + \bar{V}^* \tag{1.2a}$$

$$\bar{Q} = [\bar{Q}] + \bar{Q}^* \tag{1.2b}$$

The instantaneous transport of Q in a direction parallel to V may then be written as

$$VQ = [\bar{V}][\bar{Q}] + \bar{V}^*\bar{Q}^* + V'Q' + (VQ)_p \tag{1.3}$$

where $(VQ)_p$ represents terms involving products of mean and deviation quantities. If (1.3) is averaged over the same time and space intervals used in obtaining (1.1) and (1.2), $(VQ)_p$ vanishes identically, and the large scale transport of Q may be written as

$$\left[\overline{VQ}\right] = \left[\bar{V}\right]\left[\bar{Q}\right] + \left[\bar{V}^*\bar{Q}^*\right] + \left[\overline{V'Q'}\right] \qquad (1.4)$$

The three terms on the right hand side of (1.4) represent in order; the mean motion transport, the standing eddy flux and the transient eddy flux of Q respectively. When Q represents momentum, heat or geopotential, the magnitudes of the eddy fluxes have a direct influence on the energy transformations within the atmosphere, and a knowledge of these fluxes is a necessary prerequisite to an evaluation of the energy balances with which this study is concerned.

The foregoing method of analysis has been used extensively by Professor V.P. Starr and his colleagues at M.I.T. in general circulation studies of the troposphere. These studies prove beyond reasonable doubt that eddy fluxes play a major and necessary role in the energy processes which control the general circulation of the lower atmosphere. With the more recent acquisition of high level data, most notably those resulting from the International Geophysical Year (IGY) upper air program, these techniques have been applied in a series of observational studies of the lower stratosphere (defined for the purposes of this study as that part of the atmosphere bounded by the 100 and 30 mb isobaric surfaces). These studies have culminated in a coherent descrip-

tion of the energetics of this region. In some cases, e.g. Barnes (1962) and Newell (1963a, 1965), these studies have included information on the middle stratosphere (defined here as the region between 30 and 10 mb), however, the data has heretofore been too sparse for a comprehensive description of this region.

In general circulation studies of the atmosphere, analogies have often been drawn, e.g. Newell (1966), between the energetics of certain regions and the workings of either a refrigerator or a heat engine, the differentiation being made on the basis of the direction taken by energy exchanges within and at the boundaries of the region. In the case of a refrigerator, zonal available potential energy is destroyed by radiative processes which add heat to cold and extract heat from warm latitudinal zones within the region. The heat budget deficit created by these processes is balanced by mechanical heat transport which must, by necessity, be against the temperature gradient. Since the only self contained energy source for mechanical motion is available potential energy, which in this case is lost by radiation, a refrigerated region must be forced by external means. Evidence accumulated from observational studies indicate that the lower stratosphere operates as a refrigerated region. This evidence, compiled and discussed by Newell (1965), is enumerated as follows:

(1) Radiation processes destroy zonal available potential energy; found by Newell (1963), Oort (1963) and Kennedy (1964).

(2) Eddy available potential energy is converted to zonal

available potential energy by a process of eddy heat transport against the temperature gradient; first found by Priestly (1949) and since verified extensively. (See White, 1954; Peixoto, 1960; Murakami, 1962 and Peng, 1963, 1963a). This transport is a result of mass exchange along adiabatic trajectories whose slope with respect to the horizontal is greater than the slope of the mean isentropic surfaces; phenomena hypothesized by Newell (1961, 1963b) to account for meridional ozone transports computed by himself and by Martin (1956). Sheppard (1963) has also described the countergradient heat flux in this context. Molla and Loisel (1962) have provided verification by correlating horizonal wind components with vertical velocities computed by Jensen (1961).

(3) Eddy kinetic energy is converted to zonal kinetic energy by a countergradient eddy flux of angular momentum; found by Priestly (1949), Starr (1951a), Starr and White (1954), Dickinson (1962) and Oort (1964a) among others; and elucidated by Kuo (1951) and Starr (1953).

(4) Eddy kinetic energy is converted to eddy available potential energy through a systematic forcing of cold air toward low pressure and warm air toward high pressure; found by White and Nolan (1960), Jensen (1961), Barnes (1962), Oort (1963) and Miller (1966).

Oort (1963) has conducted a comprehensive study of the lower stratosphere energy budget using IGY data and has verified the existence of the above features over three month seasonal means. In theoretical studies by Peng (1965a,b) the numerical integration of equations representing a four level quasi-geostrophic model shows an evolution of

the stratospheric circulation into a regime with features remarkably similar to those observed. Most notably, it indicates a flow of energy upward from the troposphere, thus indicating that the lower atmosphere provides the necessary forcing for the refrigerated region.

In the case of a heat engine, the region under consideration is continually supplied with zonal available potential energy through radiative processes which add heat to warm and extract heat from cold latitudinal zones. In order to balance the obvious heat budget deficit created by this differential heating, the atmosphere uses the zonal available potential energy thereby generated as a source for the mean zonal currents. This is accomplished through the well-known energy conversion processes described by Starr (1954) and Lorenz (1955) involving both zonal and eddy forms of kinetic and available potential energy. The direction and distribution of energy conversion rates in the middle latitude troposphere show that this region operates as a heat engine. Evidence compiled to date from IGY and Meteorological Rocket Network data on energy exchange processes in the middle stratosphere imply similar heat engine characteristics in this region. (See Barnes, 1962 and Newell, 1963a, 1965).

Most stratospheric studies utilizing sufficient data to make results reasonably conclusive have been based upon climatological means of three months or more. Exceptions to these long time period investigations are studies by Boville (1961), Teweles (1963) and Reed, Wolfe and Nishimoto (1963) in which energy cycles were computed in the domain of wave number using equations presented by Saltzman (1957). Findings

indicate that energy exchange processes as represented by long term means may be unrepresentative when viewed within a shorter time scale. In view of the observed time scale of major changes which take place in stratospheric circulation patterns, e.g. the late winter breakdown of the polar vortex, a month by month statistical study of the energy budget in this region is of obvious value. The advent of the IQSY computer-analyzed chart program of the Environmental Science Services Administration (ESSA) has now made suitably reduced data available for such an investigation. Also, complete data at 10 mb now makes it possible to conduct a like investigation of the middle stratosphere energy budget. The aim of this study is to initiate these investigations by an analysis of the horizontal eddy exchange processes within these regions.

II. NOTATION AND DEFINITIONS

x,y,P = coordinates in eastward and northward directions plus pressure coordinate

t = time

u = west wind component (positive if from west)

v = south wind component (positive if from south)

$\omega = \frac{dP}{dt}$ = "vertical" velocity in pressure coordinates

$\vec{c} = (u,v,\omega)$ = three dimensional velocity vector

φ = latitude

λ = longitude

H = geopotential height

a = radius of earth

g = acceleration due to gravity

Ω = earth's angular velocity

$f = 2\Omega \sin\varphi$ = Coriolis parameter

$\Psi = gH$ = geopotential

ρ = density

α = specific volume

T = Kelvin temperature

θ = potential temperature

R = gas constant for dry air

C_p = specific heat at constant pressure

D_N = frictional force in the -N coordinate direction

τ_λ = frictional torque about earth's axis of rotation

Q = rate of nonadiabatic heating per unit mass

$dm = a^2 \cos\varphi \, d\lambda \, d\varphi \frac{dP}{g}$ = increment of mass

$$\gamma = -\alpha \left(\frac{1}{\theta} \frac{\partial \tilde{\bar{\theta}}}{\partial P} \right)^{-1} = \left(\frac{\tilde{\bar{T}}}{\bar{T}} - \frac{P C_p}{R} \frac{\partial \tilde{\bar{T}}}{\partial P} \right)^{-1}$$ = stability parameter

$$\Gamma = \frac{R[\bar{T}]}{P C_p} - \frac{\partial [\bar{T}]}{\partial P}$$ = static stability parameter

A & B = dummy variables.

$$\bar{A} = \frac{1}{\Delta t} \int_{t_1}^{t_2} A \, dt \approx \frac{1}{N} \sum_{r=1}^{N} A_r$$ = the time averaged of A at a given grid point and level where N is the number of days in a month (2.1)

$A' = A - \bar{A}$ = deviation from the time average (2.2)

$$\overline{AB} = \frac{1}{\Delta t} \int_{t_1}^{t_2} AB \, dt \approx \frac{1}{N} \sum_{r=1}^{N} A_r B_r$$ = the time average of AB at a given grid point and level (2.3)

$\overline{A'B'} = \overline{AB} - \bar{A}\,\bar{B}$ = the temporal covariance of A and B at a given grid point and level. (Transient eddy covariance) (2.4)

$$\sigma(A) = \sqrt{\overline{A^2} - \bar{A}^2}$$ = the time standard deviation of A at a given grid point and level (2.5)

$$[A] = \frac{1}{2\pi} \int_0^{2\pi} A \, d\lambda \approx \frac{1}{36} \sum_{j=1}^{36} A_j$$ = zonal average of grid point values of A at a given latitude and level (2.6)

$A^* = A - [A]$ = deviation from the zonal average at a given grid point and level. (2.7)

$A^*B^* = (A - [A])\,(B - [B])$ = spatial covariance of A an B at a given grid point and level. (standing eddy covariance). (2.8)

$[\bar{A}^* \bar{B}^*]$ = the zonal average of the spatial covariances of the time averages of A and B at a given latitude and level. (2.9)

$[\overline{A'B'}]$ = the zonal average of the temporal covariances of A and B at a given latitude and level. (2.10)

$\sqrt{[\bar{A}^{*2}]} = \sqrt{[\bar{A}^2] - [\bar{A}]^2}$ = the space standard deviation of the time average of A at a given latitude and level. (2.11)

$$\tilde{A} = \frac{1}{2\pi(1-\sin\varphi_b)} \int_{\varphi_b}^{\frac{\pi}{2}} \int_{0}^{2\pi} A \cos\varphi \, d\lambda \, d\varphi \approx \frac{\pi}{36(1-\sin\varphi_b)} \left\{ \sum_{i=b+1}^{N} [A]_i \cos\varphi_i + \frac{1}{2} [A]_b \cos\varphi_b \right\}$$

= the area average of A at a given level north of latitude φ_b where N is the number of equally spaced latitude bands north of latitude φ_b. (2.12)

$[A]'' = [A] - \tilde{A}$ = deviation of the zonal average from the area average at a given latitude and level. (2.13)

$[A]_d = [A]_l - [A]_f$ = the difference between the zonal averages of A on the first and last day of the month at a given latitude and level. (2.14)

$$\left[A\right]''_d = \left[A\right]''_L - \left[A\right]''_F = \text{the difference between the deviations of the zonal averages of A from the area averages of A on the first and last day of the month at a given latitude and level.} \quad (2.15)$$

$$\left[\overline{AB}\right] = \left[\overline{A}\right]\left[\overline{B}\right] + \left[\overline{A}^*\,\overline{B}^*\right] + \left[\overline{A'B'}\right] = \text{resolution of the time and space mean of AB into mean and eddy components.} \quad (2.16)$$

$$\left[AB\right]_E = \left[\overline{A'B'}\right] + \left[\overline{A}^*\,\overline{B}^*\right] \quad (2.17)$$

$M([\bar{u}] + a\Omega\cos\varphi)\, a\cos\varphi$ = mean absolute zonal angular momentum.

$M_r = [\bar{u}]\, a\cos\varphi$ = mean relative zonal angular momentum.

$S(B)$ = seasonal trend of B.

$F(R)_\varphi$ = horizontal flux of relative angular momentum through latitude boundary φ.

$F(R)_p$ = "vertical" flux of relative angular momentum through isobaric surface P.

$F(E)_\varphi$ = horizontal flux of earth's angular momentum through latitude boundary φ.

$F(E)_p$ = "vertical" flux of earth's angular momentum through isobaric surface P.

$D(B)$ = rate of dissipation of B due to frictional torque.

$K_Z = \frac{1}{2}\int \left([\bar{u}]^2 + [\bar{v}]^2\right) dm$ = mean zonal kinetic energy.

$K_E = \frac{1}{2}\int \left([u]_E^2 + [v]_E^2\right) dm$ = eddy kinetic energy.

$A_Z = \frac{1}{2}\int \gamma [\bar{T}]^{*2} dm$ = zonal available potential energy.

$A_E = \frac{1}{2}\int \gamma \left[\overline{T^{*2}}\right] dm$ = eddy available potential energy.

$C(K_E, K_Z)$ = rate of conversion from eddy kinetic energy into zonal kinetic energy.

$C(A_Z, K_Z)$ = rate of conversion from zonal available potential energy into zonal kinetic energy.

$A(K_Z)$ = rate of advection of zonal kinetic energy.

$W_e(K_Z)$ = rate at which work is done by eddy stresses at boundary of volume.

$W_p(K_Z)$ = rate at which work is done by pressure forces at boundary of volume.

$C(A_E, A_Z)$ = rate of conversion from eddy available potential energy into zonal available potential energy.

$G(A_Z)$ = rate of generation of zonal available potential energy by radiational heating and/or cooling.

III. DATA AND THEIR REDUCTION

The data used in this study are daily (1200z) and monthly mean grid point values of geopotential height and temperature at the 100, 50, 30 and 10 mb levels which were provided on magnetic tape by the National Weather Records Center at Asheville, North Carolina. These data were read at points on the National Meteorological Center's (NMC) 1977-point octagon grid of the northern hemisphere from charts prepared by the NMC Upper Air Branch during their IQSY stratospheric chart analysis program. Methods of chart analysis, including station coverage and raw data interpretation, are given elsewhere and will not be repeated here (see Finger et al., 1965 and Staff, Upper Air Branch NMC, 1967).

The data as received on magnetic tape was reduced through the use of a 7094 IBM electronic computer as follows:

Grid values were linearly interpolated to a 5° latitude-longitude grid (LLG) in order to organize the data into a zonally symmetric field compatible with the analysis techniques described in Section I. Daily and mean monthly geostrophic wind components were then computed at LLG points for each 5° of latitude and 10° of longitude for the northern hemisphere beginning at 20° north latitude. A ten degree grid size in both latitude and longitude was used for computations at and south of 60°. The longitude interval was increased to 20° for the v component computation north of this demarcation.

Finite difference approximations used in the wind computations were: (see II for notation)

$$u_{i,j} = \frac{g}{fa}\left(\frac{H_{i-1,j} - H_{i+1,j}}{\varphi_{i+1} - \varphi_{i-1}}\right)$$

$$v_{i,j} = \frac{g}{fa\cos\varphi_i}\left(\frac{H_{i,j-1} - H_{i,j+1}}{\lambda_{j+1} - \lambda_{j-1}}\right) \qquad (20^\circ \le \varphi_i \le 60^\circ)$$

$$v_{i,j} = \frac{g}{fa\cos\varphi_i}\left(\frac{H_{i,j-2} - H_{i,j+2}}{\lambda_{j+2} - \lambda_{j-2}}\right) \qquad (\varphi_i > 60^\circ)$$

where subscripts i and j refer to 5° latitude and longitude intervals measured northward from 15° and westward from 0° respectively.

Variations in the above procedure were required at several LLG points on the 20° latitude band due to the absence of interpolated height values at 15°. This was caused by the proximity of the original grid boundary. When values were not available at 15°, wind components were computed in the original grid coordinates at the point nearest the affected LLG point, resolved into LLG coordinates and assumed to be valid at the affected point. Since the largest distance separating any two points involved was approximately 120 km, this was assumed to be a reasonable procedure. Also, numerous hand computations of wind components using both grid scales at the 20° boundary indicated that

the difference in grid size had little or no effect on the computed wind values.

In Fig. 1 we have compared a part of a hemispheric analysis of interpolated height values with the NMC analysis from which the interpolated chart was derived. Some of our computed geostrophic wind vectors have been plotted upon the interpolated analyses. It is immediately obvious that our wind computation scheme provides a true and adequate representation of the scales of motion with which we are concerned.

The following quantities were computed for each month at each LLG point. (Parenthetical numbers following each quantity or list of quantities refer in order to the expressions from II which were used in the computations. Values of $\bar{T}$, $\bar{H}$ and $\bar{u}$ were obtained or computed directly from the interpolated monthly mean charts).

$\overline{u'^2}$, $\overline{v'^2}$, $\overline{T'^2}$, $\overline{u'v'}$, $\overline{v'T'}$ (2.3) (2.4);

$\bar{u}^{*2}$, $\bar{v}^{*2}$; $\bar{T}^{*2}$, $\bar{u}^*\bar{v}^*$, $\bar{v}^*\bar{T}^*$ (2.6) (2.7) (2.8);

$\sigma(u)$, $\sigma(v)$, $\sigma(T)$ (2.3) (2.5).

The following zonal and area averages and deviations from area averages were then computed from the foregoing values.

$[\bar{u}]$, $[\bar{T}]$, $[\bar{H}]$, $[\overline{u'^2}]$, $[\overline{v'^2}]$, $[\overline{T'^2}]$,

$[\bar{u}^{*2}]$, $[\bar{v}^{*2}]$, $[\bar{T}^{*2}]$, $[\overline{u'v'}]$, $[\overline{v'T'}]$,

$[\bar{u}^*\bar{v}^*]$ $[\bar{v}^*\bar{T}]$, $[\sigma(u)]$, $[\sigma(v)]$, $[\sigma(T)]$ (2.6);

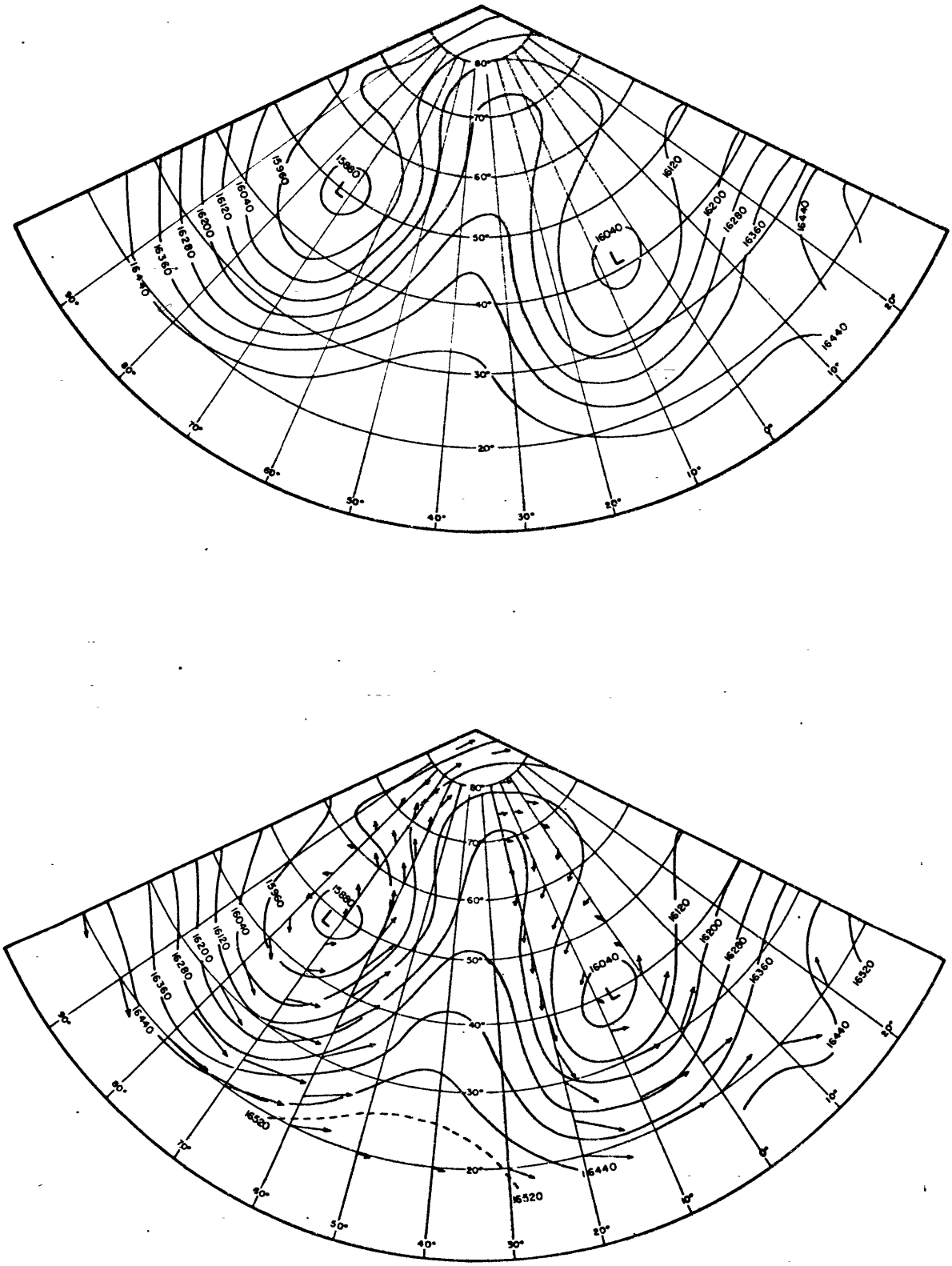

Figure 1: Analyses of original geopotential heights (upper diagram) and interpolated heights (lower diagram). Units: gpm
Arrows are geostrophic winds.
Wind scale: 10^{o} of latitude = 40 m sec^{-1} at 60^{o} north.

$\widetilde{\overline{T}}$ (2.6) (2.12); $\left[\overline{T}\right]''$ (2.6) (2.12) (2.13).

Additional computations gave values of $\left[u\right]_d$ (2.6) (2.14) and $\left[T\right]''_d$ (2.6) (2.12) (2.13) (2.15).

Monthly values of the following quantities are presented in tabular form at the end of this study.

$$\left[\overline{u}\right], \left[\overline{T}\right], \left[\overline{H}\right], \left[\overline{u'v'}\right], \left[\overline{u}^*\overline{v}^*\right], \left[\overline{v'T'}\right], \left[\overline{v}^*\overline{T}^*\right]$$

$$\left[\sigma(u)\right], \left[\sigma(v)\right], \left[\sigma(T)\right], \sqrt{\left[\overline{u}^{*2}\right]}, \sqrt{\left[\overline{v}^{*2}\right]}, \sqrt{\left[\overline{T}^{*2}\right]}.$$

A discussion of these quantities is given in Section VI in the context of their effects on momentum and energy balances.

IV. PRESENTATION AND DISCUSSION OF EQUATIONS

The conservation equations for the mean absolute zonal angular momentum, the mean zonal kinetic energy and the mean zonal available potential energy will be derived in this section. The quantities will be defined as the relevant equations are presented. Since terms involving conversions of eddy kinetic and eddy available potential energy arise in the derivations, definitions of these forms of energy will also be given. Although we are only able to calculate certain terms in the equations, primarily those involving horizontal eddy fluxes, entire expressions will be presented in order to place the evaluated terms in the proper context. Previous authors have discussed these equations extensively. (Kuo, 1951; Starr, 1951b; Lorenz, 1955; Dickinson, 1962; and Oort, 1963 among others). Also, the energy equations complete with derivation methods have been compiled by Saltzman (1957) and Peixoto (1965). The derivations given here will consequently be brief, and the notation, listed in Section II, will conform closely to that used by previous authors.

Derivations are based upon the following fundamental set of equations governing the atmosphere:

(1) Equations of motion

$$\frac{du}{dt} = v\left(f + u\frac{\tan\varphi}{a}\right) - \frac{1}{a\cos\varphi}\frac{\partial\Psi}{\partial\lambda} - D_\lambda \qquad (4.1)$$

$$\frac{dv}{dt} = -u\left(f + u\frac{\tan\varphi}{a}\right) - \frac{1}{a}\frac{\partial\Psi}{\partial\varphi} - D_\varphi \qquad (4.2)$$

$$\frac{\partial\Psi}{\partial P} = -\alpha \qquad (4.3)$$

(2) Equation of continuity

$$\frac{1}{a\cos\varphi}\frac{\partial u}{\partial \lambda} + \frac{1}{a\cos\varphi}\frac{\partial v\cos\varphi}{\partial \varphi} + \frac{\partial \omega}{\partial P} = 0 \qquad (4.4)$$

(3) Energy equation (first law of thermodynamics)

$$Q = C_p \frac{T}{\theta}\frac{d\theta}{dt} \qquad (4.5)$$

(4) Equation of state

$$P = \rho R T \qquad (4.6)$$

A. Angular momentum equation

The mean absolute zonal angular momentum, $M = \left([\bar{u}] + \Omega a\cos\varphi\right) a\cos\varphi$, is defined as the relative angular momentum per unit mass of air about the earth's axis of rotation due to the time mean and zonal mean wind plus the momentum due to the earth's rotation. To derive the equation for the time rate of change of M within a given volume we first multiply the zonal equation of motion by a cos φ, the distance to the earth's axis of rotation. Using the equation of continuity, (4.4), we may write the result as

$$\frac{\partial u a\cos\varphi}{\partial t} + \nabla\cdot\vec{c}\, u a\cos\varphi + \nabla\cdot\vec{c}\,\Omega a^2\cos^2\varphi = -\frac{\partial \psi}{\partial \lambda} - \tau_\lambda \qquad (4.7)$$

Averaging over a time period of length $t_2 - t_1$, and integrating over the mass of a polar cap north of latitude φ and between isobaric surfaces P_1 and P_2 $(P_1 > P_2)$ gives

$$\int a\cos\varphi\,\frac{u_2-u_1}{c_2-c_1}\,dm = \int_{(at\ \varphi)}^{P_1}\int_{0}^{2\pi} \overline{uv}\,a^2\cos^2\varphi\,\frac{d\lambda dP}{g} + \int_{(at\ P_2)}^{\frac{\pi}{2}}\int_{0}^{2\pi} \overline{uw}\,a^3\cos^2\varphi\,\frac{d\lambda d\varphi}{g}$$

$$-\int_{(at\ P_1)}^{\varphi}\int_{0}^{2\pi} \overline{uw}\,a^3\cos^2\varphi\,\frac{d\lambda d\varphi}{g} + \int_{(at\ \varphi)}^{P_2}\int_{0}^{2\pi} \overline{v}\Omega\,a^3\cos^3\varphi\,\frac{d\lambda dP}{g}$$

$$-\int_{(at\ P_1)}^{\varphi}\int_{0}^{2\pi} \overline{w}\Omega\,a^4\cos^3\varphi\,\frac{d\lambda d\varphi}{g} + \int_{(at\ P_2)}^{\frac{\pi}{2}}\int_{0}^{2\pi} \overline{w}\Omega\,a^4\cos^3\varphi\,\frac{d\lambda d\varphi}{g}$$

$$-\int \tau_\lambda\,dm \qquad (4.8)$$

where use has been made of the divergence theorem, and the assumption is made that the integral of the pressure torque term, $\int \frac{\partial\psi}{\partial\lambda}\,dm$, vanishes by virtue of our volume being above all terrain.

If we now average (4.8) around a latitude circle and express the integrands of the first three terms on the right hand side in their mean and eddy components according to (2.16) and (2.17), we obtain the equation for the time rate of change of M within the volume. We write it symbolically as

$$S(M) = F(R)_\varphi + F(R)_{P_2} - F(R)_{P_1} + F(E)_\varphi + F(E)_{P_2} - F(E)_{P_1} + D(M) \qquad (4.9)$$

Equation (4.9) expresses the necessity for a balance between the following processes.

(1) The "seasonal correction"; Oort (1963):

$$S(M) = \int \frac{[u]_d}{t_2 - t_1} \, a \cos\varphi \, dm$$

This term represents the total change of the mean zonal absolute angular momentum within the volume during the time period, $t_2 - t_1$. It would be zero only if a particular time interval were chosen, e.g., if the total momentum in the volume were periodic in time and we averaged over an integral number of periods. This term decreases in importance with an increase in $t_2 - t_1$, as one would expect, since over long time periods the total momentum in the volume does not change.

(2) The transport of relative angular momentum through the latitudinal boundary by mean meridional motions and horizontal eddy fluxes:

$$F(R)_\varphi = \underset{(at\ \varphi)}{\int_{p_2}^{p_1}\int_0^{2\pi}} [\bar{u}][\bar{v}]\, a^2\cos^2\varphi \, \frac{d\lambda dp}{g} + \underset{(at\ \varphi)}{\int_{p_2}^{p_1}\int_0^{2\pi}} [uv]_E \, a^2\cos^2\varphi \, \frac{d\lambda dp}{g}$$

(3) The transport of relative angular momentum through the isobaric boundaries by mean "vertical" motion and "vertical" eddy fluxes:

$$F(R)_{p_2} - F(R)_{p_1}$$

where $$F(R)_p = \underset{(at\ p)}{\int_{\varphi}^{\frac{\pi}{2}}\int_0^{2\pi}} [\bar{u}]\,[\bar{\omega}]\, a^3\cos^2\varphi \, \frac{d\lambda d\varphi}{g} + \underset{(at\ p)}{\int_{\varphi}^{\frac{\pi}{2}}\int_0^{2\pi}} [u\omega]_E \, a^3\cos^2\varphi \, \frac{d\lambda d\varphi}{g}$$

(4) The transport of the earth's angular momentum through the latitudinal and isobaric boundaries by horizontal and "vertical" motions respectively:

$$F(E)_{\varphi} + F(E)_{p_2} - F(E)_{p_1}$$

where

$$F(E)_{\varphi} = \int_{p_2}^{p_1}\int_{0}^{2\pi} [\bar{v}]\, \Omega\, a^3 \cos^3\varphi \, \frac{d\lambda\, dp}{g}$$

and

$$F(E)_{p} = \int_{\varphi\,(at\ p)}^{\pi/2}\int_{0}^{2\pi} [\bar{\omega}]\, \Omega\, a^4 \cos^3\varphi \, \frac{d\lambda\, d\varphi}{g}$$

(5) Dissipation by frictional torque:

$$D(M) = -\int \left[\bar{\tau}_{\lambda}\right] dm$$

This term contains all the effects of sub-grid scale boundary eddies plus internal and boundary effects of molecular viscosity.

B. Zonal kinetic energy equation

The mean zonal kinetic energy, $K_Z = \frac{1}{2}\int \left([\bar{u}]^2 + [\bar{v}]^2\right) dm$, is defined as the kinetic energy due to the time mean and zonal mean horizontal circulation within a volume of the atmosphere containing the mass, $\int dm$. To derive the equation for the time rate of change of K_Z within a given volume we multiply (4.1) by $[\bar{u}]$ and (4.2) by $[\bar{v}]$

and average the result over the time period, $t_2 - t_1$, and around a latitude circle. Using the continuity equation, (4.4), and equation (4.3), under the assumption of hydrostatic equilibrium, the results may be written as

$$[\bar{u}]\frac{[u]_d}{t_2-t_1} + \frac{1}{a\cos\varphi}\left\{\frac{\partial}{\partial\varphi}\left([\bar{u}]\,[\overline{uv}] - [\bar{v}]\,\frac{[\bar{u}]^2}{2}\right)\cos\varphi\right\}$$

$$+\frac{\partial}{\partial p}\left\{[\bar{u}]\,[\overline{u\omega}] - [\bar{\omega}]\,\frac{[\bar{u}]^2}{2}\right\} - \frac{[uv]_E}{a}\cos\varphi\frac{\partial}{\partial\varphi}\frac{[\bar{u}]}{\cos\varphi}$$

$$-[u\omega]_E\frac{\partial[\bar{u}]}{\partial p} = [\bar{u}][\bar{v}]\left(f + [\bar{u}]\frac{\tan\varphi}{a}\right) - [\bar{u}][\bar{D}_\lambda] \qquad (4.10)$$

and

$$[\bar{v}]\frac{[v]_d}{t_2-t_1} + \frac{1}{a\cos\varphi}\left\{\frac{\partial}{\partial\varphi}\left([\bar{v}][\overline{vv}] - [\bar{v}]\frac{[\bar{v}]^2}{2}\right)\cos\varphi\right\} + \frac{\partial}{\partial p}\left\{[\bar{v}][\overline{v\omega}] - [\bar{\omega}]\frac{[\bar{v}]^2}{2}\right\}$$

$$-\frac{[vv]_E}{a}\frac{\partial}{\partial\varphi}[\bar{v}] - [v\omega]_E\frac{\partial[\bar{v}]}{\partial p} = -[uu]_E[\bar{v}]\frac{\tan\varphi}{a} - [\bar{u}][\bar{v}]\left(f + [\bar{u}]\frac{\tan\varphi}{a}\right)$$

$$-\frac{1}{a}\frac{\partial}{\partial\varphi}[\bar{v}][\bar{\Psi}] - \frac{\partial}{\partial p}[\bar{\omega}][\bar{\Psi}] + [\bar{\Psi}]\frac{[\bar{v}]}{a}\tan\varphi$$

$$-[\bar{\omega}][\bar{\alpha}] - [\bar{v}][\bar{D}_\varphi] \qquad (4.11)$$

Adding (4.10) and (4.11) and writing terms in a somewhat different form gives

$$[\bar{u}]\frac{[u]_d}{t_2-t_1} + [\bar{v}]\frac{[v]_d}{t_2-t_1} = \frac{-1}{a\cos\varphi}\left\{\frac{\partial}{\partial\varphi}\left([\bar{v}]\frac{[\bar{u}]^2}{2} + [\bar{u}][uv]_E\right)\cos\varphi\right\}$$

$$-\frac{1}{a\cos\varphi}\left\{\frac{\partial}{\partial\varphi}\left([\bar{v}]\frac{[\bar{v}]^2}{2} + [\bar{v}][vv]_E\right)\cos\varphi\right\} - \frac{\partial}{\partial P}\left\{[\bar{\omega}]\frac{[\bar{u}]^2}{2} + [\bar{u}][u\omega]_E\right\}$$

$$-\frac{\partial}{\partial P}\left\{[\bar{\omega}]\frac{[\bar{v}]^2}{2} + [\bar{v}][v\omega]_E\right\} + \frac{[uv]_E}{a}\cos\varphi\frac{\partial}{\partial\varphi}\frac{[\bar{u}]}{\cos\varphi} + [u\omega]_E\frac{\partial[\bar{u}]}{\partial P}$$

$$+\frac{[vv]_E}{a}\frac{\partial[\bar{v}]}{\partial\varphi} + [v\omega]_E\frac{\partial[\bar{v}]}{\partial P} - [uu]_E[\bar{v}]\frac{\tan\varphi}{a} - \frac{1}{a\cos\varphi}\frac{\partial}{\partial\varphi}[\bar{v}][\bar{\psi}]\cos\varphi$$

$$-\frac{\partial}{\partial P}[\bar{\omega}][\bar{\psi}] - [\bar{\omega}][\bar{\alpha}] - [\bar{u}][\bar{D}_\lambda] - [\bar{v}][\bar{D}_\varphi] \qquad (4.12)$$

Integrating (4.12) over a polar cap north of latitude φ and between isobaric surfaces P_1 and P_2 we obtain the balance equation for the mean zonal kinetic energy. Following Oort (1963) and Peixoto (1965) we write the result symbolically as

$$S(K_Z) = C(K_E, K_Z) + C(A_Z K_Z) + A(K_Z) + W_e(K_Z) + W_p(K_Z) + D(K_Z) \qquad (4.13)$$

where terms which are small due to the relative magnitude of $[\bar{v}]$ are ignored. ($[\bar{v}]$ calculated from geostrophic winds is of course zero,

however, we obtain values of this parameter by an indirect method to be explained later; see Section V and Table 5). Equation (4.13) expresses the necessity for the balance which must exist between the average time change of the mean zonal kinetic energy within our polar cap and the processes which take part in its production or dissipation. The terms in (4.13) are:

(1) The "seasonal correction":

$$S(K_Z) = \int [\bar{u}] \frac{[u]_d}{t_2 - t_1} \, dm$$

A similar term was discussed in regard to zonal angular momentum. Analogous remarks apply to this term in its relationship to the zonal kinetic energy.

(2) The rate of conversion of eddy kinetic energy to zonal kinetic energy due to Reynold's stresses within the volume:

$$C(K_E, K_Z) = \int [u v]_E \cos\varphi \frac{\partial [\bar{u}]}{\partial \varphi a \cos\varphi} \, dm + \int [u \omega]_E \frac{\partial [\bar{u}]}{\partial p} \, dm$$

This term appears with opposite sign in the conservation equation for eddy kinetic energy, K_E, (see Oort, 1963) where K_E is given by

$$K_E = \frac{1}{2} \int ([u^2]_E + [v^2]_E) \, dm$$

and is defined as the kinetic energy due to the time and zonally averaged horizontal eddy motions within a volume containing the mass,

$\int dm \cdot C(K_E, K_Z)$ represents a process of energy exchange between the mean eddy motions and the motion of the mean zonal flow; the direction of the process is dependent upon the eddy transport of momentum relative to the gradient of angular rotation. For example, if there is an eddy flux of momentum from an area of low angular rotation to one of higher rotation, the kinetic energy of the mean motion is increased at the expense of the kinetic energy of the eddy motion.

(3) The rate of conversion from zonal available potential energy to zonal kinetic energy due to a mean motion of warm air toward low pressure and cold air toward high pressure:

$$C(A_Z, K_Z) = -\int [\bar{\omega}][\bar{\alpha}]\, dm$$

When this term involves integration over a hemispheric pressure surface, the integrand may be approximated by $[\bar{\omega}]''[\bar{\alpha}]''$, since by continuity $\int \omega\, dP \equiv 0$ within the approximation of zero mass exchange across an equatorial boundary. In our case, with a latitudinal boundary at 20°, this approximation is not entirely valid.

(4) The rate of advection of kinetic energy through the boundaries by mean meridional motions:

$$A(K_E) = \int_{P_2\,(\text{at }\varphi)}^{P_1}\int_0^{2\pi} [\bar{v}]\frac{[\bar{u}]^2}{2}\, a\cos\varphi\, \frac{d\lambda\, dP}{g}$$

$$+ \int_{\varphi\,(\text{at }P_2)}^{\pi/2}\int_0^{2\pi} [\bar{\omega}]\frac{[\bar{u}]^2}{2}\, a^2\cos\varphi\, \frac{d\lambda\, d\varphi}{g} - \int_{\varphi\,(\text{at }P_1)}^{\pi/2}\int_0^{2\pi} [\bar{\omega}]\frac{[\bar{u}]^2}{2}\, a^2\cos\varphi\, \frac{d\lambda\, d\varphi}{g}$$

(5) The rate at which work is done on the volume due to Reynold's stresses at the boundary:

$$W_e(K_z) = \int_{P_2\,(\text{at }\varphi)}^{P_1}\int_0^{2\pi} [\bar{u}][uv]_E\, a\cos\varphi\, \frac{d\lambda\, dP}{g} + \int_{\varphi\,(\text{at }P_2)}^{\pi/2}\int_0^{2\pi} [\bar{u}][u\omega]_E\, a^2\cos\varphi\, \frac{d\lambda\, d\varphi}{g} - \int_{\varphi\,(\text{at }P_1)}^{\pi/2}\int_0^{2\pi} [\bar{u}][u\omega]_E\, a^2\cos\varphi\, \frac{d\lambda\, d\varphi}{g}$$

(6) The rate of advection of potential energy into the volume, or equivalently, the rate at which work is done on the volume by mean pressure forces at the boundary:

$$W_p(K_z) = \int_{P_2\,(\text{at }\varphi)}^{P_1}\int_0^{2\pi} [\bar{v}][\bar{\Psi}]\, a\cos\varphi\, \frac{d\lambda\, dP}{g} + \int_{\varphi\,(\text{at }P_2)}^{\pi/2}\int_0^{2\pi} [\bar{\omega}][\bar{\Psi}]\, a^2\cos\varphi\, \frac{d\lambda\, d\varphi}{g}$$

$$- \int_{\varphi\,(\text{at }P_1)}^{\pi/2}\int_0^{2\pi} [\bar{\omega}][\bar{\Psi}]\, a^2\cos\varphi\, \frac{d\lambda\, d\varphi}{g} .$$

(7) The rate of dissipation of kinetic energy due to the effects of sub-grid scale boundary eddy stresses plus internal and boundary effects of molecular viscosity:

$$D(K_Z) = -\int [\bar{u}][\bar{D}_\lambda]\, dm$$

C. Zonal available potential energy equation

The mean zonal available potential energy, $A_Z = \frac{1}{2} C_p \int \gamma [\bar{T}]''^2 dm$, is defined as the maximum amount of potential energy which is available, by virtue of a variance of the time averaged and zonally averaged temperature on an isobaric surface, for conversion into kinetic energy under an adiabatic redistribution of mass. The equation for A_Z, first derived by Lorenz (1955) based upon a concept introduced by Margules (1903), is obtained from the first law of thermodynamics (4.5) written in spherical polar coordinates as

$$\frac{\partial \theta}{\partial t} = -u \frac{\partial \theta}{a \cos\varphi \partial \lambda} - \frac{v}{a} \frac{\partial \theta}{\partial \varphi} - \omega \frac{\partial \theta}{\partial P} + \frac{\theta Q}{C_p T} \qquad (4.14)$$

If (4.14) is multiplied by $[\bar{\theta}]''$ and the stability parameter, γ, averaged in time and around a latitude circle, and integrated over a polar cap north of latitude φ and between isobaric surfaces P_1 and P_2, the resulting equation may be written as

$$S(A_Z) = C(A_E, A_Z) + C(A_Z, K_Z) + G(A_Z) \qquad (4.15)$$

where boundary terms and terms involving triple correlations have been

neglected. Equation (4.15) expresses the necessity for a balance between the following processes:

(1) The "seasonal correction":

$$S(A_Z) = C_p \int \gamma [\bar{T}]'' \frac{[T]''_d}{t_2 - t_1} \, dm$$

(2) The rate of conversion from eddy available potential energy to zonal available potential energy due to eddy fluxes of sensible heat within the volume:

$$C(A_E, A_Z) = C_p \int \gamma [vT]_E \frac{1}{a} \frac{\partial}{\partial \varphi} [\bar{T}] \, dm + C_p \int \gamma \frac{T}{\theta} [\omega T]_E \frac{\partial [\bar{\theta}]''}{\partial p} \, dm$$

This term appears with opposite sign in the conservation equation for eddy available potential energy, A_E, (see Lorenz, 1955 and Oort, 1964b) where

$$A_E = \frac{1}{2} C_p \int \gamma \left[\overline{T^{*2}} \right] dm$$

and is defined as the maximum amount of potential energy which is available, by virtue of the latitudinal variance of temperature on an isobaric

surface, for conversion into kinetic energy under an adiabatic redistribution of mass. $C(A_E, A_Z)$ represents a process of redistribution of temperature variance on an isobaric surface.

This process has simultaneous effects on the variance of temperature within latitudinal zones, which represents eddy available potential energy, and the variance of mean zonal temperature over the isobaric surface, which represents zonal available potential energy. For example, a horizontal eddy flux of heat down the mean zonal temperature gradient results in an increase of temperature variance within latitudinal zones, and eddy available potential energy is created at the expense of zonal available potential energy.

(3) The rate of conversion from zonal available potential energy into zonal kinetic energy:

$$C(A_Z, K_Z) = \int [\bar{\omega}]'' [\bar{\alpha}]'' \, dm$$

A similar term with opposite sign appears in equation (4.13) and was described in paragraph B. (3) of this section.

(4) The rate of generation of zonal available potential energy by non-adiabatic processes, considered in this study to be confined to radiational heating and cooling:

$$G(A_Z) = \int \gamma [\bar{T}]'' [\bar{Q}]'' \, dm$$

The magnitude of this term depends upon the correlation of the hemispheric variance of zonally averaged diabatic heating rates and the hemispheric variance of zonally averaged temperature. For example, if a particular latitude band receives an excess of radiational heating in relationship to the hemispheric average, and its temperature is initially higher than the hemispheric average, then the radiation process increases the zonal available potential energy. This may be described simply as a zonally symmetric heating of the atmosphere where it is warm and cooling where it is cold. The reverse process destroys zonal available potential energy.

As stated earlier in this section, we will be unable to evaluate all terms in the foregoing equations. Since daily fields of "vertical" motion were not computed, we are unable to make direct calculations of "vertical" eddy fluxes and mean "vertical" motions. Thus, integrals involving these directly obtained quantities cannot be evaluated. Also, terms involving mean meridional motions cannot be evaluated with directly obtained values of $[\bar{v}]$, since our geostrophic approximation does not allow a direct calculation of this quantity, i.e. $\oint \frac{g}{fa\cos\varphi} \frac{\partial H}{\partial \lambda} d\lambda \equiv 0$. It is possible to make indirect approximations of $[\bar{v}]$ and $[\bar{\omega}]$ by considering them as forced motions resulting from heat and momentum sources and sinks. However, the assumptions we must make in their calculation essentially reduce their usefulness in the evaluation of the energy and momentum integrals to a check on the internal consistency of our set of equations. Nevertheless, these indirectly obtained approximations to

$[\bar{v}]$ and $[\bar{\omega}]$ are of value in making qualitative estimates of the mean hemispheric motion in the meridional plane. The next section deals with the calculation of these quantities.

V. MEAN MERIDIONAL AND MEAN "VERTICAL" MOTIONS

A set of equations for the computation of $[\bar{v}]$ and $[\bar{\omega}]$ may be derived from the fundamental governing equations (4.1), (4.4) and (4.5) by methods of time and space averaging analogous to those described in previous sections of this paper. This set of equations was first derived by Saltzman (1961) and has been used, either in its entirety or in part, by Dickinson (1962), Teweles (1963), Gilman (1963, 1964), Newell and Miller (1965) and others. The equations we intend to use differ from Saltzman's only in our assumption of a non-steady state of the space averaged zonal motion; and therefore, derivations will not be repeated here. The reader is referred to Saltzman's original paper for details. The equations may be written as

$$[\bar{\omega}]\frac{\partial[\bar{u}]}{\partial P} - Z[\bar{v}] = G - \frac{[u]_d}{t_2 - t_1} \tag{5.1}$$

$$\frac{1}{a\cos\varphi}\frac{\partial}{\partial\varphi}[\bar{v}]\cos\varphi + \frac{\partial[\bar{\omega}]}{\partial P} = 0 \tag{5.2}$$

$$\frac{[\bar{v}]}{a}\frac{\partial[\bar{T}]}{\partial\varphi} - \Gamma[\bar{\omega}] = h \tag{5.3}$$

where (5.1), (5.2) and (5.3) are time and space averaged forms of the zonal equation of motion, the continuity equation and the steady-state energy equation respectively. Here

$Z = f - \frac{1}{a\cos\varphi}\frac{\partial[\bar{u}]\cos\varphi}{\partial\varphi}$, the mean zonal vorticity,

$$G = -\frac{1}{a\cos^2\phi}\frac{\partial}{\partial\phi}[uv]_E\cos^2\phi - \frac{\partial}{\partial p}[u\omega]_E + [\bar{D}_\lambda]$$, the momentum forcing function,

and

$$h = \frac{[\bar{Q}]}{c_p} - \frac{1}{a\cos\phi}\frac{\partial}{\partial\phi}[vT]_E\cos\phi - \frac{\partial}{\partial p}[\omega T]_E + \frac{R}{c_p p}[\omega T]_E$$, the heat forcing function.

Other notation is defined in II. G and h contain all sources and sinks of momentum and heat which operate as forcing mechanisms for the mean motion. The momentum sources and sinks consist of momentum convergence or divergence due to large scale horizontal and "vertical" eddy processes plus dissipation due to friction. The heat sources and sinks consist of convergence or divergence of heat due to large scale horizontal and "vertical" eddy processes plus diabatic heating and cooling.

It is obvious from equations (5.1) to (5.3) that if we consider the forcing functions and all mean state variables except $[\bar{v}]$ and $[\bar{\omega}]$ as being determined, then the equations must be satisfied identically and simultaneously by $[\bar{v}]$ and $[\bar{\omega}]$. Considering the uncertainty involved in the determination of the forcing functions and the mean state variables, it would be somewhat fortuitous to find solutions to two of the equations which would simultaneously satisfy the third. When this problem was discussed with Dr. R.E. Dickinson, he suggested that the most unreliable of the specified variables was probably the diabatic heating rate, $[\bar{Q}]$, and that a reasonable approach to the problem would be a simultaneous

solution to the equations considering $[\bar{Q}]$ as a third unknown. A computer program is being developed at the present time by Mr. D.G. Vincent for carrying out this computation using relaxation techniques. However, at the time of this writing the computations have not been completed, and our values of $[\bar{v}]$ and $[\bar{\omega}]$ are those obtained as first approximations for use in the computer program. They were calculated for the months of January, April and July using equations (5.1) and (5.3) with the following assumptions:

1) $$[\bar{\omega}] = -\frac{h}{\Gamma} \tag{5.4}$$

where

$$h \approx \frac{[\bar{Q}]}{C_p} - \frac{1}{a\cos\varphi}\frac{\partial}{\partial\varphi}[vT]_E \cos\varphi$$

This assumption was based upon a comparison of the following relative orders of magnitude of the terms involved:

a. From our values of $[vT]_E$,

$$\frac{1}{a\cos\varphi}\frac{\partial}{\partial\varphi}[vT]_E \cos\varphi \sim 10^{-5} \text{ to } 10^{-4} \ ^{o}C \text{ sec}^{-1}$$

b. From the radiative heating rates of Kennedy (1964), which were used in the computations,

$$\frac{[\bar{Q}]}{C_p} \sim 10^{-5} \ ^{o}C \text{ sec}^{-1}$$

c. From the "vertical" eddy heat convergences of Miller (1966),

$$\frac{\partial}{\partial P}[\omega T]_E \sim 10^{-6} \ ^{o}C \ sec^{-1}$$

and

$$\frac{R}{C_p P}[\omega T]_E \sim 10^{-7} \ ^{o}C \ sec^{-1}$$

d. From our own $[\bar{v}]$ calculations plus those of Dickinson (1962) and Teweles (1963) and our measured values of $\frac{\partial[\bar{T}]}{\partial \varphi}$,

$$\frac{[\bar{v}]}{a}\frac{\partial[\bar{T}]}{\partial \varphi} \sim 10^{-6} \ ^{o}C \ sec^{-1}$$

2) $$[\bar{v}] = \frac{-G + \frac{[u]_d}{t_2 - t_1} + [\bar{\omega}]\frac{\partial[\bar{u}]}{\partial P}}{Z_1} \qquad (5.5)$$

where $[\bar{\omega}]$ was calculated from (5.4) and $\frac{\partial[\bar{u}]}{\partial P}$, $\frac{[u]_d}{t_2 - t_1}$ and Z_1 were computed from our data. G was determined by

$$G \approx -\frac{1}{a\cos^2\varphi}\frac{\partial}{\partial \varphi}[uv]_E \cos^2\varphi$$

based upon the following relative order of magnitude considerations:

($[\bar{D}_\lambda]$ was assumed to be zero due to the uncertainty involved in estimates of eddy viscosity coefficients).

a. From our values of $[uv]_E$,

$$\frac{1}{a\cos^2\varphi}\frac{\partial}{\partial\varphi}[uv]_E\cos^2\varphi \sim 10^{-3}\ \text{cm sec}^{-2}$$

b. From the "vertical" eddy momentum convergences of Miller (1966),

$$\frac{\partial[u\omega]_E}{\partial p} \sim 10^{-4}\ \text{cm sec}^{-2}$$

In order to obtain $[\bar{\omega}]$ at all levels, assumptions concerning the temperature lapse rates were required at the 100 mb and 10 mb boundaries. By comparing the measured lapse rates in the layers adjacent to the boundaries to the supplemental U.S. standard atmospheres, Cole et al. (1965), percentage corrections to the standards for the adjacent layers were obtained. These corrections were then applied to the standard lapse rates for the 100 and 10 mb levels. The results were used for computing Γ at these levels. In all cases the lapse rates at 100 mb were insignificant in the determination of Γ and were considered to be zero. The percentage corrections at 10 mb varied from zero to about 15 percent.

Values of $[\bar{v}]$ were obtained at intermediate isobaric levels, i.e., 75, 40 and 20 mb, by linear finite differencing between the 100, 50, 30 and 10 mb levels.

It should be noted that the order of magnitude considerations in I) and 2) above are based upon the calculations for levels at and

below 30 mb; and therefore, our assumptions above this level are questionable. However, since calculations have not been made of daily "vertical" motion fields at these higher levels, expediency prompted our use of these assumptions in the 30 to 10 mb layer.

Our values of $\left[\overline{v} \right]$ and $\left[\overline{\omega} \right]$ are tabulated at the end of this study and will be discussed in the next section.

VI. RESULTS AND DISCUSSION

The results of this study will be divided into six general categories. These categories are: (A) the monthly mean climatological features of the 1965 stratosphere; (B) the horizontal eddy transport of angular momentum; (C) the momentum budget; (D) the horizontal eddy transport of sensible heat; (E) the zonal kinetic energy budget and (F) the zonal available potential energy budget. These categories will be discussed in the order listed. All referenced tables and figures are compiled at the end of the study. In most cases, the figures referred to will be meridional cross section of relevant quantities for the months of January, March, April, July and October; and unless otherwise indicated, all references to "monthly cross sections" imply these five months. These months were chosen on the basis of their representativeness of seasonal regimes and interseasonal changes.

The isopleth spacing on some of the cross sections was a problem due to large variations in the parameters portrayed. A word is in order concerning how this spacing was handled. In most cases the isopleths representing the maximum interval portrayed were drawn as solid lines. Intermediate lines representing values of unity or larger were dashed, and when values less than unity were required for adequate portrayal, dotted lines were used.

A. Monthly climatological features

(1) Mean zonal wind, temperature and geopotential height:

Tables 1, 2 and 3 give values of $[\bar{u}]$, $[\bar{T}]$ and $[\bar{H}]$ respectively at each 5^{o} of latitude and for each month and level. Monthly cross sections of $[\bar{u}]$ and $[\bar{T}]$ are shown in Figs. 2a through 2e and 3a through 3e. Isobaric surfaces representing $[\bar{H}]$ at 100, 50, 30 and 10 mb are superimposed on the cross sections. A discussion of $[\bar{H}]$ will not be given, since its climatological features in relationship to the temperature and wind fields are obvious from the cross sections.

In January the zonal wind is westerly throughout the region. The dominant feature is the downward extension of the polar-night jet with a maximum velocity of 44 m sec^{-1} at 10 mb and 65^{o}. Following the locus of maximum wind downward, we find it remains near 65^{o} until we reach 50 mb. It moves rapidly southward between 50 and 100 mb extending into the upper portion of the middle latitude tropospheric jet which appears at 32.5^{o} and 100 mb. A maximum velocity of 26 m sec^{-1} occurs at this point.

The meridional temperature distribution in January appears to be "typical" for the early winter months (see Newell, 1965 and Hare, 1960). Cold dense air is centered over the pole at 30 mb, and the semipermanent cold region of the lower equatorial and subtropical stratosphere appears at 100 mb and 20^{o}. An extension of warm air from the subtropical middle stratosphere separates these cold regions producing the temperature gradient reversal which is common to the lower stratosphere in the winter. It is of particular significance that the gradient of $[\bar{T}]$ at 10 mb in January has the same direction as the gradient of $[\bar{T}]$ in

the troposphere. The importance of this feature will become apparent in later discussion of zonal available potential energy.

In Fig. 2a there exists a locus of zeros of the vertical derivative of $[\bar{u}]$ which begins just above 30 mb at 20° and slopes downward and northward crossing the 100 mb surface at 55°. Figure 3a indicates a locus of zeros of the horizontal derivative of $[\bar{T}]$ along the approximate same line. We note, therefore, that the thermal wind relation holds, as one would expect in view of our geostrophic approximation. This does, however, speak well for the original data and its reduction. Similar comparisons of cross sections for other months also show this satisfaction of the thermal wind relationship.

In March the polar vortex has weakened considerably (27 m sec^{-1} at 10 mb) but is still very much in evidence. The locus of maximum velocity has moved slightly northward at all levels. The extension of the tropospheric jet at 100 mb persists from January in both location and intensity. A slight easterly circulation appears at 20° at 30 and 10 mb in conjunction with middle and high latitude warming. This warming appears in the March temperature distribution (Fig. 3b) and signals the onset of the breakdown of the polar vortex. The temperatures at 85° north at the 30 and 10 mb levels shows an increase of 15 to 25°K over the January values. Table 2 indicates that this warming was relatively gradual in this particular year in contrast to other more dramatic occurrances, e.g. the sudden warmings of 1957 and 1958 (see Reed et al., 1963 and Teweles, 1963). At 100 mb in March the temperatures have not changed

appreciably from January except for slight warming at high latitudes.

In April the polar vortex has virtually disappeared. Some vestige is apparent at 30 and 50 mb. The center of maximum wind has propagated downward in apparent response to a warming aloft and has, in effect, become an extension of tropospheric jet whose main upward extension still persists at 100 mb and 22.5°. The easterlies which appeared at 20° in the middle stratosphere in March have increased and propagated northward into middle latitudes.

The April temperature profile indicates that the evolution into a "typical" summer temperature regime (see Newell, 1965 and Hare, 1960) is almost complete. The high latitude zonal temperature gradient at 10 mb is now reversed due to warming over the pole. A slight residual of cold air over the pole remains at 100 mb, still giving a temperature gradient reversal in middle latitudes at this level.

The July velocity cross section (Fig. 2d) shows strong easterly circulation at 50 mb and above with a maximum velocity of -36 m sec^{-1} at 20° and 10 mb. The westerly tropospheric jet still dominates the circulation at 100 mb, having moved northward to middle latitudes. Maximum velocity has decreased to 9 m sec^{-1} at this level.

The July temperature profile (Fig. 3d) shows that warming has continued over the pole during the spring months. Total temperature changes from January to July at 85° north vary from 25 to 40 °K at different levels. In conjunction with quasi-constant temperatures at

low latitudes, this results in a southward temperature gradient at all levels.

The climatological changes described above show a relatively gradual evolution from the winter temperature and circulation distributions of the 1965 stratosphere into the markedly different summer regime. During the late summer months the reverse of this evolution process takes place, and by October (see Figs. 2e and 3e) "typical" winter distributions of $[\bar{u}]$ and $[\bar{T}]$ are again established.

Figures 8 and 11 show zonal cross sections of January values of $\bar{u}$ and $\bar{T}$ from which $[\bar{u}]$ and $[\bar{T}]$ at 60^{o} north were derived. These cross sections show the large longitudinal dependence of $\bar{u}$ and $\bar{T}$ and indicate the necessity for adequate spatial sampling in any type of statistical analysis scheme based upon zonal means. They also indicate that a consideration of longitudinal variation is essential in the computation of many important physical processes in the stratosphere. One of particular note, of course, is radiational heating which becomes a function of longitude through its temperature dependence.

(2) Mean "vertical" and meridional motions: Tables 4 and 5 give values of $[\bar{\omega}]$ and $[\bar{v}]$ respectively for the months of January, April and July, our restriction to these months being caused by the availability of radiational heating rates. The spatial distribution given is a consequence of our computation scheme. We reiterate at this point that values of $[\bar{\omega}]$ were computed under the assumption that they are a forced response to radiational heating plus eddy heat convergence, while values

of $[\bar{v}]$ are assumed to be a response in the form of Coriolis torque to momentum advection by $[\bar{\omega}]$, forcing by eddy momentum convergence and the effects of mean monthly zonal accelerations.

In the following discussion of $[\bar{\omega}]$ and $[\bar{v}]$ references will be made to momentum and heat convergences. The reader is referred to cross sections of momentum and heat transport shown in Figs. 4a through 4e and 5a through 5e, respectively, from which areas of convergence of momentum and heat may be inferred.

We see from the values of $[\bar{\omega}]$ in Table 4 that in January subsidence occurs in middle latitudes at all levels. This is in response to both radiational cooling and eddy heat divergence. In general, eddy effects are the same order of magnitude as radiation at lower levels but increase in relative importance with height becoming an order of magnitude larger at 10 mb in some cases. In subtropical latitudes there is rising motion at low levels which decreases in magnitude with height and reverses to subsidence between 30 and 10 mb. North of 55^{o} there is rising motion in response to eddy heat convergence at all levels. This is offset somewhat by the increase in radiational cooling rates at these higher latitudes. These large cooling rates provide the main forcing for the small region of subsidence which occurs at the 100 and 50 mb levels near the pole.

It should be noted at this point that radiational cooling rates used north of 75^{o} were extropolated values, and results based upon them are subject to the attendant errors.

The mean meridional motion in January (Table 5) shows evidence of an extension of the tropospheric three-cell circulation pattern into the lower stratosphere. This was also found by Teweles (1963), Dickinson (1962) and Newell and Miller (1964) from computations similar to those used here. There is generally northward motion in the subtropics, southward motion in middle latitudes and a reversal back to a northward flow in the sub-polar latitudes. With increasing height, this general pattern remains the same but shifts northward in response to a change in the areas of maximum eddy activity associated with the different circulation regime of the middle stratosphere, e.g. there is large momentum convergence into the polar vortex which is not accounted for by acceleration of the mean zonal flow. There appears to be an indirect circulation associated with the polar vortex similar to that found about the tropospheric jet. Teweles (1963) also found evidence of this feature of the lower stratosphere.

The distribution of the "vertical" motion in April is similar to that found in January, however, values have generally decreased by a half to a full order of magnitude. Main differences in the "vertical" flow pattern appear at 30 and 10 mb, as one might expect, since this is the area of major changes in the zonal circulation during the spring. The high latitude rising motion has decreased in both intensity and extent due to a decrease in eddy heat convergence. The rising motion at low latitudes, which was confined to 30 mb and below in January, now extends to 10 mb. Middle latitude subsidence due to eddy heat divergence is a persistent feature.

The mean meridional motion in April shows a general southward drift at 75 mb. Above this level the deceleration of the polar vortex plus continued eddy momentum convergence gives mean southward motion at high latitudes. At low latitudes and high levels the increase in the zonal easterlies is insufficient to balance the momentum divergence, and a mean northward flow results.

In July the mean "vertical" motion at 50 and 30 mb is determined primarily by forcing due to radiational effects. Since radiational cooling takes place at all latitudes north of 30^{o} at 50 and 30 mb, we observe sinking motion north of this demarcation at these levels, while upward motion due to radiational heating occurs to the south of 30^{o}. At 10 mb the effects of both types of forcing become small, and little can be said concerning the true nature of the "vertical" motion at this level. At 100 mb radiational cooling effects dominate at high latitudes giving sinking motion, while forcing by eddies gives rising motion south of 45^{o}.

The emergence of the mean meridional motions for July into a coherent pattern is somewhat remarkable in view of the complicated distribution of the orders of magnitude of terms involved in its calculation. We will not attempt to describe the interrelation of all the terms at different latitudes and levels. A comparison of the momentum transport in Fig. 4d with the distribution of $[\bar{v}]$ in Table 5 indicates that forcing by standing eddy momentum convergence is one of the most significant terms.

It is difficult to assess the quantitative accuracy of our values of $[\bar{v}]$ and $[\bar{\omega}]$. In regard to order of magnitude; our values of $[\bar{\omega}]$, when averaged between January and April and between levels, compare favorably to Miller's (1966) 75 and 40 mb values which are means for the period January through March 1958. In general our January values are a half to a full order of magnitude larger than Miller's three-month averages. In comparing our values of $[\bar{\omega}]$ to the monthly adiabatic values computed by Teweles (1963) for the 100 to 50 mb layer, we find quite good correspondence in sign and magnitude in January. Our values are somewhat larger than Teweles' in April but still compare well in sign. July values do not compare well in sign, but orders of magnitude are comparable, i.e. both are quite small. Our monthly values of $[\bar{v}]$ compare well with Teweles' 1958 values computed by a similar method. In checking our values of $[\bar{\omega}]$ and $[\bar{v}]$ against continuity we find qualitative satisfaction in most regions, a fact which lends credence to their accuracy and the method of computation.

B. Eddy transport of angular momentum

As noted previously, meridional cross sections of momentum transport are shown in Figs. 4a through 4e. Specifically, these figures show the meridional distribution of transient eddy transport (upper diagrams) and standing eddy transport (lower diagrams) of mean relative zonal angular momentum per centimeter of vertical distance across a complete latitude circle. These transports are given by

$$\int_{p_2}^{p_1}\int_{0}^{2\pi} \overline{u'v'}\, a^2 \cos^2\varphi \, d\lambda \, \frac{dP}{g} \qquad (1\ cm)$$

and

$$\int_{p_2}^{p_1}\int_{0}^{2\pi} \overline{u^*}\,\overline{v^*}\, a^2 \cos^2\varphi \, d\lambda \, \frac{dP}{g} \qquad (1\ cm)$$

respectively (see equation (4.9). The integration over pressure for a centimeter of vertical distance at each isobaric level was accomplished by approximating $\int_{1\,cm} \frac{dP}{g}$ with the standard density for the level. Values of $[\overline{u'v'}]$ and $[\overline{u}^*\overline{v}^*]$ are given in Tables 6 and 7 respectively. The following series of commentaries, outlined by month, summarize the significant features of the momentum transports during the year.

(1) January, Fig. 4a: In the middle stratosphere maximum northward momentum transport by both transient and standing eddies occurs just to the south of the main axis of the polar-night jet. To the north of the jet southward transport by standing eddies takes place. Momentum convergence into the region of maximum zonal flow results. In the 50 to 30 mb region of the lower stratosphere the same general features exist except that the areas of maximum transport are slightly south of their middle stratosphere location.

At 100 mb the transports are a half to a full order of magnitude larger than those found at 10 mb. Maximum convergence at the 100 mb level due to both transient and standing eddies is north of the region of maximum zonal wind, while the region of the largest northward transport coincides with the region of maximum zonal wind. This relative distribution of eddy momentum flux and zonal wind is a somewhat unexpected phenomenon that persists at 100 mb throughout the late winter and spring. Compensating effects, one of which we have already considered, i.e. Coriolis torque due to mean meridional motions, are obviously necessary in order to maintain momentum balance in this region.

(2) March, Fig. 4b: The area of largest transport by both standing and transient eddies is still south of the region of maximum zonal flow at 50 mb and above, and convergence into the polar vortex at these high levels is a persistent feature. The character of the standing eddy activity shows a marked change from January. The region of large southward transport has virtually disappeared except for some small residual at 100 mb and 55°, and a center of strong northward transport is now located near 50 mb at 55°. The northward transient eddy fluxes at the higher levels have increased somewhat over the January values. These increased northward fluxes into the region of maximum zonal motion are unexpected features at the high levels in view of the deceleration of the zonal flow which has taken place since January. Convergence of momentum into the region of maximum zonal motion has shown some slight

decrease, however.

At 100 mb the magnitude of the standing eddy transport has decreased markedly, while a considerably smaller decrease has occurred in the transient eddy activity. Maximum momentum convergence is still north of the maximum zonal wind at this level.

(3) April, Fig. 4c: The main change observed in the April momentum transports is a decrease to insignificant values in the standing eddy flux at the higher levels. Also, a change to southward standing eddy transport has occurred in middle latitudes at 100 mb. The transient eddies give northward transport at all levels in middle latitudes and southward transport at 50 and 100 mb north of 60°. This produces a region of quite large convergence in the approximate location of the residual of the polar vortex. A net momentum convergence persists north of the tropospheric jet extension at 100 mb.

(4) July, Fig. 4d: The transient eddy transports in the middle stratosphere are insignificant. At 100 mb they show some slight activity producing southward, divergent, momentum flux at all latitudes. At high levels the standing eddy fluxes show some coherent pattern, but values are too small to bear serious consideration. At 100 mb the standing eddy pattern continues to show momentum divergence out of the region of maximum zonal motion.

(5) October, Fig. 4e: The distribution of transient eddy momentum transport in October shows considerable resemblance to its April

counterpart. Magnitudes are slightly smaller. Convergence into the accelerating polar vortex is taking place with maximum northward transport to the south of the maximum zonal wind. Transient eddies are also producing momentum convergence into the region of the upward tropospheric jet extension. The standing eddy transports in October have a distribution similar to that of the transient eddies, i.e. they are producing momentum convergence into the regions of accelerating zonal motion. Magnitudes of the standing eddy transports are somewhat larger than those due to the transient eddies.

In Figs. 9 and 10 we have shown zonal cross sections of January values of $\overline{u'v'}$ and $\bar{u}^*\bar{v}^*$ from which values of $\left[\overline{u'v'}\right]$ and $\left[\bar{u}^*\bar{v}^*\right]$ for 60° north latitude were computed. As in similar cross sections of $\bar{u}$ and $\bar{T}$, Figs. 8 and 11, we see a strong dependence of these parameters on longitude. We will return to a further discussion of some aspects of this dependence in our considerations of kinetic energy exchanges.

In summarizing the eddy momentum transports for the year we may make the following general observations. Transports due to standing eddies are usually larger than those due to transient eddies. In the middle stratosphere in the winter, the transports by both standing and transient eddies are such that momentum convergence takes place into the region of maximum westerly zonal flow. This feature is also found in the 50 to 30 mb levels of the lower stratosphere. However, at 100 mb the eddies display a somewhat disconcerting tendency to transport momentum out of the region of maximum westerly zonal flow. During the

summer, transports are found to be quite small, especially at higher levels, indicating that eddy activity plays a much smaller role in the stratospheric circulation during this part of the year.

A comparison of our values of $\left[\overline{u'v'}\right]$ and $\left[\bar{u}^*\bar{v}^*\right]$ with the three month mean values computed from IGY data by Murakami (1962) and Peng (1962, 1965c) shows the following main differences. In general, our time covariances are smaller than those computed from IGY data. A comparison of our time standard deviations of u and v (Tables 10 and 11) with those computed by Murakami and Peng indicate that during the summer this difference may be caused by smaller time variations in u and v, while in the winter, our lower values are apparently due to lack of correlation. However, the difference in the time periods of averaging of our data and that obtained during the IGY makes comparison of results based upon temporal statistics difficult and inconclusive. Our values of $\left[\bar{u}^*\bar{v}^*\right]$ are much larger in the winter than values computed from IGY data, while in the summer months, the orders of magnitude are comparable.

C. The momentum budget

Tables 16, 17 and 18 show a comparison of monthly values of the seasonal correction term, S(M), and the transient eddy and standing eddy parts of the horizontal flux term, $F(R)_\varphi$, of equation (4.9) for the 100 to 50, 50 to 30 and 30 to 10 mb layers. These terms were evaluated by finite difference approximations for polar caps north of 20, 45 and 60°. Monthly values of the total mean absolute zonal angular

momentum, M, in caps north of 20^{o} are also included in the tables. We did not calculate terms in equation (4.9) involving $[\bar{v}]$ and $[\bar{\omega}]$ even though we had values of these quantities available for January, April and July. The reader will recall that we computed $[\bar{v}]$ and $[\bar{\omega}]$ by assuming a balance between certain terms in the momentum equation. A comparison of term involving these quantities in the integrated form of the same equation would obviously be redundant.

Our comparison of the seasonal correction term and the horizontal eddy flux terms gives an approximation to the angular momentum deficit which must be accounted for by terms in equation (4.9) which we have not evaluated. These terms and the processes which they represent were described in detail in Section IV. The deficits are listed in the tables along with the values of S(M) and the eddy parts of $F(R)_{\phi}$. A negative deficit indicates that there is a surplus of momentum change in the polar cap, and a depletion process is required in order to establish a momentum balance. The following comments, outlined by layer, give the main features of the evaluated terms and resulting deficits.

(1) Table 16, 100 to 50 mb layer: In all months except March the eddies provide a net flow of angular momentum into a polar cap north of 20^{o}*. In general, the momentum transports by the standing eddies are

*March is an exception due to a large, negative, standing eddy flux at 20^{o} and 100 mb. 20^{o} boundary values of $[\bar{u}^{*}\bar{v}^{*}]$ for various months and levels appear to be spurious; however, these values were carefully checked and are correct within the accuracy of our data and computation procedures.

larger than those by the transient eddies at the 20° boundary. Their sum is such that it accounts for the seasonal changes within a cap north of this boundary during all months except September, October and November, a period of large increase in westerly zonal momentum. Little can be said concerning the relative magnitudes of transient and standing eddy momentum transports at 45°, since they vary in importance from month to month. We still find that the eddies give a net flow of momentum into a cap north of this latitude during most of the year. It is also evident that the sum of the eddy transports at 45° is sufficient to give negative deficits in the cap north of this boundary during all months except July, August and September. In these months the seasonal correction term begins to increase as a result of the late summer and fall accelerations of the zonal flow, and the eddies are apparently unable to provide the momentum for these accelerations. At the 60° latitude boundary we note a large eddy transport of momentum southward during the winter months giving large deficits in a cap north of this latitude during December, January and February. During the rest of the year behavior is similar to that found in the polar cap bounded by 45°.

(2) Table 17, 50 to 30 mb layer: Transports in this layer are smaller than those in the 100 to 50 mb layer because of the smaller density plus, in some cases, less eddy activity. Due to the sporadic nature of the flux terms, little can be said concerning the differences in the transports at the different latitude boundaries in this layer. In general, the standing eddies give the largest contribution during

all months at all three latitudes. Negative deficits predominate in the three volumes during the year, except during the late summer and fall months when the mean zonal flow experiences the largest positive acceleration.

(3) Table 18, 30 to 10 mb layer: The momentum transports in this layer are generally larger than those in the 50 to 30 mb layer. In view of the decrease in density with height, a large amount of eddy activity is obviously present. Thus, we see an indication of the relatively active nature of the middle stratosphere in comparison to the 50 to 30 mb region. The polar caps north of 20° and 45° in the 30 to 10 mb layer show characteristics similar to caps with the same latitude boundaries between the 100 and 50 mb surfaces, i.e. the sums of the eddy momentum transports and seasonal corrections result in negative deficits in all months except those in which the large positive zonal accelerations take place. We find that the standing eddy transports are somewhat larger than those due to the transient eddies at both 20° and 45° in this layer. At 60° the two types of eddy processes vary in relative importance from month to month.

In Table 19 we have compared three month averages of our values of S(M), the eddy part of $F(R)_{\varphi}$ and the total mean relative zonal angular momentum, M_r, for a 100 to 30 mb layer with similar terms computed from IGY data by Oort (1963). Oort's values were computed for polar caps bounded by the 100 and 30 mb isobaric surfaces, however, his vertical surfaces were at 30° and 60°. We are therefore only able

to make direct comparison of values in polar caps with 60^{o} boundaries. However, we have also included a comparison of our values for a polar cap north of 20^{o} to Oort's values for a polar cap north of 30^{o}. It should be pointed out that Oort's covariances used in the integrals were computed from three month averages; and therefore, are not quantities which are directly comparable to our values computed from monthly means. However, we may still make meaningfull comparisons between general orders of magnitude of the relevant terms and the approximate seasonal trends which they represent. We see from Table 19 that our values compare reasonably well with Oort's both in magnitude and sign.

In summary we find that the momentum budgets for the three polar caps show negative deficits during most months, the exceptions being those months in which the large seasonal increases in momentum take place. As mentioned earlier, deficits must be accounted for by terms in equation (4.9) which we have not calculated. Our values of $\left[\overline{v}\right]$ which were computed by balancing terms in the momentum equation represent a possible momentum source or sink for these deficits. Other possibilities are vertical eddy momentum fluxes, frictional dissipation, and transport of the earth's angular momentum by mean "vertical" motion. Calculations of daily "vertical" motion fields are required, however, before any sort of definite conclusion can be reached concerning how these sources and sinks combine to provide momentum balance.

D. Eddy transport of sensible heat

Monthly cross sections of the meridional distribution of horizontal eddy heat transports are shown in Figs. 5a through 5e. Transports are computed as the rate of energy flow per centimeter of vertical distance across a complete latitude circle due to transient eddies (upper diagram),

$$C_p \int_{1\,cm} \int_0^{2\pi} \overline{v'T'}\, a\cos\varphi\, d\lambda \frac{dp}{g}$$

and due to standing eddies (lower diagram),

$$C_p \int_{1\,cm} \int_0^{2\pi} \overline{v}^*\overline{T}^*\, a\cos\varphi\, d\lambda \frac{dp}{g}$$

where the integration over pressure for a centimeter of vertical distance is accomplished by approximating $\int_{1\,cm} \frac{dp}{g}$ by the standard density at each isobaric level. Values of $\left[\overline{v'T'}\right]$ and $\left[\overline{v}^*\overline{T}^*\right]$ are given in Tables 8 and 9 respectively. We will discuss briefly, by month, the significant features appearing on the cross sections. First, however, note the apparent spuriousness of various values of both $\left[\overline{v'T'}\right]$ and $\left[\overline{v}^*\overline{T}^*\right]$ at 20°. Similar characteristics appeared in values of $\left[\overline{u}^*\overline{v}^*\right]$, and, as noted earlier, careful checking of these

quantities indicated that they were correct. Similarly, our covariances of v and T appear to be correct. Possibilities for the cause of these apparently spurious values are differences in wind computation procedures at various points at the 20° boundary and scarcity of original data at low latitudes. We should by no means discount the possibility that these values are correct and represent true, complicated interactions in the subtropical regions between circulation regimes of the tropics and those of middle latitudes. However, when values were found to be obviously in error they were ignored in the analyses, our criterion being the reasonableness of heating rates computed from eddy heat convergences between 20 and 25°.

(1) January, Fig. 5a: Northward transport by both transient and standing eddies predominates with a region of maximum flux by both types of eddies appearing near 55°. Largest values occur at 100 mb and generally decrease with height above this level. Strong convergence takes place at all levels north of the 55° axis of maximum transport with equally large divergence south of this demarcation. In general, the standing eddy fluxes are twice as large as those due to transient eddies during this month.

(2) March, Fig. 5b: Northward transport by both the transient and standing eddies still predominates. However, there has been a large change in the character of the transient eddy flux since January. A center of maximum transport is now located at 65° and 50 mb producing

a region of heat convergence between this latitude and the pole. It is of course tempting, and no doubt correct, to associate this increase of eddy activity with the warming over the pole which took place between March and April (see Table 2). However, the standing eddy flux, although maintaining its general spatial distribution, shows a marked decrease from January, and thus counteracts the effects of the increased transient eddy activity. Nonetheless, as we shall see in later computations, the combined transports provide adequate heating to account for both radiational losses and the mean seasonal temperature increase which took place between March and April.

(3) April, Fig. 5c: The large transient eddy transports which appeared in middle latitudes in March have subsided dramatically, e.g. they have decreased by an order of magnitude at high levels in some cases. Standing eddy fluxes have also decreased somewhat in most regions, an exception being a significant increase at 100 mb in lower middle latitudes.

(4) July, Fig. 5d: Fluxes above 50 mb have decreased to insignificant values. A somewhat coherent pattern of small, predominantly negative standing eddy transports appears in the middle stratosphere. The transient eddy fluxes at high levels, mostly positive, show a somewhat more organized spatial distribution than their standing eddy counterparts, but magnitudes are equally small. At 100 mb transports are generally northward with main transient eddy activity appearing in middle latitudes. Standing eddy fluxes show two maxima at 100 mb;

one is at 55° and another is at or equatorward of 20°.

(5) October, Fig. 5e: Northward transport by both transient and standing eddies again predominates with both type fluxes showing maxima in middle and subpolar latitudes. The low latitude maximum at 100 mb which was in the subtropics in July now appears at 40°. It appears that the character of both the standing and transient eddy heat fluxes are returning to a somewhat "typical" winter distribution.

Zonal distributions of January values of $\overline{v'T'}$ and $\overline{v^*T^*}$ from which we computed the quantities $[\overline{v'T'}]$ and $[\overline{v}^*\overline{T}^*]$ for 60° north are shown in Figs. 12 and 13. We see a large longitudinal variation in these values which is not unlike that found in values of $\overline{u'v'}$ and $\overline{u}^*\overline{v}^*$. The longitudinal dependence of these parameters further accents the need for adequate spatial sampling in statistical analyses based upon zonal averages.

The most noteworthy feature of the eddy heat transports throughout the year is the predominantly northward transport at all latitudes and levels. This is significant, as we shall see later, in available potential energy conversions.

It is interesting to compare the magnitudes of the observed mean rates of change of heat energy within a polar cap during the period of the spring warming to rates predicted by the sum of the horizontal eddy transports across the latitude boundary and radiational cooling within the cap. We made this comparison for polar caps bounded by 60° north

latitude and the 100, 50, 30 and 10 mb surfaces for the period 15 March to 15 April. The three rates were computed by finite difference approximations of the following integrals.

(a) Mean rate of change of energy within the cap:

$$C_p \int \frac{[\bar{T}]_2 - [\bar{T}]_1}{\Delta t} \, dm$$

Subscripts 1 and 2 indicate values for March and April respectively. Δt = 31 days.

(b) Rate of energy increase in the cap due to radiational processes:

$$C_p \int \bar{Q} \, dm$$

The heating rates, $\bar{Q}$, are values given for April by Kennedy (1964). Extrapolation was required north of 75°.

(c) Rate of energy increase in the cap due to horizontal eddy heat transport:

$$C_p \int_{p_2 \text{ (at } 60^\circ)}^{p_1} \int_0^{2\pi} [vT]_E \, a \cos\varphi \, d\lambda \, \frac{dp}{g}$$

The results of our computations in units of 10^{19} ergs sec^{-1} are as follows:

(i) 100 to 50 mb layer

Mean rate of change of energy within the cap = 44.2

Energy increase due to radiational processes = -98.1

Energy increase due to eddy heat transport = 170.3

(ii) 50 to 30 mb layer

Mean rate of change of energy within the cap = 18.4

Energy increase due to radiational processes = -29.2

Energy increase due to eddy heat transport = 93.2

(iii) 30 to 10 mb layer

Mean rate of change of energy within the cap = 17.4

Energy increase due to radiational processes = -41.2

Energy increase due to eddy heat transport = 117.3

We must remain aware of the many factors neglected in the above computations when drawing conclusions concerning the results, e.g. the strong temperature dependence of radiational heating. However, it appears that the horizontal eddy processes provide more than enough heat transport to account for the warming over the pole. We have, of course, seen some indication of this same result in the form of our previously computed negative values of $[\bar{\omega}]$ at high latitudes in April.

E. The zonal kinetic energy budget

Figures 6a through 6d are monthly meridional cross sections, July excluded, of rates of conversion from transient and standing eddy kinetic energy to mean zonal kinetic energy. (Upper and lower diagrams in the figures show transient and standing eddy conversions respectively). Conversion rates were computed by finite difference approximations of (see equation 4.13)

$$\int_{1cm} [\overline{u'v'}] \cos\varphi \frac{\partial}{\partial\varphi} \frac{[\bar{u}]}{a\cos\varphi} \frac{dp}{g}$$

and

$$\int_{1cm} [\bar{u}^* \bar{v}^*] \cos\varphi \frac{\partial}{\partial\varphi} \frac{[\bar{u}]}{a\cos\varphi} \frac{dp}{g}$$

where $\int_{1cm} \frac{dp}{g}$ was approximated by the standard density at each level. Units are zonal mean rates of energy conversion per unit volume.

As in our previous discussions of eddy momentum and eddy heat transports, we will briefly review the main features of the meridional distribution of the energy conversion rates. We will then consider the volume integrals of these conversion rates for three polar caps bounded by the 100, 50, 30 and 10 mb surfaces and by a vertical surface at 20° north latitude. We will also consider the relationship between these integrals and the other terms in the zonal kinetic energy equation.

The main monthly features of the meridional distributions of the kinetic energy conversions are as follows:

(1) January, Fig. 6a: Considering first the upper diagram in Fig. 6a, we see that the transient eddies provide kinetic energy to the mean zonal flow throughout most of the region. Maximum energy conversions occur near the axes of the main zonal wind systems, i.e. the polar vortex and the tropospheric jet. There is a tendency for the transient eddies to extract kinetic energy from the mean motion in an area to the north of the tropospheric jet extension at 100 mb due to a momentum flux out of the region of maximum angular rotation. South of the jet the zonal flow gains kinetic energy from the transient eddies. Small negative transient eddy conversion rates occur at 100, 50, and 30 mb at high latitudes.

Considering the kinetic energy exchanges between the standing eddies and the mean zonal motion during January, we find that south of 50° the meridional distribution of the standing eddy exchanges is quite similar to that of the transient eddy counterpart. However, north of this latitude the standing eddy conversion process shows a reversal in sign, with eddy kinetic energy increasing at the expense of the kinetic energy of the mean zonal flow. This is caused by the large southward standing eddy transports of momentum down the gradient of mean zonal rotation in this region. We may gain some insight into why these negative values occur by observing Fig. 10, a zonal cross section at 60° north latitude of the January grid point values of $\overline{u}^{*}\overline{v}^{*}$. We see

that the largest negative values occur near 160° east and 80° west longitude. They are a consequence of the asymmetric nature of the polar vortex caused by the particular mean January location of a semipermanent ridge of high pressure over the northern pacific (see Staff, Upper Air Branch NMC, 1967). This ridge is a common feature of the winter stratosphere which has been discussed by Hare (1960), Boville (1960), Wilson and Godson (1963) and Sawyer (1964). As a result of the location of this ridge, air moving northward on the eastern side of a broad, semipermanent trough over northern Asia has a deficit of zonal momentum with respect to the zonal mean, while southward moving air on the eastern side of the ridge has an excess of zonal momentum with respect to the zonal mean. A net transport of momentum out of the polar vortex results, and standing eddy kinetic energy is produced at the expense of zonal kinetic energy.

(2) March, Fig. 6b: Again we will confine our attention initially to the transient eddy part of the kinetic energy conversion process. We find little change in the general spatial distribution since January. Positive values, somewhat smaller than those observed in mid-winter, are found at all levels in the upper middle latitudes. Largest values still occur at 10 mb where the large positive gradients of angular rotation to the south of the polar vortex coincide with large positive values of $[\overline{u'v'}]$. The transient eddies still gain kinetic energy from the mean flow in the area immediately to the north of the tropospheric jet extension at 100 mb, while an area of negative conversion also appears

near the pole at all levels due to southward momentum transport in these regions.

Looking now at the standing eddy part of the kinetic energy conversions for March, we see that the large area of negative values which was present at high latitudes in January has disappeared, and positive values predominate at all levels above and including 50 mb. This large change in the character of the standing eddy kinetic energy conversion process appears to be a response to a mean westward shift of the Northern Pacific Ridge. It has moved from its January position over the Aleutians to a March location near the Kamchatka Peninsula. This results in an increase in the pressure gradient to the east of the trough over Asia, and the large negative spatial covariances which occurred in this area in January have given way to positive values. Similarly, a decrease in the gradient to the west of a semipermanent trough over North America where negative covariances occurred in January now gives positive values of $\overline{u}^{*}\overline{v}^{*}$. We surmise that the position of the Northern Pacific Ridge, the so-called "Aleutian High", has a large influence on the energetics of the lower and middle stratosphere.

(3) April, Fig. 6c: Kinetic energy exchanges between the transient eddies and the mean zonal flow have decreased to insignificant values in a region above 50 mb and south of 45^{o} latitude. North of 45^{o} at 30 mb and above there is an area where the vestigal polar-night jet still receives kinetic energy from the transient eddies. At 100 mb two areas of negative values of transient eddy conversions are in

evidence. One, located at 35°, is caused by momentum transport out of the region of maximum westerly flow in the tropospheric jet, while another, in subpolar latitudes, is caused by southward eddy momentum transport down the angular momentum gradient of the receding polar vortex.

The standing eddy part of the kinetic energy exchange process in April is too small to be worthy of note except at 100 mb. At this level there is an area in middle latitudes where the standing eddies are gaining kinetic energy from the weakening polar vortex. The reverse process is occurring in the region of the tropospheric jet extension.

(4) October, Fig. 6d: We see in Fig. 6d that in general, kinetic energy is being transferred from both the transient and standing eddies into the accelerating zonal circulation systems of the autumn stratosphere.

A summary of the general character of the monthly exchange processes throughout the year between the eddy and zonal forms of kinetic energy is provided by Tables 20, 21, and 22. Here we have tabulated terms from equation (4.13) which were evaluated for our three stratospheric regions of interest. The evaluated terms are: the volume integrals of the conversion terms described above, i.e. the horizontal eddy parts of $C(K_E, K_Z)$; the seasonal correction term, $S(K_Z)$; the horizontal parts of the eddy work term, $W_e(K_Z)$, and the term representing the conversion from zonal available potential energy to zonal kinetic energy, $C(A_Z, K_Z)$. Values of $C(A_Z, K_Z)$ were computed for January, April and July only, since these were the only months for which values of $[\overline{\omega}]$ were available.

Values of this term may also be inferred from balance requirements of zonal available potential energy. This method of obtaining $C(A_Z, K_Z)$ should give values which are approximately equal to those obtained by direct computation using our forced fields of $[\overline{\omega}]$; for essentially, both methods of calculation are based upon a forced balance between dominant terms in different forms of the zonally averaged energy equation. Values of $C(A_Z, K_Z)$ obtained by both methods are included in the tables, their similarity indicating the internal consistency of our set of equations.

Additional quantities which we have included in Table 20, 21 and 22 are: the sum of the horizontal eddy parts of $C(K_E, K_Z)$ and the horizontal part of the boundary work term, $W_e(K_Z)$; the monthly mean zonal kinetic energy, K_Z ; the monthly mean eddy kinetic energies, $K_{Et.e.}$ and $K_{Es.e.}$, and the deficits in the rates of production of mean zonal kinetic energy. The deficits represent the sum of the terms in equation (4.13) which we were unable to evaluate. The reader is referred to Section IV for a description of these terms and the processes which they represent. The term $C(A_Z, K_Z)$ is included in these processes, since it was not included in the calculation of the deficits. We note the following features of the evaluated terms in the zonal kinetic energy equation for each of the three polar caps considered.

(1) Table 20, 100 to 50 mb layer: Values of the seasonal correction term, $S(K_Z)$, effectively portray the seasonal changes in the circulation regimes of the lower levels of the 1965 stratosphere.

Comparing these values to the changes in $[\bar{u}]$ shown by Figs. 2a through 2e we find the following compatible relationships. The largest negative values of $S(K_Z)$ occur during the March and April breakdown of the polar vortex. (We have seen previously that the vortex extended well into this lower layer of the stratosphere in 1965). Positive values of $S(K_Z)$ occur during the June period of the establishment of the summer polar anticyclone. (This major zonal circulation system also extended well below 50 mb in this particular year). Negative values of $S(K_Z)$ again occur as the anticyclone recedes in the late summer, and large positive seasonal corrections appear during the rapid acceleration of both the tropospheric jet and the polar vortex in the fall.

A large amount of month to month irregularity appears in the 100 to 50 mb volume integrals of the horizontal eddy conversion terms, $C(K_E,K_Z)_{t.e.}$ and $C(K_E,K_Z)_{s.e.}$. We saw some indication of this sporadic behavior in our discussion of the meridional distributions of these quantities. We find similar irregularities in the horizontal parts of the boundary work term, $W_e(K_Z)$. However, the sum of the eddy conversions within the volume and the eddy stresses at the boundary shows a large amount of month to month regularity. Thus, it appears that these terms represent conjunctional processes which work to provide a temporally consistent source of zonal kinetic energy to the volume. In general, this source of energy is a maximum during the fall and early winter months when the zonal kinetic energy is increasing; it decreases during the spring deceleration of the zonal flow and reaches a minimum

during the late summer.

We see from the deficits that in the 100 to 50 mb layer the eddies provide sufficient energy to account for seasonal changes. However, when major kinetic energy sinks are considered, e.g. our approximated values of the term $C(A_Z, K_Z)$, we find a requirement for additional sources of kinetic energy.

(2) Table 21, 50 to 30 mb layer: In this layer we find the same compatibility between the seasonal correction term and the temporal changes in the zonal circulation which we observed in the 100 to 50 mb layer. The positive values of $S(K_Z)$ during the summer formation of the polar anticyclone are somewhat larger than those in the 100 to 50 mb layer, as one would expect due to the stronger easterly circulation in the 50 to 30 mb layer during the summer. Values of $S(K_Z)$ are generally small during other months, thus reflecting the relative quiescent nature of this layer of the stratosphere during the winter.

It is difficult to reconcile the sums of the terms representing the horizontal eddy kinetic energy exchange processes in this layer with the seasonal trend term. However, we see from the deficits that in general the eddy processes provide sufficient energy to offset the seasonal changes. Notable exceptions are shown by the positive deficits in May and June. These positive values suggest that the summer polar anticyclone receives its energy from sources other than eddy processes.

We still find at these higher levels, as in the 100 to 50 mb layer, that if we consider the energy sinks which must be present, e.g. $C(A_Z,K_Z)$, then the horizontal eddies do not provide sufficient energy to balance the zonal kinetic energy budget.

(3) Table 22, 30 to 10 mb layer: In this layer we still find that the seasonal correction term reflects the changes in the mean zonal flow which take place during the year. Values of $S(K_Z)$ have increased over those found in the 50 to 30 mb layer indicating the increase in the zonal circulation with height. During the spring and early summer the internal kinetic energy conversion processes and the boundary stresses show a conjunctional relationship somewhat similar to that found in the 100 to 50 mb layer, i.e. sporadic values combine to give a net production of zonal kinetic energy. In the winter this production generally continues but is supplied by the horizontal eddy processes within the volume which are much larger than the effects of boundary stresses and dominate the sum of the terms $C(K_E,K_Z)$ and $W_e(K_Z)$.

The negative conversion values which occur in December are a result of warming over the pole which took place between November and December (see Table 2) and caused an equatorward movement of the polar vortex. The eddy momentum transports in this layer were poleward in middle latitudes during December resulting in momentum flux down the gradient of angular rotation.

The deficits which result from the evaluated terms between 30 and 10 mb show similarity to those in the 50 to 30 mb layer, i.e.

there is sufficient kinetic energy production by the horizontal eddies to balance the seasonal changes except in the summer months during the acceleration of the polar anticyclone. Our estimates of $C(A_Z, K_Z)$ at this level indicate that in general we need additional energy sources in order to provide a zonal kinetic energy balance.

In Table 23 we have compared three month averages of our values for terms in the zonal kinetic energy equation for the 100 to 30 mb layer with values computed by Oort (1963). Oort's values are based upon three month means of IGY data for the entire northern hemisphere, and as such, are not directly comparable to our values. However, the two sets of calculations are similar enough to give some measure of the reliability of our results. We see a large disparity between the present values and Oort's values of $C(K_E, K_Z)$ and $W_e(K_Z)$. However, the sums of the terms are not unreasonably dissimilar when one considers the differences in the methods of computation. This indicates that the location of the latitude boundary has a large effect on the relative magnitudes of these terms. In all cases our present values of the sums are the smallest, as one would expect in view of the smaller volume considered. Other terms in Table 23 are in reasonable agreement.

In summarizing the effects of the horizontal eddies on the kinetic energy balances of the three layers, we find that in general, the horizontal eddies provide a source of kinetic energy for the mean zonal motion. This source exists as a result of both boundary and internal stresses and is the most consistent from month to month in

the 100 to 50 mb and 30 to 10 mb layers. In the middle layer, 50 to 30 mb, the eddy source of kinetic energy tends to be small and somewhat sporadic. In the 100 to 50 mb layer the horizontal eddy source of energy is provided in about equal amounts by boundary and internal stresses. This is true throughout the year. In the higher layers the internal stresses provide the main source of energy during the winter, while boundary stresses become the most important in the summer. This change with season in the relative importance of the two energy sources is due to the large seasonal change in the circulation regimes in the higher levels, i.e. eddy activity is confined to high latitudes in the winter polar vortex, while in summer it appears at low latitudes on the periphery of the summer anticyclone.

Although the eddies provide kinetic energy to the mean zonal flow throughout most of the year, we find that if we consider terms in the zonal kinetic energy equation which represent energy sinks, e.g. $C(A_Z, K_Z)$ which we have approximated for representative months, then additional kinetic energy sources are required. Using our values of $[\bar{v}]$ and $[\bar{\omega}]$ we find that the advection terms, $A(K_Z)$, is generally quite small. Oort (1963) has found that the "vertical" eddy boundary stresses and the "vertical" eddy part of $C(K_E, K_Z)$ are generally small compared to other terms. Assuming that friction operates as a dissipative mechanism, the most likely source for the zonal kinetic energy deficit appears to be the pressure work term, $W_p(K_Z)$. However, any soundly based conclusions await the future calculation of more reliable values of $[\bar{\omega}]$, $[\bar{v}]$ and daily values of the "vertical" motion.

F. The zonal available potential energy budget

Figures 7a through 7e are monthly meridional cross sections of rates of conversions from eddy available potential energy to zonal available potential energy, where upper diagrams represent conversions due to transient eddies and lower diagrams represent conversions due to standing eddies. Conversion rates were computed from finite difference approximations of (see equation(4.15))

$$C_p \int_{1cm} \gamma \left[\overline{v'T'}\right] \frac{1}{a} \frac{\partial[\overline{T}]}{\partial \varphi} \frac{dP}{g}$$

and

$$C_p \int_{1cm} \gamma \left[\overline{v}^*\overline{T}^*\right] \frac{1}{a} \frac{\partial[\overline{T}]}{\partial \varphi} \frac{dP}{g}$$

where units are rates of zonal available potential energy production per unit volume. We again approximated $\int_{1cm} \frac{dP}{g}$ by the standard density at each level. We recall from our discussion of heat transport that eddy fluxes of sensible heat are predominately northward throughout the lower and middle stratosphere during the entire year. Thus, we see from the above integrals that the sign of the mean available potential energy conversion at a particular latitude depends upon the sign of the mean zonal temperature gradient at that latitude.

This particular fact should be kept in mind in the following discussion of causative processes.

The monthly cross sections of values computed from the above integrals allow us to make the following remarks concerning the monthly meridional distributions of zonal available potential energy conversion rates.

(1) January, Fig. 7a: In January the distribution of zonal available potential energy conversions by transient eddies bears strong resemblance to the distribution of conversions by the standing eddies. This is due to the similarity which we saw earlier between the two types of eddy heat transport. Zonal available potential energy is destroyed by both transient and standing eddies in a region above and poleward of a line which coincides with the delineation of the reversal in the horizontal temperature gradient. Maximum destruction rates occur at all levels between 60° and 65° north, with largest negative values at 100 mb. The standing eddy contribution to these negative values is about twice as large as the contribution due to the transient eddies. Positive conversion rates occur below and equatorward of the locus of the horizontal temperature gradient reversal, i.e. in the region of forced motion with countergradient heat flux in the lower winter stratosphere. Largest positive conversion rates by both types of eddies are found at 100 mb between 40° and 45°. Standing eddies give a somewhat larger contribution than transient eddies in this region.

(2) March, Fig. 7b: We again find a great deal of similarity in the distribution of the transient and standing eddy conversions. These distributions have not changed appreciably from January, although magnitudes of the two conversion processes have become approximately equal. The forced region of positive conversions is still found in the lower middle and subtropical latitudes at low levels with an upper boundary between 30 and 10 mb. The region of maximum standing eddy activity has moved slightly northward in response to a poleward shift of the maximum temperature gradient.

(3) April, Fig. 7c: The similarity in the distribution of both types of eddy conversion persists. However, there has been a dramatic change in the distributions since March. The areas of negative conversion rates have virtually disappeared, and the eddies are now creating zonal available potential energy throughout most of the stratosphere. This large change is caused by warming over the pole and the consequent reversal of the horizontal gradient of $[\overline{T}]$ at high latitudes. The result is a countergradient heat flux throughout most of the stratosphere.

(4) July, Fig. 7d: Conversion rates by both transient and standing eddies above 50 mb are small and insignificant. Between 100 and 50 mb there is a broad region through middle latitudes where both the transient and standing eddies transport heat against the temperature gradient to increase the zonal available potential energy.

(5) October, Fig. 7e: The available potential energy conversions have returned to a meridional distribution somewhat similar to that found in January and March. This is of course due to a return of the stratospheric temperature regime to a "typical" winter distribution. The eddies continue to move heat energy poleward resulting in a countergradient heat flux below 30 mb in middle and subtropical latitudes. Zonal available potential energy is still being created in this region of forced motion, however, all other regions now show decreases in zonal available potential energy as a result of eddy fluxes of heat down the temperature gradient.

Tables 23, 24, and 25 provide a synthesis of the foregoing meridional distributions of available potential energy conversions in the form of volume integrals over our three polar caps of interest, i.e. volumes bounded by the 20^{o} latitude surface and the 100, 50, 30 and 10 mb surfaces. These volume integrals are the horizontal components of $C(A_E, A_Z)$ in equation (4.15). Other terms in the zonal available potential energy equation which we evaluated and included in the table are: the seasonal correction, $S(A_Z)$; the generation term, $G(A_Z)$, and the term representing the conversion of zonal available potential energy to zonal kinetic energy, $C(A_Z, K_Z)$. $G(A_Z)$ was computed from the heating rates of Kennedy (1964) for the months of January, April and July. The tables show the results of the two different methods for evaluating $C(A_Z, K_Z)$ which were discussed previously in connection with the zonal kinetic energy equation.

Tables 24, 25 and 26 also contain values of the mean monthly zonal available potential energy and an approximation to A_E, the eddy available potential energy. Our approximation to A_E is given by

$$\frac{1}{2} C_p \int \gamma \left[\overline{T}^{*2}\right] \, dm .$$

This approximation includes only the effects of the variance of monthly mean temperatures on an isobaric surface, and as such, gives somewhat smaller values than an evaluation of the entire expression for A_E which would include the mean monthly effects of the zonal variances of all daily values of temperature (see Section IV).

The values given in Tables 24, 25 and 26 show the following features concerning the changes of the zonal available potential energy and the processes by which they are effected.

(1) Table 24, 100 to 50 mb layer: The seasonal correction term shows monthly increases in zonal available potential energy during the late winter and spring as a consequence of the increases in temperature variance during this period (see Figs. 3a, 3b, 3c). The horizontal parts of the eddy conversion term show large negative values during January and February. In March their sum is negative. This indicates that the layer, when considered in its entirety, does not appear to be a forced region during these months. The driven region south of 50°N is offset in the integrals by a region north of 50°N in which zonal availble potential energy is being

transformed to eddy available potential energy. But the integrals do not include a contribution from the zone between 20°N and the equator. The present finding, ostensibly opposite to previous work, illustrates the necessity for considering the stratosphere in separate meridional sections, thereby allowing one to delineate the boundaries where important physical processes change character. The generation term for the 100 to 50 mb layer shows a destruction of zonal available potential energy for the three months in which it was computed.

(2) Table 25, 50 to 30 mb layer: The seasonal correction term in this layer is comparatively small and, as in the case of its counterpart in the zonal kinetic energy equation, reflects the relatively inactive nature of this part of the stratosphere. The horizontal eddy conversion terms decrease the zonal available potential energy during early fall and winter in this layer and increase it during the remainder of the year. Values of the generation term show continued destruction of zonal available potential energy during all seasons.

(3) Table 26, 30 to 10 mb layer: Values of the seasonal corrections have magnitudes which are comparable to those found in the 100 to 50 mb layer, although they show little similarity in other respects. They have a coherent pattern in sign which may be associated with changes in the mean zonal temperature variance observed in Figs. 3a through 3e. Large negative zonal available potential energy conversion rates by both the standing and transient eddies occur in this layer during the early winter months and decrease markedly during the late winter and spring,

e.g. a reduction by almost two orders of magnitude occurs in the standing eddy conversions between January and July. The sum of the eddy conversion rates is positive from April to August and returns again to large negative values by mid-winter. Values of the generation term are positive during January, indicating that a self-contained energy source exists in the middle stratosphere during the winter. Similar results have been found by Newell (1963) and Kennedy (1964). However, as shown by our negative values of $G(A_Z)$ in April and July, this energy source does not exist in the middle stratosphere throughout the year.

In Table 27 we have made a comparison between values given by Oort (1963) and our present values for terms in the zonal available potential energy equation for the 100 to 30 mb layer. We made a similar comparison in the case of the zonal kinetic energy budget in which we described differences between Oort's and our methods of calculation. Similar remarks apply here. We see from Table 27 that our values compare favorably with Oort's in some cases, however, large differences occur in the case of horizontal eddy conversion terms in the January through March period. The terms are of large magnitude but of opposite sign, a dissimilarity which probably is due to the difference in the latitude boundaries used in the two calculations. We know that positive values of this term result from eddy motions which force heat against the gradient. From our January and March cross sections of horizontal eddy conversion rates (Figs. 7a and 7b) we may infer that by taking a boundary at 20^{o} we have neglected a large region where this forcing takes place.

This further accents the point made earlier that it is necessary to consider meridional distributions of eddy processes in the stratosphere in order to obtain a true picture of the energetics of this region of the atmosphere.

In summarizing the zonal available potential energy balance for the stratosphere we find a large seasonal and month to month variation in the processes by which this balance is effected. This variation is largely dependent upon the temperature gradient, since the horizontal eddy transport of heat is predominantly poleward. The forced region where heat is transferred against the gradient is confined to the lower stratosphere and latitudes south of 50^{o} during the early winter but includes the entire lower stratosphere plus part of the middle stratosphere after the breakdown of the polar vortex.

We find that the lower stratosphere acts as a refrigerated region in the sense that it loses zonal available potential energy by radiation throughout the year. However, this energy is not supplied by horizontal eddy processes in all regions and all seasons; particularly, during the winter at high latitudes these eddy processes act as a sink for zonal available potential energy. Consequently, there exists a requirement for a large source of zonal available potential energy in this region during the winter season. During the summer months in the lower stratosphere the horizontal eddies act as a source of zonal available potential energy, however, seasonal changes and large radiational destruction rates offset this source, and large deficits still result. Approximations of

the term $C(A_Z,K_Z)$ which result from balancing this deficit correspond well to values of the same term obtained from direct calculations using our values of $[\bar{\omega}]$. We conclude tentatively that this term is a major source of zonal available potential energy.

The middle stratosphere resembles the tropospheric heat engine during the winter. It has a self-contained source of zonal available potential energy due to radiational processes, and the horizontal eddies convert this zonal available potential energy into eddy available potential energy. One may assume that this eddy potential energy is eventually converted into the kinetic energy of the mean zonal flow, however, we cannot draw definite conclusions until an investigation of the processes which effect this change can be made. This investigation awaits the calculation of daily values of ω . The conversion of zonal available potential energy into eddy available potential energy by the horizontal eddies during the winter is much larger than the generation of zonal available potential energy by radiation, and large deficits occur. Approximations of the term, $C(A_Z,K_Z)$, obtained from balancing these deficits in the zonal available potential energy equation for the middle stratosphere agree well with results obtained from what we consider to be reasonably accurate values of $[\bar{\omega}]$. During the summer the middle stratosphere acts as a refrigerated region with zonal available potential energy being destroyed by radiation. The horizontal eddies act as a source for the zonal available potential energy by driving heat against the temperature gradient.

VIII. SUMMARY AND CONCLUSIONS

A statistical analysis of daily hemispheric maps of stratospheric temperature and geopotential has been made in this study to determine the influence of large-scale horizontal eddy processes on the zonal momentum and energy budgets. An entire year of data was examined, on a monthly basis, in order to compare the month to month changes in the basic parameters with the changes that would be expected from the action of the large-scale horizontal eddy processes. Much of the previous work has dealt with long term seasonal averages or specific cases. This work was intended to be complimentary and to represent a first step in the establishment of a monthly climatology of the momentum and energy budgets. As we were attempting to account for changes, most of our attention was focussed on the spring breakdown of the polar vortex and its reestablishment in the fall, but diagnostic studies of the January and July months were also made. Our findings and the conclusions derived therefrom are summarized as follows.

(1) Horizontal eddy momentum transports and the zonal angular momentum budget. The statistical parameters which represent zonal angular momentum and its horizontal eddy transport displayed monthly variations during 1965 which would obviously be blurred by seasonal averaging. This variation indicates the value in calculating these parameters over carefully selected time periods. Whether periods of one month are suitable or not is a moot point, however, our findings certainly indicate that monthly averages give meaningful results and

provide a more detailed representation of the processes which we are trying to describe than do seasonal means. In both the middle and lower stratosphere we found that the spatial distribution of horizontal eddy momentum transports display a month to month variation which coincides closely with changes in the zonal circulation. This does not mean that in all cases we found the eddy processes operating as one might presuppose, i.e. they did not always work as a driving mechanism for the mean zonal circulation. A contrary case in point was found to occur in the lower stratosphere during the winter and spring months when eddy momentum convergence took place north of the region of maximum angular rotation with no apparent mean zonal acceleration. However, our object in this study was not to substantiate presuppositions. Our intent was to establish the relationship between the horizontal eddy momentum transports and the mean zonal circulations in order to facilitate future investigations of how the horizontal eddies and all other dynamic and thermodynamic processes work together to produce major physical changes.

The results of our monthly evaluation of eddy momentum transports and their relationship to the major zonal circulation regimes have been described in detail previously. We briefly reitterate our findings here. First the horizontal eddies provided momentum to the polar-night jet at all levels. The eddy activity decreased with the breakdown of the vortex in the spring and increased with its reestablishment in the fall, however, it cannot be concluded from our findings

whether the breakdown and reestablishment were a cause or a result of changes in the eddy momentum fluxes. Secondly, the horizontal eddy momentum transports apparently had little effect on the polar anticyclone which was found at 50 mb and above in the 1965 summer stratosphere. Thirdly, in the case of the upward extension of the tropospheric jet, the eddies tended to transport momentum out of the region of maximum zonal motion during the winter and spring, while during the summer and fall they transported momentum into the region of maximum zonal flow.

(2) Eddy heat transports. We found that eddy heat fluxes vary from month to month in a manner not unlike their angular momentum counterparts. Thus, there is also much to be gained from viewing these fluxes and the processes in which they are involved, over a time scale shorter than a season. As a result of our eddy heat transport calculations, we found that the eddy heat fluxes are compatible with either the mean zonal distribution of temperature changes or manifestations of these temperature changes in the form of physically plausable mean "vertical" motions. Our most significant finding in regard to eddy heat flux was the fact that the magnitude of the horizontal eddy heat transport into the polar region was sufficient to account for the rapid warming which took place during March and April.

(3) Effects of horizontal eddies on the zonal kinetic energy budget. As in the case of eddy momentum and eddy heat transports, we found that a carefully selected time scale is also essential to

a proper description of the zonal kinetic energy budget of the stratosphere. This fact may of course be inferred from the dependence of kinetic energy exchange on horizontal eddy momentum fluxes and the mean zonal circulation. Our results indicate that in most months and regions the eddies acted as a source of zonal kinetic energy. Exceptions were mostly confined to small values of energy sinks which occurred during the mid-summer months in the 50 to 30 mb layer. A more notable exception was the large zonal kinetic energy sink found in the 30 to 10 mb layer in December. We found that although the eddies provide a source of zonal kinetic energy, this source is usually not sufficient to balance the energy sink resulting from a conversion of zonal kinetic energy into zonal available potential energy. We have concluded tentatively that the most likely additional source of zonal kinetic energy needed to achieve the required balance is the pressure work term at the boundaries of the region. However, this cannot be firmly established until daily "vertical" motion fields are computed.

(4) Effects of horizontal eddies on the zonal available potential energy budget. We found that processes which affect the zonal available potential energy budget are also best viewed within a time scale shorter than a season. As in the case of zonal kinetic energy, this fact may be inferred from the monthly variations in the parameters upon which zonal available potential energy and its conversions depend, e.g. spatial temperature variances and horizontal eddy heat transports. Our results concerning the zonal available potential energy budget of the 1965

stratosphere may be summarized as follows. The lower stratosphere operated as a refrigerated region during 1965. It lost zonal available potential energy by radiation, and this energy was resupplied by mechanical means. The horizontal eddies were a significant source of supply only in certain regions and certain months; and therefore provided only a part of the required zonal available potential energy. Conversion of zonal kinetic energy to zonal available potential energy apparently provided the remainder. This is based upon an assumption that conversions of zonal available potential energy by "vertical" eddy processes are small. One cannot fully substantiate this assumption until daily "vertical" motion fields are computed.

The middle stratosphere acted as a refrigerated region during the 1965 summer. However, during the winter it had characteristics commonly displayed by the tropospheric heat engine, i.e. it had a self contained source of zonal available potential energy which was converted to eddy available potential energy. We are left in doubt concerning the ultimate disposition of this energy, although we assume that it was eventually converted into the kinetic energy of the mean zonal flow. However, we again find that daily "vertical" motion fields are required before this assumption can be verified.

This study has by no means provided a complete explanation of the circulation of the 1965 stratosphere. Although it answered many questions it asked many more which will require further investigation. For example, how were complete balances of mass, momentum, heat and

energy achieved in the 1965 stratosphere. An answer to this question should be of immediate concern. An approximate answer may be obtained through the following sequence of investigations. (1) A resolution of our tentative forced mean "vertical" and mean meridional motions into accord with mass conservation and radiational heating, (2) a computation of daily "vertical" motion fields, (3) a subsequent calculation of complete monthly momentum, heat and energy budgets for the three stratospheric regions considered in this study. A more difficult question, but one which is by no means less intriguing, concerns the effects of the zonal distribution of significant statistical parameters on the momentum, heat and energy budgets. The reasons for these distributions is an ultimate question which should be answered. The answers to the foregoing questions will improve our ability to explain the behavior of the lower and middle stratosphere, and hopefully, they will also enable us to fortell this behavior and its cause or effect in adjacent layers of the atmosphere.

Table 1
Monthly Values of Mean Zonal Wind $[\overline{u}]$, for 1965

		JANUARY, 1965				FEBRUARY				MARCH			
	p(mb)	100	50	30	10	100	50	30	10	100	50	30	10
Lat.	85	5.0	8.7	12.1	16.3	3.5	7.9	10.4	13.5	6.9	9.4	10.8	12.7
	80	8.9	15.1	20.5	27.9	6.7	13.7	18.0	23.4	11.8	15.9	18.2	21.0
	75	12.3	19.7	26.4	36.3	10.1	18.4	23.8	30.8	15.2	19.7	22.4	25.7
	70	15.0	23.0	30.0	41.7	13.1	21.9	27.6	35.4	16.2	20.3	23.0	26.8
	65	16.6	24.8	31.2	43.8	15.1	23.3	28.4	36.4	14.6	17.9	20.3	24.3
	60	17.6	24.8	30.3	42.5	16.2	22.3	26.4	34.0	12.4	14.7	16.4	19.7
	55	18.6	23.1	27.0	37.8	16.5	19.8	22.4	28.6	11.5	12.3	12.8	14.7
	50	19.5	19.5	20.9	29.9	16.4	16.0	16.8	21.2	12.3	10.3	9.2	10.0
	45	20.5	14.9	13.9	20.8	17.5	12.1	11.0	13.8	14.9	8.6	5.9	5.9
	40	22.5	11.3	8.8	13.9	20.7	9.5	6.9	9.1	19.2	7.6	3.8	3.4
	35	24.4	9.0	5.9	10.8	24.5	8.1	4.8	7.7	23.6	7.1	3.0	3.0
	30	25.1	7.2	4.3	10.0	26.7	7.1	3.9	8.1	25.9	6.2	2.5	3.4
	25	23.0	5.4	3.2	8.1	25.7	6.8	3.6	7.4	24.6	5.0	1.3	2.1
	20	17.7	3.3	2.0	3.6	21.7	6.9	3.5	4.0	20.8	4.0	-.4	-1.5
		APRIL				MAY				JUNE			
	85	3.6	5.4	5.1	3.5	.9	-.8	-2.0	-2.7	.1	-.9	-1.3	-2.2
	80	6.5	8.8	8.3	5.4	1.3	-1.3	-3.1	-4.8	.0	-1.6	-2.5	-4.2
	75	9.1	10.5	9.5	5.7	1.7	-1.3	-3.4	-6.2	.2	-2.3	-3.8	-6.3
	70	10.7	10.7	9.0	4.7	2.5	-.9	-3.2	-6.8	.6	-2.8	-5.0	-8.2
	65	10.8	9.3	7.2	3.0	3.6	-.1	-2.6	-6.3	1.5	-2.9	-5.7	-9.5
	60	10.1	7.4	5.1	1.5	5.1	.7	-1.9	-5.3	2.8	-2.6	-5.9	-10.0
	55	9.5	5.7	3.3	.7	6.8	1.3	-1.5	-4.6	4.4	-2.3	-6.0	-10.2
	50	9.4	4.0	1.5	.6	8.4	1.4	-1.7	-4.1	6.5	-2.0	-5.9	-10.1
	45	10.6	2.7	.0	1.0	9.9	.7	-2.3	-3.6	8.9	-2.1	-5.9	-10.0
	40	13.4	2.3	-.6	1.9	11.9	-.1	-3.2	-3.1	10.8	-2.8	-6.5	-10.4
	35	17.2	2.7	-.4	2.5	13.6	-.7	-4.0	-3.1	10.6	-4.5	-8.4	-12.0
	30	20.2	2.8	-.3	1.6	13.8	-1.6	-5.2	-4.6	7.7	-7.3	-11.7	-15.3
	25	20.6	1.9	-1.1	-1.4	12.3	-3.0	-7.0	-8.5	2.7	-12.5	-17.1	-21.7
	20	18.4	.3	-2.9	-6.3	10.1	-4.6	-9.4	-13.9	-2.8	-20.5	-24.6	-31.2

Table 1 (con't)
Monthly Values of Mean Zonal Wind, $[\bar{u}]$, for 1965

		JULY				AUGUST				SEPTEMBER			
	p(mb)	100	50	30	10	100	50	30	10	100	50	30	10
Lat.	85	.2	-.9	-1.4	-1.6	-.3	-.5	-.6	-1.0	.9	1.1	1.4	2.7
	80	.1	-1.8	-2.7	-3.2	-.2	-.9	-1.2	-1.8	2.0	2.1	2.5	4.6
	75	-.2	-2.7	-4.0	-5.2	.5	-1.0	-1.8	-2.4	3.3	3.2	3.6	6.0
	70	-.1	-3.3	-5.2	-7.1	1.9	-.8	-2.1	-2.9	4.8	4.1	4.3	7.0
	65	.8	-3.5	-5.9	-8.5	3.7	-.2	-2.1	-3.1	6.2	4.6	4.5	7.6
	60	2.4	-3.2	-6.2	-9.5	6.0	.7	-1.8	-3.3	7.7	4.9	4.4	7.8
	55	4.8	-2.8	-6.4	-10.5	8.4	1.3	-1.8	-4.2	9.4	5.0	4.1	7.1
	50	7.3	-2.6	-6.6	-11.6	10.2	1.0	-2.4	-5.6	11.3	4.7	3.5	5.4
	45	8.8	-3.3	-7.3	-12.6	10.3	-.6	-3.8	-7.4	12.6	3.8	2.1	2.9
	40	8.2	-4.9	-8.9	-14.2	8.3	-3.2	-6.3	-10.0	12.8	2.0	-.1	-.3
	35	5.0	-7.2	-11.4	-16.4	4.5	-6.3	-9.7	-13.2	10.6	-1.0	-3.6	-4.6
	30	-.1	-10.7	-15.2	-19.9	-.3	-10.0	-13.7	-16.9	6.1	-5.0	-8.2	-9.7
	25	-5.5	-16.4	-21.0	-26.2	-5.4	-14.8	-18.7	-22.0	.7	-9.6	-13.3	-15.7
	20	-10.6	-24.9	-28.9	-36.0	-10.0	-21.1	-25.0	-29.2	-4.8	-14.5	-18.9	-23.1

	OCTOBER				NOVEMBER				DECEMBER			
85	2.7	3.9	5.2	7.7	-.9	-.1	1.2	4.1	1.9	1.2	1.0	1.0
80	5.5	7.3	9.3	13.8	-.8	.8	2.7	8.4	3.5	2.4	2.1	2.3
75	8.5	10.4	12.7	18.6	.5	2.8	5.0	13.4	5.1	3.8	3.2	3.6
70	11.1	12.5	14.8	21.9	2.9	5.7	8.1	18.0	6.7	5.4	4.6	4.9
65	12.8	13.3	15.3	22.7	6.3	8.7	11.4	21.1	8.6	7.3	6.5	6.5
60	14.0	12.9	14.4	21.6	10.3	11.9	14.5	23.0	11.2	9.6	8.7	9.1
55	15.1	12.2	12.9	19.7	14.6	14.9	17.0	24.4	14.6	12.4	11.2	12.9
50	16.0	11.2	11.0	16.9	18.6	16.3	17.6	25.2	18.4	14.6	13.1	17.1
45	16.4	9.4	8.6	13.5	21.5	15.9	16.2	24.7	22.2	15.7	14.1	20.3
40	16.1	7.2	6.3	10.0	23.2	14.0	13.7	22.1	25.3	15.8	14.2	21.9
35	14.5	4.5	3.7	6.4	23.3	11.0	10.3	17.5	26.7	14.1	13.4	22.3
30	12.0	1.3	.1	2.5	21.5	7.3	6.3	12.1	25.8	11.0	11.7	22.0
25	8.8	-2.3	-4.1	-2.4	17.9	3.6	2.1	6.9	22.4	7.6	9.3	20.8
20	5.2	-6.2	-9.1	-8.9	13.6	.1	-1.9	1.8	17.8	4.9	6.5	18.9

Table 4

Monthly Values of Mean Temperature, $[\overline{T}]$, for 1965. Units: ^{o}C

Lat.	p(mb)	JANUARY 100	50	30	10	FEBRUARY 100	50	30	10	MARCH 100	50	30	10
	85	-67.6	-73.9	-74.7	-69.1	-68.5	-72.3	-70.2	-57.9	-62.3	-61.5	-58.9	-48.8
	80	-66.8	-72.1	-72.7	-68.2	-67.3	-70.1	-68.2	-57.8	-61.1	-60.3	-58.0	-49.0
	75	-65.1	-69.5	-70.2	-66.3	-64.8	-67.0	-65.6	-57.1	-58.9	-58.5	-56.7	-49.0
	70	-62.7	-66.5	-67.2	-63.4	-62.0	-63.8	-62.9	-55.8	-57.0	-56.6	-55.3	-48.6
	65	-60.1	-63.1	-63.8	-60.0	-59.4	-60.8	-60.4	-54.0	-55.7	-55.1	-54.0	-47.9
	60	-57.7	-60.0	-60.6	-56.6	-57.0	-58.2	-58.2	-51.9	-54.8	-54.1	-53.0	-47.2
	55	-55.9	-57.6	-58.0	-53.7	-55.2	-56.3	-56.5	-49.9	-54.3	-53.5	-52.5	-46.5
	50	-55.5	-56.3	-56.1	-51.4	-54.6	-55.5	-55.3	-48.5	-54.3	-53.6	-52.5	-45.9
	45	-56.6	-56.6	-55.4	-49.4	-55.7	-55.9	-54.9	-47.5	-55.6	-54.6	-53.0	-45.2
	40	-59.3	-58.0	-55.5	-47.8	-58.6	-57.3	-55.1	-46.9	-58.4	-56.6	-53.9	-44.7
	35	-63.4	-59.8	-55.9	-46.4	-62.9	-59.3	-55.7	-46.3	-62.7	-58.8	-54.9	-44.5
	30	-67.9	-61.5	-55.9	-44.9	-67.9	-61.2	-56.0	-44.9	-67.7	-60.9	-55.3	-43.9
	25	-72.1	-62.7	-55.8	-43.6	-72.5	-62.8	-56.0	-43.7	-72.4	-62.6	-55.3	-43.2
	20	-75.3	-63.5	-55.6	-43.1	-75.9	-63.9	-56.1	-43.3	-75.8	-63.9	-55.5	-43.3
		APRIL				MAY				JUNE			
	85	-54.1	-49.9	-46.9	-39.1	-45.4	-43.5	-43.2	-35.2	-43.5	-41.0	-40.3	-31.2
	80	-52.8	-49.3	-47.1	-39.7	-45.5	-44.0	-43.6	-35.4	-43.7	-41.5	-40.9	-31.7
	75	-51.5	-48.8	-47.6	-40.7	-46.2	-44.9	-44.5	-35.9	-44.4	-42.4	-41.9	-32.3
	70	-50.7	-49.0	-48.4	-41.7	-47.3	-46.3	-45.7	-36.7	-45.7	-43.8	-43.1	-32.9
	65	-50.6	-49.8	-49.6	-42.9	-48.5	-47.8	-47.1	-37.6	-47.3	-45.5	-44.5	-33.8
	60	-51.2	-51.0	-50.7	-43.8	-49.9	-49.2	-48.4	-38.3	-49.0	-47.2	-45.7	-34.5
	55	-52.3	-52.2	-51.9	-44.1	-51.7	-50.7	-49.5	-38.8	-51.0	-49.0	-47.0	-34.9
	50	-54.1	-53.5	-52.7	-43.9	-54.0	-52.2	-50.4	-39.2	-53.6	-51.0	-48.2	-35.4
	45	-56.8	-55.0	-53.4	-43.2	-57.3	-53.9	-51.2	-39.2	-56.9	-53.1	-49.4	-36.2
	40	-60.0	-56.7	-53.9	-42.2	-61.3	-55.8	-51.8	-39.0	-61.3	-55.3	-50.4	-37.1
	35	-63.6	-58.5	-54.2	-41.3	-65.3	-57.6	-52.2	-38.8	-66.1	-57.3	-51.3	-37.8
	30	-67.6	-60.0	-54.1	-40.7	-69.1	-59.1	-52.4	-38.5	-70.1	-58.9	-51.9	-38.2
	25	-71.7	-61.4	-54.0	-40.5	-72.7	-60.4	-52.7	-38.3	-73.1	-60.2	-52.5	-38.4
	20	-75.0	-62.7	-54.3	-40.8	-75.6	-61.7	-53.4	-38.6	-74.8	-61.6	-53.5	-39.0

Monthly Values of Mean Temperature, $[\overline{T}]$, for 1965. Units: ^{o}C

Lat.	p(mb)	JULY 100	JULY 50	JULY 30	JULY 10	AUGUST 100	AUGUST 50	AUGUST 30	AUGUST 10	SEPTEMBER 100	SEPTEMBER 50	SEPTEMBER 30	SEPTEMBER 10
	85	-43.1	-41.3	-40.9	-31.3	-44.9	-43.9	-44.5	-35.3	-48.7	-50.6	-52.2	-46.6
	80	-43.7	-41.9	-41.4	-31.5	-45.3	-44.4	-44.8	-35.7	-48.9	-50.7	-52.1	-46.3
	75	-44.6	-42.7	-42.2	-31.9	-45.8	-45.1	-45.1	-36.0	-49.0	-50.9	-52.0	-45.9
	70	-45.7	-43.9	-43.2	-32.5	-46.4	-46.0	-45.8	-36.2	-49.3	-51.0	-51.9	-45.1
	65	-47.1	-45.2	-44.2	-33.0	-47.5	-47.1	-46.6	-36.3	-50.0	-51.3	-51.8	-44.1
	60	-48.8	-46.8	-45.2	-33.5	-49.3	-48.5	-47.5	-36.4	-51.2	-51.9	-51.7	-42.8
	55	-51.0	-48.7	-46.4	-34.1	-51.8	-50.1	-48.3	-36.6	-52.9	-52.6	-51.6	-41.6
	50	-54.1	-50.9	-47.7	-35.0	-54.9	-51.9	-49.0	-37.0	-55.3	-53.6	-51.5	-40.8
	45	-58.3	-53.2	-48.9	-36.0	-59.0	-53.8	-49.7	-37.6	-58.5	-54.7	-51.5	-40.5
	40	-62.9	-55.3	-50.0	-37.0	-63.2	-55.6	-50.4	-38.5	-62.4	-55.8	-51.6	-40.4
	35	-67.1	-57.0	-50.9	-37.9	-67.0	-57.0	-51.2	-39.2	-66.6	-57.1	-51.9	-40.5
	30	-69.9	-58.4	-51.5	-38.6	-69.7	-58.3	-51.8	-39.6	-70.2	-58.4	-52.3	-40.6
	25	-71.8	-59.6	-52.2	-39.0	-71.8	-59.4	-52.5	-39.8	-72.9	-59.6	-52.9	-40.6
	20	-73.7	-61.0	-53.3	-39.7	-73.5	-60.6	-53.2	-40.1	-74.9	-60.8	-53.6	-40.7

		OCTOBER				NOVEMBER				DECEMBER			
	85	-53.8	-59.2	-62.1	-58.8	-56.9	-63.3	-68.5	-68.3	-54.9	-57.3	-58.8	-59.5
	80	-53.7	-58.7	-61.3	-57.6	-57.2	-63.0	-68.2	-67.1	-54.6	-57.5	-59.0	-59.4
	75	-53.4	-57.8	-60.1	-56.0	-57.1	-62.3	-66.9	-64.9	-54.6	-57.6	-59.1	-59.2
	70	-53.0	-56.7	-58.6	-54.3	-56.6	-61.2	-64.4	-62.1	-54.7	-57.6	-59.0	-58.9
	65	-52.9	-55.9	-57.3	-52.4	-56.0	-60.0	-61.9	-59.3	-55.0	-57.7	-58.9	-58.4
	60	-53.4	-55.5	-56.3	-50.2	-55.6	-58.9	-60.2	-56.9	-55.5	-57.9	-59.4	-57.9
	55	-54.5	-55.6	-55.4	-48.0	-55.4	-58.2	-58.9	-54.9	-56.0	-58.2	-59.8	-57.3
	50	-56.4	-56.0	-54.7	-46.3	-56.1	-57.7	-57.7	-52.9	-56.8	-58.7	-59.5	-56.1
	45	-59.0	-56.7	-54.1	-44.9	-58.1	-58.0	-56.7	-50.7	-58.3	-59.6	-59.1	-53.6
	40	-62.3	-57.6	-53.8	-43.8	-61.3	-58.7	-55.9	-48.3	-61.0	-60.8	-59.1	-50.4
	35	-66.1	-58.5	-53.6	-43.3	-65.1	-59.8	-55.3	-46.6	-64.7	-62.1	-59.0	-48.1
	30	-69.8	-59.3	-53.5	-42.7	-69.2	-61.0	-55.0	-45.1	-68.9	-63.3	-58.2	-46.3
	25	-73.1	-60.1	-53.5	-42.0	-72.9	-62.2	-55.0	-43.7	-72.9	-63.9	-57.1	-44.6
	20	-75.5	-61.0	-53.8	-41.6	-75.9	-63.0	-55.2	-43.0	-76.1	-64.3	-56.3	-43.4

Table 5

Monthly Values of Mean Geopotential Height, $[\overline{H}]$, for 1965. Units: gpm

		JANUARY				FEBRUARY				MARCH			
	p(mb)	100	50	30	10	100	50	30	10	100	50	30	10
Lat.	85	15081	19149	22106	28603	15192	19266	22295	29042	15209	19492	22684	29706
	80	15140	19250	22246	28792	15234	19358	22415	29199	15289	19601	22810	29853
	75	15226	19394	22440	29058	15302	19489	22588	29423	15402	19751	22981	30048
	70	15336	19565	22667	29371	15395	19652	22795	29691	15532	19915	23167	30263
	65	15459	19752	22906	29705	15505	19830	23017	29972	15654	20066	23338	30464
	60	15584	19937	23135	30028	15622	20000	23222	30236	15751	20184	23472	30627
	55	15711	20108	23340	30314	15737	20149	23394	30460	15831	20277	23572	30746
	50	15837	20251	23501	30540	15845	20267	23525	30624	15906	20351	23645	30826
	45	15958	20354	23605	30693	15945	20351	23608	30728	15986	20407	23689	30872
	40	16077	20424	23664	30783	16050	20409	23654	30786	16080	20451	23713	30895
	35	16196	20474	23698	30840	16165	20453	23681	30824	16190	20488	23730	30909
	30	16309	20519	23719	30885	16282	20485	23699	30859	16304	20518	23742	30923
	25	16404	20533	23734	30923	16386	20511	23713	30892	16404	20540	23750	30937
	20	16469	20547	23742	30942	16461	20533	23724	30911	16476	20553	23752	30938
		APRIL				MAY				JUNE			
	85	15573	20056	23432	30807	16036	20692	24131	31601	16286	20965	24430	32000
	80	15615	20118	23491	30847	16045	20682	24108	31570	16286	20955	24414	31975
	75	15679	20200	23567	30896	16057	20670	24080	31523	16287	20939	24388	31932
	70	15760	20286	23643	30939	16072	20661	24053	31470	16289	20918	24353	31874
	65	15845	20365	23706	30969	16095	20657	24031	31418	16296	20895	24310	31805
	60	15922	20426	23750	30984	16126	20659	24014	31376	16312	20875	24268	31733
	55	15990	20471	23779	30990	16168	20666	24003	31342	16336	20858	24226	31662
	50	16050	20503	23794	30994	16218	20676	23994	31314	16371	20845	24186	31595
	45	16109	20522	23798	30998	16273	20683	23982	31290	16418	20833	24151	31533
	40	16174	20534	23795	31006	16334	20684	23966	31272	16475	20821	24118	31478
	35	16251	20546	23792	31018	16400	20682	23948	31257	16533	20803	24081	31423
	30	16337	20560	23791	31029	16463	20678	23928	31242	16576	20778	24038	31365
	25	16418	20570	23790	31031	16514	20669	23906	31219	16596	20743	23984	31296
	20	16480	20573	23783	31019	16549	20656	23879	31183	16595	20691	23918	31213

Table 3 (cont.)

Monthly Values of Mean Geopotential Height, $[\overline{H}]$, for 1965. Units: gpm

		JULY				AUGUST				SEPTEMBER			
	p(mb)	100	50	30	10	100	50	30	10	100	50	30	10
Lat.	85	16429	21116	24575	32123	16302	20939	24353	31793	16057	20578	23881	31021
	80	16431	21105	24558	32104	16298	20933	24345	31782	16069	20591	23897	31053
	75	16431	21087	24531	32071	16299	20924	24332	31765	16090	20613	23922	31096
	70	16428	21062	24494	32021	16307	20916	24316	31743	16122	20643	23954	31148
	65	16429	21035	24450	31960	16328	20912	24300	31720	16164	20677	23989	31205
	60	16439	21010	24406	31894	16363	20914	24286	31697	16214	20712	24022	31263
	55	16463	20988	24362	31824	16414	20922	24273	31672	16273	20747	24052	31317
	50	16504	20971	24319	31751	16477	20932	24261	31641	16342	20780	24078	31359
	45	16555	20955	24278	31678	16542	20934	24244	31602	16416	20807	24096	31385
	40	16506	20933	24234	31604	16597	20924	24216	31554	16490	20824	24103	31394
	35	16643	20903	24183	31527	16631	20900	24176	31495	16552	20828	24095	31382
	30	16654	20865	24125	31448	16640	20864	24125	31429	16591	20814	24069	31351
	25	16642	20815	24057	31363	16628	20817	24063	31356	16603	20786	24028	31302
	20	16615	20750	23978	31265	16602	20760	23994	31275	16595	20747	23976	31241

	OCTOBER				NOVEMBER				DECEMBER			
85	15603	19989	23155	29968	15636	19934	23037	29626	15414	19859	23097	29991
80	15637	20036	23215	30059	15626	19934	23052	29676	15437	19874	23110	30004
75	15693	20109	23306	30193	15623	19946	23081	29763	15471	19898	23131	30028
70	15773	20201	23417	30357	15634	19979	23132	29890	15517	19934	23160	30061
65	15866	20303	23536	30532	15668	20034	23208	30043	15576	19982	23202	30104
60	15964	20400	23647	30697	15728	20109	23303	30206	15647	20043	23257	30159
55	16066	20488	23742	30842	15815	20205	23416	30373	15735	20120	23327	30235
50	16169	20566	23822	30964	15927	20311	23533	30537	15844	20211	23409	30334
45	16268	20630	23882	31057	16051	20411	23638	30692	15968	20305	23493	30451
40	16361	20676	23923	31122	16178	20496	23723	30826	16103	20394	23573	30572
35	16440	20706	23949	31163	16298	20561	23784	30927	16237	20473	23645	30684
30	16498	20718	23958	31183	16399	20601	23820	30992	16356	20529	23701	30783
25	16538	20716	23950	31184	16476	20621	23836	31027	16450	20563	23741	30866
20	16560	20703	23929	31166	16525	20626	23835	31040	16513	20582	23766	30928

Table 4

Monthly Values of Mean "Vertical" Motion, $[\bar{\omega}]$, for January, April and July 1965. Units: 10^{-5}mb sec^{-1}

		JANUARY				APRIL				JULY			
	p(mb)	100	50	30	10	100	50	30	10	100	50	30	10
Lat.	82.5	1.301	.835	-.059	-.018	1.306	.563	.177	-.011	.355	.173	.121	.004
	77.5	.696	-.608	-.548	-.554	.032	.141	-.259	-.016	.653	.403	.214	.011
	72.5	-.433	-1.867	-1.195	-.630	-.903	-.518	-.508	-.028	.373	.345	.195	.007
	67.5	-1.646	-1.538	-.836	-.701	-.278	-.081	-.238	.039	.151	.245	.156	-.009
	62.5	-1.776	-.655	-.117	-.148	.605	.542	.190	.138	-.054	.220	.166	-.014
	57.5	-.114	.734	.504	.414	.794	.724	.367	.149	.123	.252	.200	.001
	52.5	1.349	1.503	.609	.730	.680	.520	.326	.139	.156	.221	.165	.005
	47.5	2.106	1.477	.850	.658	.526	.288	.168	.066	.279	.186	.121	-.007
	42.5	2.052	.922	.507	.404	.053	.172	.089	.027	-.066	.136	.071	-.020
	37.5	1.549	.514	.248	.200	.679	.087	.040	.000	-.360	.053	.044	-.033
	32.5	.701	.212	.112	.148	1.148	.034	-.047	-.004	-.507	.031	.010	-.050
	27.5	-.146	-.014	.031	.083	.235	.007	-.084	.000	-.394	-.019	-.016	-.054
	22.5	-1.318	-.255	-.127	.048	-1.330	-.525	-.058	-.023	.597	-.207	-.013	-.036

Table 5

Monthly Values of Mean Meridional Motion, $[\bar{v}]$, for January, April and July 1965. Units: cm sec^{-1}

		JANUARY			APRIL			JULY		
	p(mb)	75	40	20	75	40	20	75	40	20
Lat.	82.5	37.5	64.5	85.3	0.2	-4.0	-8.6	2.6	2.4	1.9
	77.5	29.2	46.2	56.3	0.5	-4.5	-12.1	1.6	1.3	0.9
	72.5	12.9	11.6	1.8	-1.0	-6.6	-16.8	-0.1	-0.2	-0.2
	67.5	5.6	-9.3	-39.2	-3.7	-12.5	-18.4	-1.0	-1.2	-1.2
	62.5	2.6	-11.4	-54.1	-4.5	-9.0	-13.9	-1.4	-1.0	0.8
	57.5	-2.7	-10.4	-37.5	-3.2	-4.9	-6.4	-0.2	0.4	0.8
	52.5	-10.3	-13.1	-25.3	-2.2	-0.4	2.3	1.1	1.2	0.6
	47.5	-15.6	-9.9	-8.2	-1.0	1.1	4.3	1.6	0.6	0.4
	42.5	-10.7	1.3	11.2	-1.8	1.4	4.1	1.0	1.0	0.6
	37.5	-3.9	5.0	17.5	-0.1	3.5	4.8	-0.1	1.2	1.1
	32.5	1.7	7.7	19.9	0.7	4.0	5.2	-5.9	-0.3	0.6
	27.5	7.9	7.3	8.2	-3.6	0.2	4.5	-11.1	-1.1	0.4
	22.5	-0.4	-6.1	0.7	-2.2	-2.3	8.9	-2.6	2.8	1.2

Table 6

Monthly Values of Zonally Averaged Time Covariances of u and v, $\boxed{u'v'}$, for 1965. Units: m^2sec^{-2}

		JANUARY				FEBRUARY				MARCH			
	p(mb)	100	50	30	10	100	50	30	10	100	50	30	10
Lat.	85	-.9	-1.2	-2.0	2.7	-.2	-.8	-1.5	-4.7	-.8	-.7	2.2	1.3
	80	-2.4	-.2	-.5	8.7	-.0	-2.0	-2.5	-10.1	-2.2	-3.1	.8	.1
	75	-2.3	2.8	5.5	18.9	-.7	-3.3	-1.5	-6.9	-3.1	-5.6	-2.4	-2.4
	70	-.7	7.5	13.8	29.1	-2.0	-3.6	.6	6.0	-2.5	-4.9	-1.0	1.6
	65	.7	8.9	17.6	38.1	-2.8	-3.7	2.1	17.0	-.8	-1.5	4.0	15.9
	60	0	5.7	14.3	41.9	-2.3	-2.3	4.5	21.5	1.4	2.4	8.1	30.8
	55	-1.7	3.3	9.4	37.8	-.7	.8	7.2	22.3	3.8	5.0	11.1	38.7
	50	-.1	3.4	8.0	29.9	1.7	3.1	7.6	19.8	5.7	5.8	12.7	38.5
	45	4.7	4.8	8.2	22.5	3.7	3.1	6.2	15.8	7.2	5.9	12.0	32.5
	40	8.8	4.1	5.6	14.8	5.9	2.1	4.1	10.9	8.6	5.3	9.0	24.3
	35	11.0	2.2	2.7	8.4	7.8	1.2	2.3	6.1	8.7	4.0	5.5	15.8
	30	10.6	1.5	1.2	4.4	6.8	.6	1.0	2.7	6.7	2.3	2.7	7.9
	25	7.4	1.4	.7	2.4	4.1	-.0	-.2	.3	4.4	1.1	1.0	2.6
	20	3.3	1.5	1.2	3.3	2.7	-.5	-1.9	-1.8	2.9	.4	-.1	-.7
		APRIL				MAY				JUNE			
	85	-1.1	.2	2.1	3.6	0	.2	.2	.3	0	.1	.1	0
	80	-3.3	-1.3	2.2	4.5	.1	.6	1.3	.8	0	.2	.1	0
	75	-5.3	-3.4	1.4	7.8	.2	1.4	2.9	2.3	.1	.3	.2	.2
	70	-5.5	-4.0	1.5	13.9	.4	2.2	4.1	4.3	.1	.2	.2	.3
	65	-3.8	-1.6	4.3	18.5	.7	2.4	4.3	5.6	.1	.1	.2	.1
	60	-1.2	1.9	7.1	19.1	1.6	2.4	4.0	6.1	.2	.1	.1	-.1
	55	1.3	3.6	7.6	16.2	2.6	2.1	3.9	6.2	.4	0	-.1	-.2
	50	3.7	3.6	6.3	11.4	3.0	1.5	3.2	5.2	.6	-.1	-.2	0
	45	5.8	3.2	4.7	6.9	3.4	1.0	2.2	3.4	.8	-.1	.1	0
	40	8.2	2.6	3.5	4.3	4.5	.9	1.3	1.9	1.1	.1	.3	-.1
	35	9.5	2.0	2.2	2.7	5.3	.6	.5	.9	1.5	.2	.5	-.1
	30	9.5	1.3	1.1	1.4	5.5	.2	-.2	.1	1.6	.2	.7	.2
	25	8.0	.8	.4	-.1	5.4	0	-.6	-.9	1.1	-.1	.6	.5
	20	2.5	0	-.7	-2.2	3.7	-.6	-1.2	-3.5	-.3	-2.1	-.7	-.3

Table 6 (cont'd)

Monthly Values of Zonally Averaged Time Covariances of u and v, $[\overline{u'v'}]$, for 1965. Units: $m^2 sec^{-2}$

		JULY				AUGUST				SEPTEMBER			
	p(mb)	100	50	30	10	100	50	30	10	100	50	30	10
Lat.	85	0	0	.2	0	-.2	-.2	0	.1	.3	.2	.3	.5
	80	-.3	.1	.2	.1	-.4	-.3	0	0	.5	.3	.5	1.2
	75	-.7	0	.1	.2	-.6	-.2	0	-.1	.6	.3	.8	1.9
	70	-1.0	-.1	.1	.4	-.5	0	0	-.2	.3	.3	.9	2.1
	65	-1.2	-.1	0	.4	0	.1	.1	-.1	-.2	.4	1.0	2.2
	60	-1.0	0	.1	.3	1.0	.2	.1	.1	-.5	.4	1.1	2.4
	55	-.7	-.1	.2	.5	2.1	.3	0	.2	-.4	.3	.9	2.3
	50	-.4	-.2	.2	.6	2.8	.4	-.1	0	-.1	.2	.8	1.8
	45	-.5	-.1	.3	.5	3.1	.5	0	-.2	.5	.2	.7	1.4
	40	-.6	0	.4	.3	3.0	.5	.2	-.3	1.4	.1	.4	1.2
	35	-.7	0	.5	.3	2.2	.5	.3	-.3	1.7	-.1	.1	.9
	30	-.5	0	.5	.1	1.5	.3	.3	.2	1.4	-.2	0	.6
	25	-.6	-.3	.3	-.4	.8	.2	0	.5	.9	-.2	.1	.6
	20	-2.1	-1.4	-.9	-2.5	-.7	.1	-1.1	1.5	.5	-.5	.7	1.7
		OCTOBER				NOVEMBER				DECEMBER			
	85	.4	.5	.1	.6	1.5	2.7	3.8	5.0	-.8	2.9	5.9	9.3
	80	.4	.6	.5	1.7	3.4	5.5	7.7	11.6	-1.8	3.9	9.8	17.5
	75	-.3	.4	.9	3.4	6.1	8.1	11.5	18.8	-3.3	.9	7.6	22.5
	70	-1.2	0	1.0	4.4	7.1	10.3	15.6	24.9	-4.7	-3.0	2.3	23.7
	65	-1.4	-.2	1.1	3.8	5.4	10.8	18.2	29.2	-4.9	-3.9	.8	25.2
	60	-.4	.3	1.4	3.6	3.2	8.9	18.1	31.0	-3.5	-2.3	2.9	27.3
	55	.9	1.1	1.8	4.7	2.1	6.2	15.4	30.6	-.5	.2	5.8	29.1
	50	2.2	1.5	2.3	6.0	2.5	4.2	10.9	26.7	3.7	3.1	8.1	29.2
	45	3.6	1.5	2.2	6.4	4.7	2.9	7.5	20.5	7.8	4.7	8.9	26.0
	40	4.7	1.5	1.8	4.9	6.9	2.1	5.1	15.3	10.2	4.4	7.8	20.7
	35	4.8	1.4	1.3	2.6	7.1	1.8	3.2	11.1	10.6	3.8	6.0	14.3
	30	3.9	.8	.6	1.2	5.1	1.1	1.5	6.2	9.7	2.8	4.2	8.7
	25	2.4	.1	-.2	.6	2.2	.4	.6	2.0	8.0	1.9	2.8	5.4
	20	.3	-.9	-2.1	-1.4	.3	-.4	-.1	1.7	5.7	1.6	1.2	6.7

Table 7

Monthly Values of Zonally Averaged Space Covariances of $\bar{u}$ and $\bar{v}$, $[\bar{u}^*\bar{v}^*]$, for 1965. Units: $m^2 sec^{-2}$

		JANUARY				FEBRUARY				MARCH			
	p(mb)	100	50	30	10	100	50	30	10	100	50	30	10
Lat.	85	-4.4	-14.3	-23.4	-33.4	-1.1	-7.6	-16.6	-18.8	-.7	-2.3	-4.1	-1.7
	80	-10.8	-31.8	-49.5	-71.6	-3.0	-17.6	-33.7	-34.5	-1.4	-1.4	-3.1	5.4
	75	-17.3	-39.7	-63.1	-84.2	-6.5	-21.8	-36.2	-31.0	-1.0	3.4	7.0	26.8
	70	-22.5	-34.0	-53.5	-57.0	-11.1	-16.4	-21.4	-12.1	-.4	10.3	21.9	54.6
	65	-23.8	-24.1	-30.4	-7.9	-14.5	-8.6	-6.9	3.7	-1.4	14.6	32.5	72.3
	60	-20.9	-15.8	-11.6	35.4	-16.9	-7.4	-2.5	15.5	-3.2	14.5	33.9	72.9
	55	-16.1	-8.6	-1.1	53.9	-15.2	-6.0	1.8	26.8	-3.8	12.1	28.3	61.2
	50	-8.2	-2.5	5.2	53.5	-6.4	.7	8.6	34.2	-1.7	9.5	20.4	43.2
	45	1.3	.7	7.0	44.2	2.9	5.3	10.7	32.9	2.0	7.6	13.9	25.5
	40	8.9	2.5	6.0	30.3	8.2	6.1	9.0	23.7	4.3	6.1	9.1	12.2
	35	12.8	3.3	4.8	18.7	9.2	4.1	5.9	13.1	3.4	3.7	5.3	4.4
	30	12.4	2.0	2.2	9.5	8.6	1.8	3.0	5.9	1.7	1.0	2.3	.7
	25	9.4	.8	-.3	2.4	7.6	1.7	1.6	2.7	-.4	-.3	.6	-.9
	20	7.6	3.0	1.4	1.8	4.9	2.9	2.1	2.4	-9.2	-1.3	-.2	-2.6
		APRIL				MAY				JUNE			
	85	.6	-.3	-.3	-.3	0	-.3	-.4	.1	-.1	-.1	-.1	0
	80	.9	-.3	-.3	0	-.1	-.1	-.1	.8	-.1	-.1	-.2	0
	75	.4	.1	.5	1.1	.1	.5	.9	2.1	.2	.2	0	.2
	70	-1.0	.2	1.3	2.4	.3	1.2	2.0	3.3	.3	.6	.4	.5
	65	-2.6	-.4	1.3	3.9	.2	1.7	2.3	3.4	.2	.9	.7	.8
	60	-3.8	-1.3	.9	5.0	-.5	1.3	1.7	2.4	.3	.9	.9	.8
	55	-4.0	-1.6	.7	4.9	-1.3	.4	.6	1.1	.3	.5	.7	.1
	50	-3.4	-1.3	.5	3.6	-1.7	-.6	-.4	0	-.4	-.1	0	-.2
	45	-3.2	-.7	.5	2.2	-2.5	-1.4	-1.0	-.8	-1.9	-.8	-.5	.1
	40	-3.9	-.7	.1	1.1	-3.8	-2.1	-1.1	-1.0	-3.5	-1.5	-.7	.3
	35	-4.7	-1.7	-1.1	0	-3.4	-2.7	-1.4	-.9	-4.3	-2.1	-.9	-.4
	30	-3.6	-2.6	-2.1	-1.4	1.4	-2.4	-1.6	-.8	-3.0	-2.1	-1.6	-1.7
	25	-.7	-1.7	-2.1	-3.1	8.9	-.4	-1.1	-.5	.2	-1.6	-2.2	-3.3
	20	-.6	1.5	-1.0	-5.9	15.7	3.4	-.5	-.5	4.0	-1.0	-2.7	-5.7

Monthly Values of Zonally Averaged Space Covariances of $\bar{u}$ and $\bar{v}$, $[\bar{u}^*\bar{v}^*]$, for 1965. Units: $m^2 sec^{-2}$

		JULY				AUGUST				SEPTEMBER			
	p(mb)	100	50	30	10	100	50	30	10	100	50	30	10
Lat.	85	-.6	-.7	-.6	-.3	-.5	-.2	-.2	-.5	.1	.2	.2	1.1
	80	-.7	-1.3	-.8	-.5	-1.1	-.6	-.5	-.7	.3	.3	.3	1.5
	75	-.4	-1.0	-.5	-.2	-1.6	-1.1	-.7	-.5	-.1	0	-.3	.8
	70	.3	0	.2	.8	-1.7	-1.0	-.5	.3	-.6	-.4	-.9	-.2
	65	1.2	1.1	1.3	1.7	-1.3	-.4	.1	1.2	-.7	-.2	-.6	-.1
	60	1.9	1.8	1.8	1.8	-1.2	.3	.8	1.5	-.7	.4	.5	1.4
	55	1.9	1.7	1.5	1.2	-1.7	.4	1.2	1.1	-.6	.8	1.2	2.4
	50	1.0	1.0	1.0	.8	-1.9	.3	.7	.7	-.8	.4	1.0	2.3
	45	.2	.5	.7	.7	-1.0	.1	.2	.4	-1.2	-.2	.4	1.7
	40	-.5	-.1	.2	.4	.6	-.2	-.3	.1	-.2	-.5	0	1.0
	35	-.5	-.5	-.5	-.3	2.0	-.5	-.7	-.2	1.9	-.4	-.1	.4
	30	2.3	-.1	-.6	-.5	2.7	-.5	-.6	-.3	4.4	0	.1	.3
	25	7.5	.8	-.2	-.2	3.8	.3	.2	.1	6.8	1.3	1.2	1.1
	20	13.7	1.9	.4	-1.4	6.2	1.5	1.0	.7	10.1	3.1	2.5	2.9
		OCTOBER				NOVEMBER				DECEMBER			
	85	.9	2.3	3.1	3.6	0	-1.0	-2.0	3.6	-.2	-2.2	-4.8	.7
	80	1.3	4.1	5.7	7.9	-.8	-1.1	-1.4	15.6	-1.6	-2.1	-2.9	11.2
	75	-.2	4.0	6.8	12.6	-3.3	.3	2.6	37.2	-3.4	-.3	2.6	31.1
	70	-2.3	2.9	6.9	16.8	-6.5	1.7	7.3	56.9	-4.6	2.5	8.9	53.0
	65	-2.2	2.2	6.7	18.5	-8.0	1.2	11.1	64.9	-5.4	4.4	15.8	72.1
	60	0	1.9	6.0	17.1	-7.4	.4	13.8	64.4	-4.8	4.4	22.4	90.6
	55	3.4	2.4	5.5	15.1	-3.9	2.5	16.6	60.6	-1.2	7.6	31.7	105.2
	50	6.2	3.1	5.2	12.7	1.3	5.3	17.1	52.6	2.6	10.0	33.4	99.9
	45	7.7	3.1	4.1	9.1	4.5	6.1	14.5	42.1	3.7	7.0	22.3	75.5
	40	8.7	2.8	3.2	5.5	5.5	5.8	11.3	31.2	3.9	4.3	11.8	47.3
	35	8.9	2.3	2.3	3.2	5.5	4.0	7.0	20.2	3.9	2.7	5.6	25.5
	30	8.2	1.9	1.3	1.7	5.1	1.8	2.6	10.4	5.1	1.1	1.3	9.8
	25	7.9	2.4	1.4	.4	4.8	.3	-.6	3.5	6.4	.7	-1.4	-2.5
	20	9.3	3.8	3.2	-.4	4.8	0	-2.2	-1.7	8.2	2.5	-.6	-8.2

Table 8

Monthly Values of Zonally Averaged Time Covariances of v and T, $[\overline{v'T'}]$. Units: $m^{o}c\ sec^{-1}$

		JANUARY				FEBRUARY				MARCH			
	p(mb)	100	50	30	10	100	50	30	10	100	50	30	10
Lat.	85	-2.3	-1.0	-2.6	-3.0	.3	-.3	-.9	-8.0	-3.3	2.8	15.4	24.6
	80	-2.3	-.4	-2.8	-2.5	.8	-.1	-1.0	-10.1	-2.0	5.7	22.6	39.3
	75	.4	2.6	1.0	3.5	.6	.9	1.4	-6.7	2.1	10.6	24.9	42.4
	70	3.0	7.1	7.7	11.0	.4	3.5	6.3	.9	6.3	16.6	27.5	41.9
	65	5.4	10.5	12.4	16.9	1.8	6.3	10.4	10.0	9.2	20.7	29.8	40.4
	60	7.1	11.7	13.6	20.4	3.8	8.0	12.3	14.2	9.8	21.3	29.8	36.3
	55	6.8	10.0	12.4	17.7	4.4	7.4	10.9	12.5	8.3	18.4	26.0	30.5
	50	5.6	6.7	8.4	10.2	3.1	4.4	7.1	8.8	6.1	13.1	18.4	21.7
	45	4.5	4.2	4.1	3.8	1.7	2.4	3.3	5.2	3.7	8.2	11.8	13.8
	40	3.1	2.5	1.5	.7	.7	1.7	1.4	3.2	1.7	4.5	6.8	8.9
	35	1.9	1.2	.4	-.4	.3	1.3	.7	1.9	.4	2.0	3.1	5.3
	30	1.3	.7	.1	-.3	.1	.9	.5	1.0	0	.8	1.2	2.7
	25	1.1	.5	.1	0	0	.6	.3	.1	-.2	.2	.6	.9
	20	2.7	-1.5	2.1	-1.2	-1.3	-.1	-.5	1.0	-.3	0	.1	.4

		APRIL				MAY				JUNE			
	85	-.2	-2.1	-4.4	.6	.1	0	.1	.7	.2	.1	0	.1
	80	-1.2	-2.5	-4.7	.9	.2	.1	.4	1.4	.4	.1	.1	.1
	75	-.4	-.5	-1.9	1.7	.1	.2	.6	1.5	.7	.2	.1	0
	70	2.0	2.8	2.5	4.7	.5	.3	.7	1.5	.7	.2	.2	.2
	65	4.2	5.3	5.5	6.9	2.0	.7	1.0	1.5	.7	.3	.3	.2
	60	5.0	5.0	5.2	5.9	3.2	1.4	1.4	1.8	1.0	.4	.3	.2
	55	4.9	3.2	3.1	4.4	3.3	2.0	1.7	1.8	1.2	.5	.4	.5
	50	4.3	1.7	1.1	2.7	2.5	1.8	1.6	1.3	1.3	.6	.4	.7
	45	3.3	1.0	.5	1.7	1.4	1.1	1.1	.7	1.5	.6	.5	.5
	40	2.6	.7	.4	1.1	.9	.6	.5	.4	1.2	.7	.5	.2
	35	2.1	.6	.3	.6	.6	.4	.3	.4	.6	.6	.4	.1
	30	.7	.4	.3	.3	-.1	.2	.2	.4	.4	.3	.2	.1
	25	-.4	.2	.1	.2	-.7	-.1	.3	.3	.1	.1	.2	.1
	20	.9	3.6	-1.0	.4	.3	-1.7	-2.8	-1.3	0	-.3	1.5	1.0

Table 8 (con't)

Monthly Values of Zonally Averaged Time Covariances of v and T, $[\overline{v'T'}]$. Units: $m^{o}c\ sec^{-1}$

		JULY				AUGUST				SEPTEMBER			
	p(mb)	100	50	30	10	100	50	30	10	100	50	30	10
Lat.	85	-.2	0	.1	.2	0	.1	.1	.1	.8	.5	.4	.4
	80	-.3	-.1	.1	.3	.1	.2	.2	.2	1.2	.9	.7	.7
	75	-.1	0	.3	.4	.3	.3	.3	.5	1.3	1.1	.9	.8
	70	.3	.3	.4	.4	.7	.5	.5	.7	1.4	1.1	1.1	1.3
	65	.7	.4	.4	.4	1.4	.7	.7	.9	1.7	1.2	1.3	1.7
	60	1.2	.5	.4	.4	1.9	.9	.7	.9	2.2	1.4	1.4	1.8
	55	1.4	.6	.4	.4	2.4	.9	.7	.7	3.0	1.7	1.4	1.6
	50	1.0	.6	.4	.2	2.4	.6	.5	.5	3.3	1.6	1.3	1.0
	45	.6	.6	.4	.2	1.3	.5	.2	.4	2.3	1.4	1.0	.4
	40	.7	.5	.3	.2	.4	.4	0	.2	1.8	1.1	.6	.3
	35	.8	.3	.2	0	.3	.3	0	.1	1.2	.6	.3	.2
	30	.3	0	.1	-.1	.4	.1	0	.1	.5	.2	.1	.2
	25	-.1	0	-.1	-.1	.3	-.1	.1	.2	.4	.1	.1	.1
	20	-3.4	1.4	-.7	-.3	-2.1	1.8	-.1	1.8	.1	-.7	1.4	1.7
		OCTOBER				NOVEMBER				DECEMBER			
	85	1.9	1.9	1.4	1.6	3.1	4.9	4.3	3.1	-3.3	-1.6	-1.3	.2
	80	2.6	2.5	2.4	2.8	4.6	8.0	7.7	4.7	-4.4	-3.3	-2.2	.4
	75	2.4	2.4	2.8	3.3	5.1	8.7	9.3	4.3	-3.0	-3.6	-2.5	.7
	70	2.4	2.4	3.1	3.5	4.7	7.9	9.1	3.9	-1.2	-2.3	-2.0	1.6
	65	2.7	2.7	3.3	3.7	3.9	6.5	7.4	4.3	-.1	-1.0	-.5	2.5
	60	2.9	2.8	3.2	4.0	3.2	5.3	5.5	4.7	1.0	.1	1.2	4.5
	55	3.4	2.6	2.7	3.7	3.0	4.5	4.7	4.3	2.0	1.1	3.2	6.2
	50	3.3	2.1	1.8	2.9	3.2	3.7	4.1	3.2	2.9	2.1	4.6	5.6
	45	2.3	1.7	1.1	1.6	2.5	2.3	2.3	2.4	3.0	2.2	3.8	4.1
	40	1.4	1.3	.7	.4	1.3	1.3	1.3	2.1	2.7	2.1	2.2	2.5
	35	.7	.8	.5	0	.9	1.0	.7	1.7	2.3	1.7	1.2	1.2
	30	.2	.4	.3	.1	.8	.6	.5	.7	1.4	1.2	.7	.2
	25	-.1	.2	.1	.1	.3	.2	.3	.1	.4	.6	.4	-.1
	20	2.2	1.6	-.9	-.6	-3.6	-.2	-.4	-.5	-1.7	-1.5	.4	-1.0

Table 8

Monthly Values of Zonally Averaged Space Covariances of $\overline{v}$ and $\overline{T}$, $[\overline{v^*}\ \overline{T^*}]$, for 1965. Units: $m^{\circ}c\ sec^{-1}$

		JANUARY				FEBRUARY				MARCH			
	p(mb)	100	50	30	10	100	50	30	10	100	50	30	10
Lat.	85	3.6	2.0	7.2	-2.5	-4.2	-5.8	-10.5	-49.8	5.1	6.7	8.0	-2.7
	80	3.8	3.0	11.4	6.8	-11.0	-11.3	-15.4	-73.2	6.3	12.0	15.5	2.6
	75	2.6	7.4	17.9	26.5	-12.9	-9.8	-10.4	-54.5	8.1	16.3	21.6	14.7
	70	4.2	15.9	29.4	48.2	-6.5	-1.5	2.3	-11.1	9.9	17.8	23.4	25.4
	65	9.5	23.1	37.2	62.0	2.3	8.6	14.3	20.5	9.2	15.1	18.8	25.0
	60	13.8	24.4	35.4	60.3	8.9	14.0	18.6	30.7	7.9	10.5	11.8	16.3
	55	14.5	20.0	26.8	46.4	11.0	12.5	15.5	25.9	7.3	6.8	6.9	8.2
	50	11.9	13.0	15.9	28.1	8.5	8.1	9.5	15.7	6.5	4.5	4.1	2.9
	45	7.4	6.4	7.1	13.0	4.3	4.2	4.6	7.4	4.9	3.2	2.8	.1
	40	3.7	3.1	3.0	4.6	2.1	2.1	2.4	3.4	2.7	1.9	1.7	-.8
	35	1.2	1.6	1.5	1.3	-.1	.7	1.3	1.6	.4	.7	.8	-.5
	30	0	.6	.8	.6	-1.1	0	.5	.9	.1	.1	.6	.1
	25	.1	.1	.3	.8	-.8	-.3	.1	.8	1.0	-.2	.4	.3
	20	1.5	.2	0	.2	-.1	-.5	-.1	.2	2.1	-.2	.3	-.1

	APRIL				MAY				JUNE			
85	-.4	-.1	1.1	2.2	0	.9	1.0	-.9	1.3	.7	.5	-.3
80	.6	1.1	2.7	4.7	.5	1.2	1.4	-1.9	1.3	.9	.6	-.4
75	2.9	3.6	4.7	6.5	.7	.9	.9	-2.7	.9	.6	.3	-.7
70	5.4	5.9	6.5	7.3	.1	.4	.1	-2.9	.6	.3	-.1	-1.0
65	5.4	5.6	6.0	6.5	-.3	-.1	-.3	-2.1	.6	0	-.3	-.8
60	3.3	3.3	3.4	4.3	-.1	-.1	-.3	-.4	.5	-.2	-.4	-.4
55	1.7	1.5	1.3	1.8	.4	.2	-.2	.5	.5	-.4	-.5	-.3
50	1.0	1.0	.4	.3	1.6	.6	-.1	.4	.3	-.5	-.5	-.2
45	1.4	1.2	.4	-.2	3.9	.9	0	0	.8	-.3	-.3	-.1
40	2.8	1.3	.5	-.5	6.3	1.0	.1	0	1.9	-.1	-.3	-.1
35	3.1	1.2	.5	-.1	6.7	.9	.1	.3	2.5	.3	-.2	0
30	2.4	.8	.5	.4	4.8	.5	0	.4	2.1	.4	-.1	.2
25	2.6	.2	.2	.2	2.7	.2	-.2	-.1	1.8	.2	0	.1
20	2.9	.1	.1	-.2	2.3	.1	-.2	-.5	2.4	.1	0	0

Monthly Values of Zonally Averaged Space Covariances of $\bar{v}$ and $\bar{T}$, $[\bar{v}^*\bar{T}^*]$, for 1965. Units: m^o c sec^{-1}

		JULY				AUGUST				SEPTEMBER			
	p(mb)	100	50	30	10	100	50	30	10	100	50	30	10
Lat.	85	2.6	2.0	1.0	-1.1	.7	.4	-.1	-.8	1.7	1.4	.8	-1.6
	80	2.7	1.9	.7	-1.7	.7	.3	-.4	-1.2	2.3	2.1	1.3	-1.7
	75	1.6	.6	-.5	-2.2	.5	.1	-.7	-1.5	2.2	2.5	1.9	-.3
	70	1.0	-.1	-1.0	-2.2	.7	.2	-.7	-1.3	2.1	2.6	2.3	.9
	65	.9	.1	-.6	-1.4	.9	.3	-.4	-.7	2.0	2.3	2.2	1.7
	60	1.1	.3	-.1	-.4	.8	.4	-.3	-.2	1.7	1.8	1.8	1.9
	55	1.1	.3	0	.1	.7	.4	-.1	.1	1.7	1.6	1.4	1.4
	50	.8	.1	-.1	.3	.9	.5	0	.2	1.9	1.3	.8	.9
	45	.3	-.1	-.3	.3	1.7	.5	0	.2	1.7	.7	.3	.8
	40	.1	-.2	-.2	.2	1.8	.3	-.1	.3	1.6	.2	.2	.8
	35	.3	0	-.1	.2	.8	0	0	.3	1.5	0	.2	.5
	30	1.1	.1	.1	.2	.2	-.1	.1	.2	1.6	0	.2	.2
	25	1.3	0	.2	.2	.5	0	.3	.1	1.7	-.1	.2	0
	20	1.3	-.2	.1	.2	.9	0	.5	.1	1.3	-.1	.1	-.1
		OCTOBER				NOVEMBER				DECEMBER			
	85	-.2	-.3	.2	0	4.8	5.9	-1.1	3.8	.2	-2.0	-1.9	-2.4
	80	1.4	1.6	2.6	1.3	8.4	11.9	1.1	12.0	4.5	5.8	7.6	7.6
	75	3.6	4.7	6.2	4.0	11.4	18.0	10.1	24.1	11.0	18.4	23.8	28.6
	70	4.7	5.9	8.0	5.8	14.2	22.3	23.1	36.8	16.2	29.7	40.4	50.8
	65	4.2	5.0	6.8	5.5	16.2	23.3	30.1	43.9	19.5	36.7	51.3	62.5
	60	3.0	3.4	4.5	4.5	16.2	21.1	28.4	41.1	21.3	37.5	51.8	60.3
	55	2.0	2.1	2.7	3.0	13.6	16.5	21.9	31.2	21.3	34.6	46.0	51.6
	50	1.7	1.5	1.8	2.0	8.6	10.4	13.8	18.6	16.9	25.7	34.0	39.5
	45	2.1	1.3	1.2	1.5	3.8	5.1	6.7	8.2	9.3	14.9	19.9	25.1
	40	2.6	1.3	1.1	1.4	1.4	2.1	2.7	3.0	3.3	6.5	8.8	13.6
	35	2.3	1.2	1.0	1.0	1.1	.9	1.3	1.2	.1	1.8	2.9	6.3
	30	1.1	.8	.7	.6	1.0	.7	.8	1.0	-.6	.4	.7	2.3
	25	.8	.3	.3	.3	1.3	.4	.4	.8	.1	.3	.2	1.5
	20	1.1	0	0	.2	1.4	0	.3	.1	1.1	.5	.3	.9

Monthly Values of Zonally Averaged Time Standard Deviations of u, $[\sigma(u)]$, for 1965. Units: m sec^{-1}

Lat.	p(mb)	JANUARY 100	50	30	10	FEBRUARY 100	50	30	10	MARCH 100	50	30	10
	85	5.9	6.5	7.9	12.0	6.0	6.4	8.0	12.1	8.0	12.4	15.9	21.0
	80	7.1	7.8	8.9	12.9	5.5	7.0	8.1	11.1	7.1	10.6	13.4	17.8
	75	7.8	8.5	9.8	13.2	5.5	6.9	8.0	10.0	6.0	3.2	10.3	14.6
	70	7.9	8.2	9.3	12.3	6.4	7.6	8.3	10.0	5.9	7.6	9.4	13.5
	65	6.5	6.4	7.5	10.1	6.9	8.1	8.6	9.4	7.0	9.1	10.9	14.9
	60	5.7	5.8	6.9	9.2	7.1	8.0	8.5	9.5	7.6	11.0	13.6	17.7
	55	7.5	8.2	9.3	12.1	6.8	7.7	8.7	10.9	7.2	11.2	14.2	18.7
	50	9.0	9.8	11.0	14.9	6.1	7.2	8.7	11.5	6.9	9.8	12.3	17.0
	45	9.3	9.2	10.3	15.0	5.7	6.4	8.1	11.4	7.3	8.1	9.6	14.0
	40	8.8	7.6	8.6	13.0	5.7	5.2	6.9	10.3	7.6	6.9	7.7	11.6
	35	8.4	5.8	6.5	10.1	6.0	4.2	5.3	8.3	7.4	5.6	6.0	9.6
	30	7.9	4.8	5.0	8.0	6.0	3.7	3.7	6.0	6.1	4.4	4.9	7.8
	25	7.6	4.3	4.6	7.2	6.1	3.6	3.4	5.0	5.3	4.0	4.3	6.7
	20	8.3	4.6	5.3	8.1	7.8	4.4	4.7	6.4	6.8	4.9	4.7	6.6
		APRIL				MAY				JUNE			
	85	5.2	8.3	11.3	15.1	2.2	1.8	2.1	2.5	2.0	1.5	1.4	1.2
	80	8.1	11.3	13.1	14.7	2.4	2.3	2.5	2.9	2.1	1.6	1.3	1.5
	75	9.9	12.8	14.0	14.2	2.6	2.6	3.0	3.2	2.0	1.5	1.3	1.6
	70	9.5	12.0	13.1	13.2	3.0	2.9	3.2	3.3	2.1	1.5	1.4	1.9
	65	7.4	9.3	10.3	11.3	3.3	2.9	3.0	3.5	2.6	1.6	1.5	2.1
	60	5.5	6.6	7.7	9.6	3.6	2.8	3.2	4.1	3.1	1.8	1.6	2.1
	55	5.2	5.7	6.8	9.2	4.0	3.1	3.8	4.7	3.4	1.9	1.6	2.2
	50	5.1	5.0	6.2	9.1	4.2	3.3	4.0	5.0	3.6	2.0	1.8	2.5
	45	5.1	4.3	5.4	8.1	4.5	3.3	3.8	5.5	3.7	2.1	2.2	2.9
	40	5.2	3.9	4.6	6.5	4.8	3.1	3.6	5.7	4.4	2.3	2.3	3.1
	35	5.3	3.3	3.7	4.9	4.7	2.9	3.2	4.9	4.9	2.8	2.6	3.4
	30	5.4	2.9	3.1	4.0	4.8	3.1	3.3	4.6	4.9	3.2	3.3	4.1
	25	5.7	3.5	3.3	4.1	5.5	3.9	3.7	4.7	5.0	3.7	4.1	5.0
	20	7.0	5.4	5.0	5.7	6.8	5.5	4.9	5.8	5.7	5.1	5.9	7.2

Table 10 (con't)

Monthly Values of Zonally Averaged Time Standard Deviations of u, $[\sigma(u)]$, for 1965. Units: m sec^{-1}

		JULY				AUGUST				SEPTEMBER			
	p(mb)	100	50	30	10	100	50	30	10	100	50	30	10
Lat.	85	2.5	1.6	1.7	1.4	2.8	1.8	1.5	1.8	3.2	2.5	2.5	2.9
	80	2.4	1.5	1.5	1.6	2.7	2.0	1.8	2.1	3.2	2.8	3.0	3.8
	75	2.1	1.4	1.4	1.8	2.7	2.0	2.0	2.4	3.3	3.1	3.5	4.7
	70	2.2	1.5	1.6	2.0	2.8	2.0	2.0	2.7	3.6	3.4	3.7	5.2
	65	2.3	1.6	1.7	2.3	2.9	2.0	2.2	3.1	4.0	3.4	3.6	5.2
	60	2.6	1.7	1.8	2.5	3.2	2.2	2.4	3.8	4.2	3.2	3.4	5.0
	55	3.1	1.8	1.7	2.4	3.6	2.3	2.8	4.2	4.2	3.0	3.3	4.9
	50	3.3	1.8	1.8	2.5	3.8	2.5	2.9	4.4	4.2	2.9	3.1	4.8
	45	3.5	2.0	2.0	2.7	3.9	2.7	3.0	4.3	4.5	3.0	3.2	4.6
	40	4.0	2.3	2.2	2.7	4.0	2.7	2.9	3.9	4.8	3.1	3.2	4.6
	35	4.0	2.3	2.3	2.8	4.1	2.5	2.4	3.3	4.7	3.1	3.3	4.3
	30	3.8	2.5	2.8	3.6	3.9	2.5	2.4	3.2	5.0	3.3	3.6	4.3
	25	3.8	3.0	3.5	4.7	3.7	2.7	2.9	3.6	5.3	3.8	4.4	5.2
	20	4.5	4.6	5.0	6.5	4.6	3.7	3.9	4.9	6.0	5.4	5.9	6.8
		OCTOBER				NOVEMBER				DECEMBER			
	85	4.3	4.4	4.9	5.9	5.7	6.8	8.6	11.9	5.4	9.3	13.0	18.2
	80	3.7	4.1	4.6	5.7	5.4	7.2	8.9	11.6	6.4	10.1	13.9	19.8
	75	3.4	3.5	4.0	5.6	5.9	7.7	9.3	11.6	6.9	10.0	13.8	20.7
	70	3.6	3.7	4.5	6.2	6.2	7.5	9.0	11.3	6.6	9.1	12.4	19.4
	65	4.2	4.4	5.1	6.7	5.6	6.4	7.7	10.3	5.8	7.8	10.4	16.1
	60	5.0	4.5	5.2	6.6	5.2	5.6	7.1	10.2	5.6	7.2	9.5	13.9
	55	5.5	4.4	5.0	6.6	5.3	5.8	7.5	11.1	6.0	7.3	9.4	14.4
	50	5.6	4.2	4.7	6.7	5.5	6.0	7.7	11.5	6.5	7.6	10.2	15.8
	45	5.2	3.9	4.4	6.6	5.9	5.9	7.5	11.4	6.7	7.9	10.9	16.3
	40	5.2	3.7	4.0	6.2	6.3	5.3	6.7	10.5	6.8	7.2	10.0	15.1
	35	5.4	3.6	3.8	5.6	5.9	4.4	5.5	8.6	6.7	5.6	7.8	12.0
	30	5.2	3.6	4.0	5.3	5.5	3.9	4.5	6.9	6.4	4.5	5.7	8.8
	25	5.3	3.7	4.3	5.8	5.5	4.1	4.4	6.7	6.6	4.7	5.6	8.9
	20	6.4	4.7	5.3	7.0	6.4	4.9	5.3	8.0	7.1	5.5	6.9	11.2

Table II

Monthly Values of Zonally Averaged Time Standard Deviations of v, $[\sigma(v)]$, for 1965. Units: m sec^{-1}

		JANUARY				FEBRUARY				MARCH			
	p(mb)	100	50	30	10	100	50	30	10	100	50	30	10
Lat.	85	5.8	6.4	8.0	11.9	6.8	6.8	8.6	13.1	8.8	13.5	17.2	22.8
	80	7.0	8.3	9.7	13.0	7.4	8.3	10.1	13.6	8.9	13.2	16.8	21.9
	75	8.3	10.1	11.5	14.5	7.8	9.5	11.3	14.2	8.9	12.9	16.1	20.8
	70	9.3	11.4	13.1	15.9	7.9	9.9	11.7	14.6	8.5	11.9	14.8	19.4
	65	9.9	11.9	13.5	16.4	7.5	9.5	11.3	14.3	8.0	10.6	13.2	17.5
	60	9.8	11.2	12.6	15.6	6.9	8.6	10.2	13.0	7.4	9.2	11.3	15.2
	55	9.5	9.8	11.0	13.9	6.6	7.4	8.9	11.4	7.2	8.0	9.6	13.0
	50	8.6	7.6	8.4	11.2	6.2	5.8	6.8	9.0	6.5	6.4	7.4	10.3
	45	7.8	5.6	5.9	8.4	5.9	4.4	4.7	6.6	5.9	5.0	5.5	8.0
	40	7.6	4.4	4.3	6.3	6.1	3.6	3.4	4.9	5.7	3.9	4.2	6.3
	35	7.9	3.8	3.5	5.1	6.4	3.1	2.8	3.8	5.8	3.2	3.4	5.1
	30	8.1	3.3	3.1	4.5	6.5	2.9	2.7	3.5	5.9	2.9	2.9	4.3
	25	7.5	3.1	2.9	4.0	6.1	2.9	2.8	3.5	5.7	2.8	2.8	3.7
	20	7.8	3.9	3.6	4.7	6.5	3.6	3.4	4.3	6.0	3.7	3.6	4.4
		APRIL				MAY				JUNE			
	85	4.3	7.0	10.7	15.4	2.4	1.9	2.1	2.5	2.1	1.5	1.6	1.3
	80	5.8	7.9	10.5	14.2	2.9	2.5	2.7	3.0	2.3	1.6	1.6	1.6
	75	7.1	8.5	10.3	13.0	3.2	2.9	3.3	3.6	2.5	1.7	1.7	1.8
	70	7.3	8.2	9.6	11.7	3.5	3.2	3.6	4.2	2.6	1.8	1.7	1.9
	65	6.7	6.9	8.1	10.2	3.7	3.2	3.5	4.2	2.7	1.7	1.6	2.0
	60	5.8	5.4	6.3	8.4	4.0	3.0	3.1	4.0	2.8	1.7	1.5	2.0
	55	5.5	4.3	5.0	6.9	4.6	2.9	3.0	4.2	3.3	1.8	1.6	2.2
	50	5.0	3.6	3.9	5.2	4.8	2.6	2.7	4.0	3.7	1.9	1.7	2.3
	45	5.0	3.0	3.0	3.9	4.7	2.4	2.4	3.5	4.0	1.9	1.8	2.3
	40	5.3	2.7	2.5	3.2	4.6	2.3	2.3	3.1	4.2	1.9	1.9	2.4
	35	5.8	2.6	2.4	3.1	4.6	2.3	2.3	3.0	4.1	2.0	2.1	2.7
	30	6.0	2.7	2.4	3.1	4.6	2.4	2.4	3.1	3.9	2.2	2.3	2.9
	25	5.8	2.8	2.5	3.3	4.3	2.6	2.7	3.4	3.7	2.5	2.7	3.2
	20	6.1	3.5	3.5	4.3	5.0	3.7	3.8	4.5	4.2	3.7	4.1	4.4

Monthly Values of Zonally Averaged Time Standard Deviation of v, $[\sigma(v)]$, for 1965. Units: m sec

		JULY				AUGUST				SEPTEMBER			
	p(mb)	100	50	30	10	100	50	30	10	100	50	30	10
Lat.	85	2.7	1.8	1.9	1.6	3.0	1.8	1.4	1.8	3.6	2.4	2.4	2.6
	80	2.9	1.8	1.8	1.7	3.0	1.8	1.5	1.9	3.6	2.5	2.4	2.7
	75	2.9	1.8	1.8	2.0	3.1	1.9	1.6	1.9	3.6	2.6	2.5	2.9
	70	3.0	1.8	1.7	2.1	3.2	1.9	1.7	2.0	3.7	2.7	2.5	3.1
	65	3.1	1.8	1.6	2.1	3.3	1.9	1.6	2.0	3.9	2.6	2.3	3.1
	60	3.3	1.8	1.6	2.0	3.5	1.9	1.6	2.0	4.4	2.6	2.2	3.0
	55	3.8	2.0	1.7	2.4	4.3	2.0	1.8	2.3	5.2	2.8	2.4	3.0
	50	3.9	2.0	1.7	2.4	4.8	2.0	1.8	2.3	5.5	2.7	2.3	2.8
	45	3.8	1.8	1.6	2.4	4.7	1.9	1.7	2.2	5.4	2.5	2.2	2.6
	40	3.7	1.8	1.9	2.6	4.2	1.9	1.8	2.4	5.0	2.3	2.1	2.4
	35	3.4	2.0	2.2	3.0	3.4	2.0	2.0	2.7	4.4	2.1	2.2	2.6
	30	3.1	2.1	2.4	3.2	2.8	2.1	2.3	3.0	3.8	2.1	2.2	2.8
	25	3.1	2.5	2.7	3.5	2.7	2.3	2.5	3.3	3.3	2.3	2.4	3.0
	20	3.9	3.7	4.1	5.0	3.6	3.4	3.7	4.4	3.9	3.2	3.5	4.2
		OCTOBER				NOVEMBER				DECEMBER			
	85	4.7	4.8	5.4	6.3	6.4	7.0	8.9	12.4	5.2	8.8	12.5	17.7
	80	4.8	5.1	5.7	6.7	6.2	7.4	9.2	12.4	5.3	8.7	12.2	17.3
	75	4.8	5.2	5.8	6.9	6.0	7.5	9.2	12.0	5.3	8.3	11.6	16.4
	70	5.0	5.0	5.5	6.9	5.9	7.4	8.9	11.4	5.3	7.7	10.7	15.5
	65	5.1	4.6	4.9	6.3	5.7	7.0	8.2	10.6	5.3	7.2	9.8	14.4
	60	5.1	4.0	4.3	5.5	5.6	6.2	7.3	9.7	5.5	6.6	8.7	12.7
	55	5.4	3.7	3.8	5.1	5.1	5.8	6.7	8.9	6.3	6.4	8.0	11.2
	50	5.6	3.3	3.3	4.5	6.3	5.1	5.8	7.9	6.8	5.8	7.0	9.4
	45	5.7	3.0	2.9	3.9	6.4	4.3	4.8	6.8	6.9	5.1	5.8	7.7
	40	5.5	2.8	2.6	3.5	6.2	3.7	3.3	5.7	6.9	4.3	4.6	6.1
	35	5.1	2.6	2.6	3.2	5.8	3.2	3.3	4.8	6.6	3.7	3.7	5.0
	30	4.6	2.4	2.5	3.2	5.3	2.9	3.1	4.3	6.1	3.2	3.2	4.5
	25	4.2	2.4	2.5	3.3	4.9	2.7	2.9	3.9	5.3	2.9	2.9	4.0
	20	4.4	3.1	3.4	4.5	5.1	3.2	3.6	4.4	5.4	3.5	3.6	4.8

Table 12

Monthly Values of Zonally Averaged Time Standard Deviations of T, $[\sigma(T)]$, for 1965. Units: ^{o} C.

		JANUARY				FEBRUARY				MARCH			
	p(mb)	100	50	30	10	100	50	30	10	100	50	30	10
Lat.	85	6.8	3.3	4.2	5.2	3.5	2.9	3.5	5.8	5.7	7.4	8.8	10.3
	80	5.1	3.8	4.5	5.2	4.0	3.6	3.8	5.7	6.3	7.7	8.6	9.3
	75	4.2	4.3	5.1	5.6	4.3	4.5	4.3	5.5	6.7	7.8	8.2	7.7
	70	4.1	4.9	5.6	6.1	4.5	5.1	4.8	5.5	6.8	7.9	8.0	6.0
	65	4.2	5.1	5.9	6.6	4.5	5.3	5.2	5.5	6.6	7.6	7.7	6.2
	60	3.9	4.9	5.7	6.7	4.2	5.0	5.2	5.4	5.8	6.6	7.2	6.0
	55	3.7	4.4	5.2	6.2	3.9	4.5	4.8	5.2	4.7	5.3	6.3	4.8
	50	3.5	3.8	4.4	5.3	3.5	3.7	4.0	4.5	3.8	4.1	5.3	3.8
	45	3.3	3.1	3.6	4.2	3.2	2.9	3.3	3.6	3.5	3.3	4.2	2.5
	40	3.2	2.6	2.8	3.5	3.2	2.7	2.7	3.0	3.3	3.0	3.4	2.6
	35	3.4	2.6	2.5	3.0	3.3	2.6	2.3	2.8	3.4	2.7	2.7	2.8
	30	3.4	2.6	2.4	2.6	3.2	2.4	2.2	2.6	3.5	2.7	2.5	1.9
	25	3.2	2.5	2.2	2.2	3.0	2.3	2.2	2.2	3.2	2.5	2.4	1.1
	20	3.1	2.4	2.2	2.0	2.8	2.3	2.2	2.1	2.8	2.2	2.3	.2
		APRIL				MAY				JUNE			
	85	6.3	5.0	4.1	4.3	1.9	1.8	1.9	2.5	2.2	1.4	1.6	1.9
	80	5.8	5.5	5.0	3.8	2.2	1.9	2.2	2.7	1.9	1.7	1.7	2.1
	75	5.0	5.6	5.2	3.7	2.2	2.2	2.2	2.8	2.1	1.8	1.8	2.1
	70	4.5	5.3	5.0	3.6	2.4	2.4	2.4	2.9	2.3	1.9	2.0	2.2
	65	4.2	4.9	4.7	3.7	2.5	2.5	2.6	2.8	2.3	1.9	2.0	2.3
	60	3.8	4.1	4.1	3.6	2.7	2.5	2.5	2.8	2.4	2.0	2.0	2.3
	55	3.4	3.4	3.5	3.4	2.7	2.5	2.6	2.9	2.6	2.0	2.1	2.3
	50	3.2	2.9	2.9	3.2	3.0	2.6	2.6	2.9	2.9	2.2	2.1	2.3
	45	3.2	2.5	2.4	2.9	3.1	2.5	2.5	2.6	3.1	2.3	2.1	2.2
	40	3.4	2.4	2.3	2.8	3.1	2.4	2.3	2.4	3.2	2.2	2.2	2.1
	35	3.2	2.4	2.2	2.9	3.1	2.2	2.2	2.2	3.1	2.2	2.0	2.1
	30	3.0	2.3	2.4	2.8	2.9	2.2	2.1	2.0	2.9	2.3	2.0	2.0
	25	2.9	2.3	2.2	2.6	2.7	2.2	2.0	1.9	2.6	2.1	2.0	1.9
	20	2.7	2.3	2.2	2.6	2.6	2.3	2.0	1.8	2.6	2.3	2.0	1.8

Monthly Values of Zonally Averaged Time Standard Deviation of T, $[\sigma(T)]$, for 1965. Units: ^{o}C.

		JULY				AUGUST				SEPTEMBER			
	p(mb)	100	50	30	10	100	50	30	10	100	50	30	10
Lat.	85	2.1	1.8	1.8	2.0	1.9	2.0	2.2	2.8	2.3	3.1	3.4	5.0
	80	2.1	1.9	1.9	2.2	2.0	2.0	2.2	2.9	2.5	3.0	3.4	4.8
	75	2.1	1.8	1.7	2.2	2.3	2.1	2.4	2.9	2.6	2.8	3.2	4.5
	70	2.2	1.8	1.9	2.2	2.3	2.2	2.4	2.9	2.5	2.6	2.9	4.0
	65	2.1	1.9	2.0	2.2	2.4	2.2	2.3	2.8	2.6	2.5	2.8	3.5
	60	2.3	1.9	2.0	2.1	2.6	2.2	2.2	2.6	2.7	2.4	2.7	3.3
	55	2.5	2.0	2.0	2.1	2.8	2.2	2.1	2.4	3.1	2.5	2.7	3.0
	50	2.7	2.1	2.0	2.2	3.2	2.2	2.1	2.3	3.3	2.5	2.5	2.7
	45	3.0	2.1	2.1	2.0	3.2	2.2	2.0	2.1	3.4	2.4	2.4	2.3
	40	3.0	2.2	2.1	2.1	3.0	2.2	2.0	2.1	3.2	2.5	2.3	2.2
	35	3.0	2.2	2.1	2.0	2.8	2.1	1.9	2.1	3.2	2.4	2.2	2.3
	30	2.9	2.2	2.0	1.9	2.6	2.0	1.9	2.0	2.9	2.3	2.0	2.1
	25	2.7	2.1	2.0	1.8	2.6	2.1	2.0	1.9	2.7	2.1	2.0	1.9
	20	2.6	2.1	2.0	2.0	2.5	2.1	1.9	1.8	2.6	2.1	2.0	1.9
		OCTOBER				NOVEMBER				DECEMBER			
	85	2.8	3.5	3.6	4.6	3.0	3.3	3.5	3.1	5.7	6.9	8.0	6.7
	80	3.0	3.4	3.8	4.4	3.3	3.6	3.6	3.2	5.6	6.7	7.6	6.3
	75	2.9	3.2	3.4	4.5	3.6	4.0	3.9	3.6	5.4	6.5	7.0	5.8
	70	2.8	3.0	3.3	4.4	3.8	4.3	4.2	4.0	5.1	6.2	6.6	5.6
	65	2.8	2.9	3.1	4.2	3.8	4.3	4.5	4.4	4.7	5.8	6.4	5.7
	60	3.0	2.7	3.0	4.0	3.7	4.1	4.4	4.5	4.3	5.4	6.1	5.8
	55	3.2	2.7	2.9	3.7	3.5	3.7	4.1	4.3	4.0	5.0	5.7	5.3
	50	3.5	2.6	2.7	3.3	3.4	3.3	3.7	3.8	4.0	4.4	4.9	4.6
	45	3.3	2.4	2.5	3.0	3.2	2.9	3.3	3.2	3.8	3.7	4.0	3.8
	40	3.2	2.4	2.4	2.6	3.3	2.8	2.9	2.8	3.5	3.1	3.2	3.3
	35	3.2	3.3	2.2	2.5	3.4	2.6	2.7	2.6	3.4	2.7	2.9	2.9
	30	3.1	2.3	2.1	2.3	3.4	2.5	2.5	2.3	3.0	2.6	2.7	2.3
	25	2.8	2.2	2.0	2.0	3.1	2.3	2.3	2.1	2.8	2.4	2.3	2.2
	20	2.6	2.1	1.9	2.0	2.7	2.3	2.1	2.0	2.5	2.3	2.1	2.1

Monthly Values of the Space Standard Deviation of $\bar{u}$, $\sqrt{[\bar{u}^{*2}]}$, for 1965.
Units: m sec^{-1}

		JANUARY				FEBRUARY				MARCH			
	p(mb)	100	50	30	10	100	50	30	10	100	50	30	10
Lat.	85	6.7	13.2	20.0	33.3	4.9	9.2	15.2	27.8	5.4	8.5	11.7	19.6
	80	7.0	12.0	17.0	27.7	7.1	10.6	14.7	24.1	4.0	6.5	9.3	16.2
	75	6.2	9.4	11.5	18.1	7.2	9.9	11.8	16.8	2.6	3.6	5.6	10.3
	70	4.6	5.2	5.2	6.7	5.5	6.4	6.7	7.7	3.3	2.5	3.0	4.5
	65	4.0	4.6	5.9	5.9	4.5	4.5	5.6	6.2	4.8	4.9	5.5	6.8
	60	5.2	8.6	11.5	16.4	6.4	8.2	10.1	14.1	5.2	6.5	8.1	11.5
	55	6.1	10.8	14.9	24.2	7.5	10.3	12.9	19.6	4.8	6.9	9.3	14.6
	50	6.1	10.7	15.2	27.1	6.9	9.8	12.9	21.3	3.8	6.3	9.1	15.4
	45	6.1	9.1	13.3	25.1	6.4	8.1	11.2	19.8	4.0	5.8	8.1	13.9
	40	7.6	7.2	10.3	19.7	7.6	6.4	8.7	16.5	5.8	5.3	6.9	11.4
	35	9.0	5.6	6.9	13.5	8.8	4.5	5.8	12.4	7.4	4.6	5.8	9.0
	30	8.3	4.0	4.1	8.7	8.2	3.3	3.6	8.9	7.2	3.7	4.8	6.9
	25	6.8	3.5	3.2	6.4	6.3	3.3	2.8	6.1	5.3	3.0	3.5	4.6
	20	7.7	4.9	5.1	7.6	6.4	4.3	3.8	5.9	5.0	3.5	3.1	3.1
		APRIL				MAY				JUNE			
	85	1.7	1.8	2.9	4.4	.6	1.4	2.3	3.0	1.4	1.0	1.0	.7
	80	2.8	2.4	2.4	3.6	.6	1.1	2.0	2.8	.9	.8	1.0	.8
	75	3.1	2.6	2.3	2.8	.5	.8	1.3	2.3	1.0	.7	1.0	1.0
	70	2.2	1.5	1.4	1.9	1.8	1.1	1.1	1.7	1.9	1.0	1.0	1.1
	65	1.4	1.3	1.6	1.4	2.6	1.7	1.6	1.7	2.7	1.6	1.2	1.3
	60	2.8	3.2	3.3	3.1	2.5	1.7	1.8	2.4	2.9	1.8	1.4	1.2
	55	3.9	3.9	3.8	4.0	2.1	1.2	1.5	3.0	2.2	1.3	1.0	1.0
	50	4.2	3.3	3.2	3.8	1.8	.9	1.3	2.9	1.5	1.0	1.2	1.3
	45	4.3	2.3	2.1	3.3	2.7	1.3	1.6	2.5	2.7	1.3	1.6	1.3
	40	4.6	1.8	1.5	3.2	3.7	1.6	1.8	2.4	3.9	1.8	1.6	1.2
	35	4.8	2.0	1.8	3.1	4.1	1.8	1.7	2.2	3.8	2.3	1.8	1.6
	30	3.9	2.5	2.5	3.0	3.8	1.8	1.7	2.2	3.0	2.4	2.4	2.6
	25	3.3	2.6	2.7	3.0	4.1	2.4	2.5	2.8	4.4	2.4	2.8	3.4
	20	5.9	3.4	3.3	4.7	7.1	4.1	3.9	4.9	7.8	4.2	4.1	4.5

Table 13 (con't)

Monthly Values of the Space Standard Deviation of $\bar{u}$, $\sqrt{[\overline{u^{*2}}]}$, for 1965.
Units: m sec^{-1}

		JULY				AUGUST				SEPTEMBER			
	p(mb)	100	50	30	10	100	50	30	10	100	50	30	10
Lat.	85	3.7	2.9	2.6	2.2	2.1	2.0	2.2	2.2	2.4	2.6	3.1	4.4
	80	2.2	1.9	1.8	1.8	1.5	1.3	1.4	1.8	1.9	1.7	2.0	3.0
	75	1.1	1.0	1.0	1.2	1.6	1.0	.9	1.3	1.9	1.5	1.4	1.8
	70	1.2	.5	.4	.8	1.8	1.0	.6	.6	2.0	1.3	1.2	1.3
	65	1.5	1.0	.9	1.4	1.3	.6	.4	.8	1.6	.9	1.0	1.5
	60	1.8	1.5	1.4	1.6	1.0	.7	.9	1.2	1.9	1.2	1.4	1.9
	55	2.1	1.5	1.3	1.3	2.0	1.2	1.3	1.3	3.1	2.0	2.0	2.3
	50	2.1	1.3	1.4	1.5	2.8	1.4	1.5	1.3	3.9	2.3	2.2	2.4
	45	2.5	1.0	1.4	1.8	2.8	1.4	1.5	1.5	4.2	2.1	2.0	2.3
	40	3.8	.8	1.2	1.5	2.7	1.3	1.4	1.5	4.8	1.9	1.7	1.8
	35	4.3	1.1	1.0	1.6	2.6	1.3	1.3	1.7	4.9	1.6	1.3	1.8
	30	3.4	1.5	1.4	2.1	2.9	1.6	1.7	2.5	4.1	1.6	1.6	2.3
	25	5.1	2.3	2.3	2.9	4.4	2.3	2.6	3.8	4.4	2.5	2.8	3.3
	20	9.7	5.1	4.2	4.8	7.3	4.2	4.4	6.0	7.2	4.1	4.6	5.5
		OCTOBER				NOVEMBER				DECEMBER			
	85	4.5	4.8	5.1	4.1	3.7	6.1	9.1	16.1	6.2	11.0	14.8	21.7
	80	4.1	4.6	5.0	5.0	4.2	6.4	9.0	15.2	5.9	10.0	13.3	19.3
	75	3.2	3.2	3.5	4.7	4.1	5.7	7.8	12.8	5.1	7.8	10.3	14.6
	70	2.1	2.0	2.6	4.5	3.5	4.2	5.3	8.7	4.4	5.2	6.4	8.6
	65	2.0	3.2	4.4	5.8	2.7	2.4	2.7	5.0	3.7	3.5	3.9	5.9
	60	3.3	4.5	5.8	6.8	2.7	3.8	5.1	8.6	3.1	4.7	6.6	12.1
	55	4.7	5.1	6.3	7.3	3.6	5.9	8.4	14.2	3.2	7.5	11.1	18.8
	50	5.8	5.0	5.6	6.9	4.4	6.9	10.1	17.4	5.0	10.3	14.5	22.9
	45	6.2	4.2	4.1	5.8	5.6	6.7	10.1	17.8	8.2	11.7	15.4	23.0
	40	5.8	3.2	3.3	5.0	6.7	5.8	8.5	15.9	10.7	11.4	14.0	19.6
	35	5.2	2.6	3.0	4.7	6.5	4.4	6.1	12.2	11.0	9.2	10.9	14.9
	30	5.0	2.7	3.0	4.5	4.6	3.3	4.4	8.3	8.7	6.1	7.2	11.6
	25	5.4	3.6	3.7	4.6	2.9	3.1	3.9	6.7	5.2	4.0	5.2	10.7
	20	7.4	5.0	5.4	6.1	5.3	4.2	4.6	7.6	4.6	4.7	6.6	12.5

Monthly Values of the Space Standard Deviation of $\bar{v}$, $\sqrt{[\bar{v}^{*2}]}$, for 1965.
Units: m sec^{-1}

		JANUARY				FEBRUARY				MARCH			
	p(mb)	100	50	30	10	100	50	30	10	100	50	30	10
Lat.	85	7.5	14.4	21.4	35.3	5.8	10.1	16.3	29.3	6.1	9.4	12.8	20.8
	80	9.1	15.0	21.4	34.4	9.2	13.0	18.2	29.5	6.0	8.9	12.2	20.0
	75	10.1	15.5	20.7	32.2	11.6	15.3	19.6	28.8	5.7	8.2	11.2	18.6
	70	10.3	14.8	18.6	28.5	12.5	16.1	19.3	26.7	5.4	7.2	9.8	16.3
	65	9.7	13.0	15.8	24.0	12.0	14.7	17.1	23.2	5.4	6.1	8.2	13.6
	60	8.5	10.3	12.4	19.1	10.4	11.9	13.6	18.6	5.5	5.3	6.7	10.8
	55	7.4	7.7	9.0	14.4	8.6	9.9	10.0	14.1	5.8	4.8	5.6	8.3
	50	6.3	5.3	6.2	10.1	6.8	6.0	6.7	10.0	5.5	4.2	4.6	6.2
	45	5.3	3.8	4.3	6.7	5.2	4.0	4.5	6.8	4.9	3.6	3.8	4.6
	40	4.5	3.0	3.2	4.6	3.8	2.7	3.1	4.7	4.0	3.0	3.1	3.3
	35	4.0	2.5	2.7	3.6	2.9	2.0	2.5	3.5	2.8	2.5	2.6	2.6
	30	3.9	2.2	2.5	3.3	3.1	1.7	2.2	3.2	2.5	2.1	2.2	2.5
	25	4.0	2.0	2.4	3.3	3.9	1.8	2.1	3.4	3.5	2.1	2.2	2.9
	20	4.2	2.9	3.3	3.8	5.4	2.7	2.6	4.0	5.6	3.6	3.5	4.2
		APRIL				MAY				JUNE			
	85	2.2	2.3	3.6	4.8	.7	1.6	2.4	3.1	1.7	1.1	1.1	.8
	80	3.3	2.9	3.5	4.7	1.2	1.5	2.4	3.2	1.5	1.0	1.1	.9
	75	4.1	3.7	3.8	4.6	1.1	1.4	2.3	3.2	1.5	1.1	1.3	1.2
	70	4.4	4.0	3.9	4.6	.9	1.3	2.0	3.1	1.8	1.3	1.4	1.4
	65	4.1	3.5	3.4	4.2	1.3	1.3	1.8	2.9	2.3	1.4	1.5	1.5
	60	3.4	2.6	2.4	3.2	1.9	1.4	1.7	2.6	2.6	1.7	1.6	1.5
	55	3.2	2.0	1.8	2.5	2.5	1.7	1.6	2.2	2.9	1.9	1.8	1.4
	50	3.2	2.0	1.8	2.3	3.0	1.8	1.5	1.9	2.8	1.9	1.7	1.3
	45	3.2	2.1	1.9	2.1	3.5	2.1	1.5	1.6	2.5	1.8	1.6	1.4
	40	3.3	2.1	1.9	2.0	4.0	2.2	1.6	1.7	2.4	1.8	1.8	1.7
	35	3.4	2.1	1.8	2.0	4.3	2.4	1.8	1.8	2.9	1.9	1.9	1.9
	30	3.8	2.1	1.7	2.3	4.5	2.5	1.9	1.9	3.4	2.0	1.8	2.1
	25	4.3	2.4	2.0	2.8	4.6	2.7	2.2	2.2	3.8	2.3	2.1	2.6
	20	5.3	3.6	3.4	4.1	4.9	3.4	3.1	3.0	4.8	3.3	3.4	4.2

Table 14 (cont'd)

Monthly Values of the Space Standard Deviation of $\bar{v}$, $\sqrt{\left[\bar{v}^{*2}\right]}$, for 1965.
Units: m sec^{-1}

		JULY				AUGUST				SEPTEMBER			
	p(mb)	100	50	30	10	100	50	30	10	100	50	30	10
Lat.	85	4.4	3.4	3.1	2.4	2.5	2.4	2.7	2.5	2.9	3.1	3.8	5.1
	80	3.8	3.0	2.7	2.3	2.2	2.1	2.3	2.4	2.9	2.8	3.3	4.6
	75	3.2	2.6	2.4	2.3	2.1	1.8	2.1	2.4	3.1	2.7	3.0	4.2
	70	2.9	2.3	2.2	2.1	2.4	1.8	1.9	2.3	3.4	2.7	2.8	3.7
	65	2.7	2.0	1.9	1.9	2.7	1.8	1.8	2.0	3.8	2.7	2.6	3.2
	60	2.6	1.8	1.7	1.6	2.8	1.8	1.6	1.7	3.9	2.5	2.3	2.6
	55	2.8	1.8	1.7	1.5	2.6	1.7	1.6	1.5	4.0	2.3	1.9	2.1
	50	3.0	1.8	1.6	1.3	2.5	1.7	1.5	1.3	3.9	1.9	1.4	1.8
	45	3.1	1.8	1.6	1.3	2.7	1.6	1.4	1.5	3.8	1.5	1.1	1.7
	40	3.3	1.9	1.6	1.5	3.0	1.7	1.5	1.8	3.6	1.4	1.1	1.9
	35	3.5	1.9	1.7	1.8	3.2	1.9	1.7	2.1	3.2	1.5	1.3	1.9
	30	3.8	2.1	2.0	2.3	3.3	2.1	1.9	2.4	3.1	1.8	1.6	1.9
	25	4.1	2.7	2.6	3.1	3.4	2.3	2.4	3.1	3.3	2.2	2.2	2.5
	20	4.8	4.0	4.1	5.1	3.9	3.0	3.5	4.9	3.5	3.0	3.5	4.0
		OCTOBER				NOVEMBER				DECEMBER			
	85	4.7	4.9	5.1	4.0	3.9	6.3	9.5	16.6	6.3	11.3	15.2	22.5
	80	4.9	5.2	5.5	4.7	5.1	7.5	10.5	17.4	6.6	11.5	15.3	22.5
	75	5.1	5.3	5.7	5.3	6.1	8.5	11.4	18.0	6.8	11.4	15.1	21.9
	70	5.2	5.0	5.2	5.3	6.8	9.0	11.7	17.9	7.2	11.3	14.7	20.8
	65	5.0	4.4	4.4	4.8	7.0	8.8	11.2	16.6	7.7	10.9	13.9	19.1
	60	4.7	3.6	3.4	3.9	6.6	7.8	9.7	14.3	7.9	10.1	12.6	16.8
	55	4.5	2.9	2.7	3.1	6.1	6.5	7.9	11.5	8.0	9.3	11.0	14.4
	50	4.4	2.4	2.2	2.8	5.2	5.0	6.1	8.8	7.5	7.6	8.8	11.7
	45	4.3	2.3	2.1	2.8	4.3	3.8	4.6	6.9	6.4	5.9	6.5	9.3
	40	4.2	2.2	2.1	2.7	3.5	2.9	3.7	5.7	4.9	4.3	4.7	7.3
	35	4.0	2.0	2.1	2.4	3.2	2.4	3.1	4.7	3.5	3.0	3.5	5.9
	30	3.9	2.0	2.1	2.4	3.4	2.0	2.4	3.6	2.8	2.3	2.9	5.1
	25	3.8	2.2	2.4	2.7	3.7	2.0	1.8	2.7	3.1	2.3	2.8	4.9
	20	4.1	3.0	3.3	3.8	4.2	2.8	2.4	2.9	4.1	3.2	3.8	6.2

Table 10

Monthly Values of the Space Standard Deviation of $\overline{T}, \sqrt{\left[\overline{T^{*2}}\right]}$, for 1965.
Units: °C

		JANUARY				FEBRUARY				MARCH			
	p(mb)	100	50	30	10	100	50	30	10	100	50	30	10
Lat.	85	1.8	2.6	3.2	2.9	1.7	2.6	3.5	3.9	1.6	1.9	2.3	3.2
	80	3.5	5.1	6.2	6.1	3.1	5.3	6.7	7.5	2.3	3.5	4.2	5.8
	75	5.1	7.5	8.8	9.0	4.6	7.7	9.2	10.4	2.9	4.8	5.8	7.4
	70	6.4	9.2	10.6	11.3	6.1	9.2	10.6	12.1	3.7	5.8	6.9	8.0
	65	6.7	9.6	11.2	12.1	6.9	9.4	10.7	12.6	4.1	6.2	7.2	7.7
	60	6.1	8.9	10.5	11.2	6.3	8.5	9.8	11.7	4.1	6.0	6.7	6.5
	55	5.0	7.3	8.8	9.2	5.2	6.8	8.0	9.8	4.0	5.2	5.7	4.9
	50	4.0	5.4	6.5	6.8	4.2	4.9	6.0	7.5	3.9	4.2	4.4	3.3
	45	3.2	3.6	4.3	4.6	3.4	3.4	4.1	5.2	3.6	3.2	3.1	2.0
	40	2.5	2.3	2.7	2.8	2.6	2.3	2.7	3.3	2.8	2.3	2.1	1.2
	35	2.0	1.7	1.7	1.5	1.5	1.4	1.7	1.8	1.7	1.5	1.3	1.0
	30	2.1	1.1	1.0	.7	1.7	.7	1.0	.9	1.6	.8	.8	1.1
	25	2.6	.6	.4	.6	2.3	.5	.8	.7	2.2	.6	.6	1.2
	20	2.7	.5	.4	.5	2.5	.9	.8	.6	2.5	.8	.5	1.1
		APRIL				MAY				JUNE			
	85	.5	.5	.4	.6	.9	.9	.6	.4	.8	.7	.5	.5
	80	1.1	1.2	1.2	1.5	1.5	1.4	1.0	.9	1.0	.9	.8	1.1
	75	1.5	1.8	1.9	2.4	1.8	1.7	1.3	1.3	.9	.8	.5	1.4
	70	1.8	2.2	2.5	3.1	1.6	1.8	1.7	1.5	.8	.8	.5	1.4
	65	1.7	2.4	2.7	3.2	1.3	1.7	1.8	1.3	1.0	.9	.6	1.1
	60	1.5	2.2	2.5	2.9	1.2	1.4	1.5	1.0	1.2	.9	.7	.8
	55	1.7	2.0	2.1	2.3	1.3	1.3	1.2	.9	1.3	.9	.8	.8
	50	2.1	1.8	1.8	1.6	1.5	1.3	.9	.8	1.3	.9	.8	.8
	45	2.5	1.6	1.4	.9	2.0	1.3	.7	.6	1.4	.8	.5	.7
	40	2.5	1.3	1.1	.9	2.6	1.1	.4	.7	1.6	.7	.5	.5
	35	2.4	1.2	.8	1.5	2.9	.9	.3	.8	2.1	.8	.6	.5
	30	2.4	1.1	.5	1.7	2.9	.9	.3	.9	2.5	.8	.5	.4
	25	2.1	.9	.4	1.6	2.5	.9	.4	.9	2.3	.8	.4	.3
	20	1.8	.8	.3	1.5	2.0	1.0	.4	.8	1.9	.8	.4	.4

Table 15 (con't)

Monthly Values of the Space Standard Deviation of $\overline{T}$, $\sqrt{\left[\overline{T^{*2}}\right]}$, for 1965.
Units: ^{o}C

		JULY				AUGUST				SEPTEMBER			
	p(mb)	100	50	30	10	100	50	30	10	100	50	30	10
Lat.	85	.8	.6	.4	.5	.3	.4	.4	.4	.6	.8	.8	.9
	80	1.2	.8	.4	1.1	.4	.4	.4	1.0	.9	1.2	1.1	1.5
	75	1.1	.7	.4	1.5	.6	.6	.6	1.2	1.1	1.3	1.3	1.5
	70	.9	.8	.7	1.5	.8	.9	.8	1.2	1.3	1.4	1.4	1.4
	65	1.0	.8	.8	1.1	1.1	1.0	.8	.9	1.5	1.5	1.4	1.4
	60	1.0	.9	.7	.8	1.3	1.0	.8	.7	1.7	1.6	1.5	1.4
	55	1.0	.9	.6	.6	1.3	1.0	.7	.5	1.9	1.6	1.5	1.2
	50	1.2	.9	.4	.6	1.0	.8	.5	.5	2.1	1.5	1.2	1.1
	45	1.4	.7	.3	.5	1.4	.6	.3	.6	2.3	1.2	.9	1.0
	40	1.9	.8	.4	.4	1.7	.6	.4	.6	2.3	.9	.8	.9
	35	2.9	.9	.6	.5	2.1	.6	.6	.5	2.5	.7	.8	.6
	30	3.4	.9	.5	.5	2.3	.5	.6	.6	2.6	.5	.5	.4
	25	2.9	.7	.5	.4	2.0	.5	.6	.6	2.2	.5	.4	.4
	20	2.1	.7	.5	.4	1.5	.5	.6	.6	1.8	.5	.4	.4
		OCTOBER				NOVEMBER				DECEMBER			
	85	.4	.4	.3	.3	1.5	1.7	.7	1.4	2.4	2.4	2.3	.9
	80	.8	.8	.6	.7	2.8	3.4	2.5	3.2	4.2	4.8	4.7	2.2
	75	1.1	1.2	1.3	1.3	3.7	5.1	4.8	5.2	5.6	6.7	6.6	3.8
	70	1.5	1.5	1.9	2.1	4.4	6.2	6.6	6.8	6.4	7.8	7.9	5.3
	65	1.8	1.8	2.3	2.5	4.9	6.7	7.6	7.5	6.6	8.2	8.4	6.0
	60	2.0	2.0	2.4	2.4	4.8	6.5	7.6	7.3	6.1	7.6	7.9	5.7
	55	2.3	2.1	2.4	2.0	4.2	5.6	6.6	6.5	5.2	6.5	6.9	5.1
	50	2.3	2.0	2.2	1.6	3.2	4.3	5.1	5.2	3.9	5.0	5.7	4.6
	45	2.3	1.6	1.8	1.1	2.2	2.9	3.4	3.6	2.6	3.5	4.4	4.2
	40	2.7	1.2	1.3	1.1	1.6	1.9	2.2	2.2	1.8	2.4	3.2	3.8
	35	2.8	.9	1.0	1.2	1.4	1.3	1.6	1.3	1.2	1.6	2.4	3.2
	30	2.3	.8	.8	1.1	1.8	1.0	1.4	1.0	1.6	.9	1.7	2.4
	25	1.8	.7	.5	.8	1.9	.8	.9	1.1	2.1	.7	1.2	1.7
	20	1.6	.5	.5	.5	1.9	.6	.5	.9	2.2	.8	1.1	1.2

Table 16:

Monthly values of the seasonal correction term, S(M), and the horizontal eddy flux terms, $F(R)_{\varphi}$, in the angular momentum balance for 1965 for polar caps north of 20°, 45° and 60° (100 to 50 mb. layer). Units: 10^{24} gm cm sec^{-2}; t. e. = transient eddy; s. e. = standing eddy. Also, total angular momentum, M, for cap north of 20°. Units: 10^{32} gm cm^2 sec^{-1}

	Jan.	Feb.	March	April	May	June
North of 20°						
S(M)	.5	-1.5	-5.6	-5.7	-8.1	-7.0
$F(R)_{\varphi}$ t. e.	2.8	1.3	1.9	1.4	1.8	-1.4
$F(R)_{\varphi}$ s. e.	6.1	4.5	-6.1	.5	11.0	1.7
Deficit	-8.4	-7.3	-1.4	-7.6	-20.9	-7.3
M	13.7	13.7	13.7	13.4	13.3	13.1
North of 45°						
S(M)	-1.4	-1.1	-2.6	-2.7	-2.4	-.8
$F(R)_{\varphi}$ t. e.	3.1	2.2	4.3	2.9	1.4	.2
$F(R)_{\varphi}$ s. e.	.7	2.7	3.1	-1.3	-1.3	-.9
Deficit	-5.2	-6.0	-10.0	-4.3	-2.5	-.1
North of 60°						
S(M)	-.7	-.3	-1.0	-2.8	-.5	-.4
$F(R)_{\varphi}$ t. e.	.9	-.8	.6	.1	.7	0
$F(R)_{\varphi}$ s. e.	-6.0	-4.0	1.8	-.8	.1	.2
Deficit	4.4	4.5	-3.4	-1.1	-1.3	-.6

Table 16: (con't)

Monthly values of the seasonal correction term, S(M), and the horizontal eddy flux terms, $F(R)_{\phi}$, in the angular momentum balance for 1965 for polar caps north of 20°, 45° and 60° (100 to 50 mb. layer). Units: 10^{24} gm cm sec^{-2}; t. e. = transient eddy; s. e. = standing eddy. Also, total angular momentum, M, for cap north of 20°. Units: 10^{32} gm cm^2 sec^{-1}

	July	Aug.	Sep.	Oct.	Nov.	Dec.
North of 20°						
S(M)	-.5	3.8	8.9	8.9	5.2	1.5
$F(R)_{\phi}$ t. e.	-2.0	-.3	0	-.3	-.10	4.2
$F(R)_{\phi}$ s. e.	9.0	4.4	7.6	7.6	2.8	6.2
Deficit	-7.5	-.3	1.3	1.6	2.5	-8.9
M	13.0	13.0	13.2	13.4	13.6	13.7
North of 45°						
S(M)	.3	1.8	2.7	3.3	-1.2	1.8
$F(R)_{\phi}$ t. e.	-.2	1.2	.2	1.7	2.5	4.1
$F(R)_{\phi}$ s. e.	.2	-.3	-.5	3.5	3.5	3.5
Deficit	.3	.9	3.0	-1.9	-7.2	-5.8
North of 60°						
S(M)	.2	.7	.9	1.6	-1.9	2.8
$F(R)_{\phi}$ t. e.	-.2	.2	0	0	2.0	-.9
$F(R)_{\phi}$ s. e.	.6	-.1	0	.3	-1.1	-.1
Deficit	-.6	.6	.9	1.3	-2.8	1.8

Table 17:

Monthly values of the seasonal correction term, S(M), and the horizontal eddy flux terms, $F(R)_\varphi$, in the angular momentum balance for 1965 for polar caps north of 20°, 45°, and 60° (50 to 30 mb. layer). Units: 10^{24} gm cm sec^{-2}; t. e. = transient eddy; s. e. = standing eddy. Also, total angular momentum, M, for cap north of 20°. Units: 10^{32} gm cm^2 sec^{-1}.

	Jan.	Feb.	March	April	May	June
North of 20°						
S(M)	.2	-1.5	-3.1	-1.9	-3.1	-2.9
$F(R)_\varphi$ t. e.	.6	-.6	.1	-.2	-.4	-.6
$F(R)_\varphi$ s. e.	1.0	1.2	-.3	.1	.7	-.9
Deficit	-1.4	-2.1	-2.9	-1.8	-3.3	-1.4
M	5.4	5.4	5.3	5.2	5.2	5.1
North of 45°						
S(M)	-.8	-.4	-2.0	-1.4	-1.0	-.6
$F(R)_\varphi$ t. e.	1.7	1.2	2.3	1.0	.4	0
$F(R)_\varphi$ s. e.	1.0	2.1	2.8	0	-.3	-.2
Deficit	-3.5	-3.7	-7.1	-2.4	-1.1	-.4
North of 60°						
S(M)	-.4	-.1	-.8	-1.3	-.1	-.3
$F(R)_\varphi$ t. e.	1.3	.1	.7	.6	.4	0
$F(R)_\varphi$ s. e.	-1.8	-.6	3.2	0	.2	-.1
Deficit	.1	.4	-1.7	-1.9	-.7	-.2

Table 17 (con't)

Monthly values of the seasonal correction term, S(M), and the horizontal eddy flux terms, $F(R)_\varphi$, in the angular momentum balance for 1965 for polar caps north of 20°, 45°, and 60° (50 to 30 mb. layer). Units: 10^{24}gm cm sec^{-2}; t. e. = transient eddy; s. e. = standing eddy. Also, total angular momentum, M, for cap north of 20°. Units: 10^{32} gm cm^2 sec^{-1}.

	July	Aug.	Sep.	Oct.	Nov.	Dec.
North of 20°						
S(M)	.4	2.1	4.3	4.1	2.3	-.2
$F(R)_\varphi$ t. e.	-.5	-.2	0	-.7	-.1	.6
$F(R)_\varphi$ s. e.	.5	.6	1.3	.2	-.5	.4
Deficit	.4	1.7	3.0	4.6	2.9	-1.2
M	5.0	5.1	5.2	5.3	5.4	5.4
North of 45°						
S(M)	.2	1.0	1.5	1.8	-.4	.6
$F(R)_\varphi$ t. e.	0	.1	.1	.5	1.4	1.8
$F(R)_\varphi$ s. e.	.2	0	0	.9	2.7	3.8
Deficit	0	.9	1.4	.4	-4.5	-5.0
North of 60°						
S(M)	.2	.3	.6	.8	-1.0	1.3
$F(R)_\varphi$ t. e.	0	0	.1	.1	1.8	0
$F(R)_\varphi$ s. e.	.2	.1	.1	.5	.9	1.8
Deficit	0	.2	.4	.2	-1.7	-.5

Table 18:

Monthly values of the seasonal correction term, S(M), and the horizontal eddy flux terms, $F(R)_\varphi$, in the angular momentum balance for 1965 for polar caps north of 20°, 45° and 60° (30 to 10 mb. layer). Units: 10^{24} gm cm sec^{-2}; t. e. = transient eddy; s. e. = standing eddy. Also, total angular momentum, M, for cap north of 20°. Units: 10^{32} gm cm^2 sec^{-1}.

	Jan.	Feb.	March	April	May	June
North of 20°						
S(M)	.5	-2.8	-4.8	-1.6	-3.7	-3.6
$F(R)_\varphi$ t. e.	1.0	-.9	-.2	-.7	-1.1	-.2
$F(R)_\varphi$ s. e.	.7	1.0	-.6	-1.6	-.2	-1.9
Deficit	-1.2	-2.9	-4.0	.7	-2.4	-1.4
M	5.5	5.4	5.3	5.3	5.2	5.0
North of 45°						
S(M)	-1.6	-.7	-3.3	-1.1	-1.3	-.8
$F(R)_\varphi$ t. e.	4.0	2.9	5.8	1.5	.7	0
$F(R)_\varphi$ s. e.	6.7	5.7	5.2	.4	-.2	-.1
Deficit	-12.3	-9.3	-14.3	-3.0	-1.8	-.7
North of 60°						
S(M)	-.6	-.2	-1.5	-1.3	0	-.3
$F(R)_\varphi$ t. e.	3.7	1.7	2.5	1.7	.7	0
$F(R)_\varphi$ s. e.	1.6	.9	7.0	.4	-.3	.1
Deficit	-5.9	-2.8	-11.0	-3.4	-.4	-.4

Table 18 (con't)

Monthly values of the seasonal correction term, S(M), and the horizontal eddy flux terms, $F(R)_\varphi$, in the angular momentum balance for 1965 for polar caps north of 20°, 45° and 60° (30 to 10 mb. layer). Units: 10^{24} gm cm sec^{-2}; t. e. = transient eddy; s. e. = standing eddy. Also, total angular momentum, M, for cap north of 20°. Units: 10^{32} gm cm^2 sec^{-1}.

	July	Aug.	Sep.	Oct.	Nov.	Dec.
North of 20°						
S(M)	.7	3.0	5.7	5.6	2.9	-.7
$F(R)_\varphi$ t. e.	-.8	.1	.6	-.8	.4	1.8
$F(R)_\varphi$ s. e.	-.2	.4	1.2	.6	-.9	-2.0
Deficit	1.7	2.5	3.9	5.8	3.4	-.5
M	5.0	5.1	5.2	5.3	5.4	5.5
North of 45°						
S(M)	.4	1.5	2.3	2.4	-.4	.3
$F(R)_\varphi$ t. e.	.1	0	.3	1.1	3.7	4.6
$F(R)_\varphi$ s. e.	.2	.1	.3	1.7	7.4	13.0
Deficit	.1	1.4	1.7	-.4	-11.5	-17.3
North of 60°						
S(M)	.3	.4	.9	1.1	-1.3	1.6
$F(R)_\varphi$ t. e.	0	0	.2	.3	3.2	2.0
$F(R)_\varphi$ s. e.	.2	.2	.1	1.5	5.1	7.4
Deficit	.1	.2	.6	-.7	-9.6	-7.8

Table 19:

Comparison of three month mean values of terms in the momentum budget for polar caps north of 20^{o} and 60^{o} with values computed by Oort 1963 for polar caps north of 30^{o} and 60^{o} (100 to 30 mb. layer). Units: 10^{24} gm cm sec^{-2}. M_r in units of 10^{32} gm cm^2 sec^{-1}.

I = January-March; II = April-June; III = July-September; IV = October-December

Polar caps north of 20^{o} and 30^{o}

	I		II		III		IV	
	Present Results	Oort (1963)	Present Results	Oort (1963)	Present Results	Oort (1963)	Present Results	Oort (1963)
S(M)	-3.7	-4.5	-9.6	-6.1	6.3	4.2	7.3	6.6
$F(R)_{\varphi}$ horizontal eddy part	4.1	14.5	4.5	8.6	6.8	4.3	6.8	15.6
M_r	.74	.82	.13	0	-.16	-.55	.61	.50

Polar cap north of 60^{o}

S(M)	-1.1	-1.3	-1.8	-.7	1.0	.7	1.2	1.1
$F(R)_{\varphi}$ horizontal eddy part	-1.6	-1.8	.5	-.4	.3	.3	1.8	2.4

Table 20:

Terms in the zonal kinetic energy equation for a polar cap north of 20° (100 to 50 mb. layer). Units: 10^{18} ergs sec^{-1} Also, total zonal kinetic energy and total eddy kinetic energy in cap. Units: 10^{25} ergs; t. e. = transient eddy; s. e. = standing eddy.

	Jan.	Feb.	March	April	May	June
$S(K_Z)$	-3.2	-4.1	-18.8	-19.0	-7.8	2.3
$C(K_E, K_Z)$t. e.	16.4	1.2	.74	-2.8	1.2	.42
$C(K_E, K_Z)$s. e.	-14.6	-7.6	11.8	-.21	4.2	-3.0
$We(K_Z)$t. e.	6.1	5.3	6.0	4.4	3.9	4.2
$We(K_Z)$s. e.	13.9	12.2	-8.9	5.1	2.5	.90
$C(K_E, K_Z) + We(K_Z)$	21.8	11.1	9.6	6.5	11.8	2.5
$C(A_Z, K_Z)$	(-89.7)*			(-17.8)		
$C(A_Z, K_Z)$	-91.6			-22.0		
Deficit	-25.0	-15.2	-28.4	-25.5	-19.6	-.2
K_Z	14.3	13.2	10.4	5.2	2.3	2.2
K_E t. e.	5.3	3.5	4.6	2.9	1.4	.97
K_E s. e.	4.2	4.4	2.1	.93	.72	.64

* parenthesized quantities have been inferred from zonal available potential energy balance requirements.

Table 20 (con't)

Terms in the zonal kinetic energy equation for a polar cap north of 20°(100 to 50 mb. layer). Units: 10^{18} ergs sec^{-1} Also, total zonal kinetic energy and total eddy kinetic energy in cap. Units: 10^{25} ergs; t. e. = transient eddy; s. e. = standing eddy.

	July	Aug.	Sep.	Oct.	Nov.	Dec.
$S(K_Z)$	-.83	-1.4	3.5	17.9	15.8	1.5
$C(K_E, K_Z)$t. e.	-1.8	3.3	1.9	6.1	1.8	11.9
$C(K_E, K_Z)$s. e.	7.9	5.6	9.9	17.5	14.1	8.5
$We(K_Z)$t. e.	5.5	.47	.47	.69	.39	10.5
$We(K_Z)$s. e.	-8.6	-9.0	-9.0	2.4	10.7	17.9
$C(K_E, K_Z) + We(K_Z)$	3.0	.4	3.3	26.7	27.0	48.8
$C(A_Z K_Z)$	(-37.9)*					
$C(A_Z K_Z)$	-47.7					
Deficit	-3.8	-1.8	-.2	-8.8	-11.2	-47.3
K_Z	2.8	2.5	2.4	5.3	9.3	11.6
K_E t. e.	.79	.89	1.3	1.8	2.8	3.5
K_E s. e.	.79	.56	.83	1.5	2.1	4.2

*parenthesized quantities have been inferred from zonal available potential energy balance requirements.

Table 21:

Terms in the zonal kinetic energy equation for a polar cap North of 20°(50 to 30 mb. layer). Units: 10^{18} ergs sec^{-1}. Also, total zonal kinetic energy and total eddy kinetic energy in cap. Units: 10^{25} ergs; t. e. = transient eddy; s. e. = standing eddy.

	Jan.	Feb.	March	April	May	June
$S(K_Z)$	-5.7	-3.0	-9.9	-5.2	1.4	6.4
$C(K_E, K_Z)$t. e.	15.8	5.9	7.4	2.00	-3.6	-.12
$C(K_E, K_Z)$s. e.	-13.9	-.07	25.9	-.23	-.59	-2.1
$We(K_Z)$t. e.	.28	-.39	.06	.08	.54	2.3
$We(K_Z)$s. e.	.49	1,1	.20	.12	-.42	3.4
$C(K_E, K_Z) + We(K_Z)$	2.7	6.5	33.2	2.0	-4.1	3.5
$C(A_Z, K_Z)$	(-72.8)*			(-6.4)		
$C(A_Z, K_Z)$	-49.8			-6.4		
Deficit	-8.4	-9.5	-43.1	-7.2	5.5	2.9
K_Z	4.8	3.8	2.0	.36	.20	1.5
K_E t. e.	2.1	1.5	2.5	1.2	.37	.23
K_E s. e.	2.6	2.3	1.0	.22	.14	.14

* parenthesized quantities have been inferred from zonal available potential energy balance requirements.

Table 21 (con't)

Terms in the zonal kinetic energy equation for a polar cap north of 20° (50 to 30 mb. layer). Units: 10^{18} ergs sec^{-1}. Also, total zonal kinetic energy and total eddy kinetic energy in cap. Units: 10^{25} ergs; t. e. = transient eddy; s. e. = standing eddy.

	July	Aug.	Sep.	Oct.	Nov.	Dec.
$S(K_Z)$	-1.4	-2.1	-2.5	6.4	3.0	-2.4
$C(K_E, K_Z)$ t. e.	-.21	.18	.19	1.5	1.9	3.0
$C(K_E, K_Z)$ s. e.	.19	.10	.96	5.9	6.6	.42
$We(K_Z)$ t. e.	2.3	.98	-.23	.95	0	.60
$We(K_Z)$ s. e.	-2.3	-2.2	-3.6	-2.0	.16	.32
$C(K_E, K_Z) + We(K_Z)$	-.02	-.94	-2.7	6.2	8.7	4.3
$C(A_Z, K_Z)$	(-9.8) *					
$C(A_Z, K_Z)$	-12.1					
Deficit	-1.4	-1.3	.2	.2	-5.7	-6.7
K_Z	2.3	1.6	.83	1.4	2.2	2.2
K_E t. e.	.20	.21	.34	.55	1.3	1.9
K_E s. e.	.14	.12	.15	.45	1.2	2.5

* Parenthesized quantities have been inferred from zonal available potential energy balance requirements.

Table 22:

Terms in the zonal kinetic energy equation for a polar cap North of 20° (30 to 10 mb. layer) Units: 10^{18} ergs sec^{-1}. Also, total zonal kinetic energy and total eddy kinetic energy in cap. Units: 10^{25} ergs; t. e. = transient eddy; s. e. standing eddy.

	Jan.	Feb.	March	April	May	June
$S(K_Z)$	-14.7	-6.2	-19.3	-3.1	3.2	10.5
$C(K_E, K_Z)$ t. e.	58.8	27.0	31.0	3.6	-1.7	.28
$C(K_E, K_Z)$ s. e.	39.7	28.5	68.2	-.54	-.88	-3.3
$We(K_Z)$ t. e.	.55	-.54	.04	.61	2.3	1.0
$We(K_Z)$ s. e.	.36	.65	.15	1.5	.45	9.4
$C(K_E, K_Z) + We(K_Z)$	99.4	55.6	99.4	5.2	.17	7.4
$C(A_Z, K_Z)$	(-108.3)*			(5.0)		
$C(A_Z, K_Z)$	-134.1			5.3		
Deficit	-114.1	-61.8	-118.7	-8.3	3.0	3.1
K_Z	8.3	5.5	2.4	.20	.50	2.8
K_E t. e.	3.2	2.4	4.2	1.7	.55	.30
K_E s. e.	6.0	4.8	2.2	.28	.17	.14

* Parenthesized quantities have been inferred from zonal available potential energy balance requirements.

Table 22 (con't)

Terms in the zonal kinetic energy equation for a polar cap North of 20^{o} (30 to 10 mb. layer). Units: 10^{18} ergs sec^{-1} Also, total zonal kinetic energy and total eddy kinetic energy in cap. Units: 10^{25} ergs; t. e. = transient eddy; s. e. = standing eddy.

	July	Aug.	Sep.	Oct.	Nov.	Dec.
$S(K_Z)$	-2.7	-5.4	-3.1	12.1	3.7	-6.0
$C(K_E, K_Z)$ t. e.	-.42	.22	1.5	5.2	15.7	-1.4
$C(K_E, K_Z)$ s. e.	-.57	.09	1.9	13.9	3.1	-15.7
$We(K_Z)$ t. e.	4.5	-.63	-2.0	1.2	.13	5.2
$We(K_Z)$ s. e.	1.5	-1.8	-4.4	-.99	.04	-6.1
$C(K_E, K_Z) + We(K_Z)$	5.0	-2.1	-3.0	19.3	19.0	-18.0
$C(A_Z, K_Z)$	(-7.0)*					
$C(A_Z, K_Z)$	-6.6					
Deficit	-7.7	-3.3	-.1	-7.2	-15.3	12.0
K_Z	4.1	2.6	1.3	2.4	4,1	3.8
K_E t. e.	.29	.30	.47	.84	2.2	3.9
K_E s. e.	.15	.17	.20	.61	2.9	5.1

* Parenthesized quantities have been inferred from zonal available potential energy balance requirements.

Table 23:

Comparison of three month mean values of terms in the zonal kinetic energy equation for a polar cap north of 20^{o} with values computed by Oort (1963) for the entire northern hemisphere (100 to 30 mb. layer). Units: 10^{18} ergs sec^{-1}; t. e. = transient eddy; s. e. = standing eddy. K_Z and K_E in units of 10^{25} ergs.

I = January - March; II = April - June

	I		II	
	Present Results	Oort (1963)	Present Results	Oort (1963)
$S(K_Z)$	-14.9	-12.6	-7.3	.4
$C(K_E, K_Z)$ t. e.	15.8	5.8	.10	14.7
$C(K_E, K_Z)$ s. e.	.5	24.2	-.65	3.2
$We(K_Z)$	12.1	.5	9.0	.2
$C(K_E, K_Z) + We(K_Z)$	28.4	30.5	8.5	18.1
K_Z	16.2	12.7	3.9	3.7
K_E t. e.	6.5	6.0	2.4	5.2
K_E s. e.	5.5	2.0	1.0	.61

Table 23: (con't)

Comparison of three month mean values of terms in the zonal kinetic energy equation for a polar cap north of 20° with values computed by Oort (1963) for the entire northern hemisphere (100 to 30 mb. layer). Units: 10^{18} ergs sec^{-1}; t. e. = transient eddy; s. e. = standing eddy. K_Z and K_E in units of 10^{25} ergs.

III = July - September; IV = October - December

	III		IV	
	Present Results	Oort (1963)	Present Results	Oort (1963)
$S(K_Z)$	-1.5	-9.2	14.1	26.5
$C(K_E, K_Z)$ t. e.	1.2	9.0	8.7	29.8
$C(K_E, K_Z)$ s. e.	8.2	4.5	17.7	14.1
$We(K_Z)$	-8.4	-.4	15.2	-.3
$C(K_E, K_Z) + We(K_Z)$	1.0	13.1	41.6	43.6
K_Z	4.1	6.5	10.7	8.4
K_E t. e.	1.2	3.2	4.0	5.0
K_E s. e.	.9	1.4	4.0	1.8

Table 24:

Terms in the zonal available potential energy equation for a polar cap north of 20° (100 to 50 mb. layer). Units: 10^{18} ergs sec^{-1}. Also, total zonal available potential energy in cap. Units: 10^{25} ergs; t. e. = transient eddy; s. e. = standing eddy.

	Jan.	Feb.	March	April	May	June
$S(A_Z)$	-1.1	5.8	2.7	7.7	8.3	5.3
$C(A_E, A_Z)$ t. e.	-18.4	-11.4	-6.2	20.1	10.9	9.8
$C(A_E, A_Z)$ s. e.	-45.2	-18.8	5.4	24.5	37.1	14.9
$C(A_Z K_Z)$	91.6			22.0		
$C(A_Z K_Z)$	(89.7)*			(17.8)		
$G(A_Z)$	-27.2			-54.7		
A_Z	5.3	5.7	5.8	7.7	10.4	12.2
A_E **	4.0	3.7	2.0	.63	.56	.32

* Parenthesized quantities are inferred as balance requirements.

** Values of A_E are probably too small due to an approximation in their calculation.

Table 24 (con't)

Terms in the zonal available potential energy equation for a polar cap north of 20° (100 to 50 mb. layer). Units: 10^{18} ergs sec^{-1}. Also, total zonal available potential energy in cap. Units: 10^{25} ergs; t. e. = transient eddy; s. e. = standing eddy.

	July	Aug.	Sep.	Oct.	Nov.	Dec.
$S(A_Z)$	-4.5	-12.0	-6.0	-8.4	-5.7	.50
$C(A_E, A_Z)$ t. e.	6.1	9.7	15.9	14.6	9.9	9.7
$C(A_E, A_Z)$ s. e.	9.6	10.0	17.7	12.3	7.3	44.4
$C(A_Z, K_Z)$	47.7					
$C(A_Z K_Z)$	(37.9)*					
$G(A_Z)$	-58.1					
A_Z	11.5	10.0	8.0	5.8	5.0	5.6
A_E**	.45	.28	.50	.62	2.2	3.4

* Parenthesized quantities are inferred as balance requirements.
** Values of A_E are probably too small due to an approximation in their calculation.

Table 25:

Terms in the zonal available potential energy equation for a polar cap north of 20^{o} (50 to 30 mb. layer). Units: 10^{18} ergs sec^{-1}. Also, total zonal available potential energy in cap. Units: 10^{25} ergs; t. e. = transient eddy; s. e. = standing eddy.

	Jan.	Feb.	March	April	May	June
$S(A_Z)$	-4.0	-.33	-.15	-.18	1.4	1.3
$C(A_E, A_Z)$ t. e.	-22.2	-11.2	-.97	1.8	1.9	1.4
$C(A_E, A_Z)$ s. e.	-49.1	-18.1	-3.3	4.2	1.6	.05
$C(A_Z, K_Z)$	49.8			6.4		
$C(A_Z, K_Z)$	(72.8)*			(6.4)		
$G(A_Z)$	-5.5			-12.6		
A_Z	1.4	.93	.50	.87	1.2	1.7
A_E**	2.3	2.1	1.0	.17	.08	.04

* Parenthesized quantities are inferred as balance requirements.

** Values given for A_E are probably too small due to an approximation in their calculation.

Table 25 (con't)

Terms in the zonal available potential energy equation for a polar cap north of 20^{o} (50 to 30 mb. layer). Units: 10^{18} ergs sec^{-1}. Also, total zonal available potential energy in cap. Units: 10^{25} ergs; t. e. = transient eddy; s. e. = standing eddy.

	July	Aug.	Sep.	Oct.	Nov.	Dec.
$S(A_Z)$	-1.7	-3.1	-1.4	1.5	-1.5	.54
$C(A_E, A_Z)$ t. e.	1.1	1.2	1.3	.34	-3.0	-.53
$C(A_E, A_Z)$ s. e.	.85	.46	1.4	-2.7	-22.9	7.4
$C(A_Z, K_Z)$	12.1					
$C(A_Z, K_Z)$	(9.8)*					
$G(A_Z)$	-13.4					
A_Z	1.6	1.1	3.7	.27	.62	.27
A_E **	.03	.03	.08	.16	1.2	1.7

* Parenthesized quantities are inferred as balance requirements.

** Values are given for A_E are probably too small due to an approximation in their calculation.

Table 26:

Terms in the zonal available potential energy equation for a polar cap north of 20° (30 to 10 mb. layer). Units: 10^{18} ergs sec^{-1}. Also, total zonal available potential energy in cap. Units: 10^{25} ergs; t. e. = transient eddy; s. e. = standing eddy.

	Jan.	Feb.	March	April	May	June
$S(A_Z)$	-9.2	-3.1	-3.3	-.94	.50	1.0
$C(A_E, A_Z)$ t. e.	-33.8	-18.1	-2.3	.74	1.1	.69
$C(A_E, A_Z)$ s. e.	-96.4	-43.3	-6.5	3.9	-.30	-.32
$C(A_Z, K_Z)$	134.1			-5.3		
$C(A_Z, K_Z)$	(108.3)*			(-5.0)		
$G(A_Z)$	12.7			-.55		
A_Z	2.6	.98	.18	.22	.25	.52
A_E **	2.6	2.7	1.1	.20	.05	.03

* Parenthesized quantities are inferred as balance requirements.

** Values of A_E are probably too small due to an approximation in their calculation.

Table 26 (con't)

Terms in the zonal available potential energy equation for a polar cap north of 20^{o} (30 to 10 mb. layer). Units: 10^{18} ergs sec^{-1}. Also, total zonal available potential energy in cap. Units: 10^{25} ergs; t. e. = transient eddy; s. e. = standing eddy.

	July	Aug.	Sep.	Oct.	Nov.	Dec.
$S(A_Z)$	-.76	-1.7	1.6	4.9	1.2	-1.5
$C(A_E, A_Z)$ t. e.	.40	.44	-.25	-3.5	-8.3	-5.6
$C(A_E, A_Z)$ s. e.	-.13	-.21	-.76	-6.2	-55.7	-36.9
$C(A_Z, K_Z)$	6.6					
$C(A_Z, K_Z)$	(7.0)*					
$G(A_Z)$	-8.0					
A_Z	.56	.26	.11	.87	2.1	1.1
A_E**	.03	.03	.07	.16	1.3	1.4

* Parenthesized quantities are inferred as balance requirements.

** Values of A_E are probably too small due to an approximation in their calculation.

Table 27:

Comparison of three month mean values of terms in the zonal available potential energy equation for a polar cap north of 20^{o} with values computed by Oort (1963) for the entire northern hemisphere (100 to 30 mb. layer). Units: 10^{18} ergs sec^{-1}; t. e. = transient eddy; s. e. = standing eddy. A_Z in units of 10^{25} ergs.

I = January - March; II = April - June

	I		II	
	Present Results	Oort (1963)	Present Results	Oort (1963)
$S(A_Z)$	.9	21.3	7.9	8.1
$C(A_E, A_Z)$ t. e.	-23.5	42.0	15.3	37.1
$C(A_E, A_Z)$ s. e.	-43.0	11.5	27.5	25.5
A_Z	6.2	25.7	11.4	30.2
A_E*	5.0	3.0	.60	1.3

* Values of A_E are probably too small due to an approximation in their calculation.

Table 27 (con't)

Comparison of three month mean values of terms in the zonal available potential energy equation for a polar cap north of 20^{o} with values computed by Oort (1963) for the entire northern hemisphere (100 to 30 mb. layer). Units: 10^{18} ergs sec^{-1}; t. e. = transient eddy; s. e. = standing eddy. A_Z in units of 10^{25} ergs.

III = July - September; IV = October - December

	III		IV	
	Present Results	Oort (1963)	Present Results	Oort (1963)
$S(A_Z)$	-9.6	-13.8	-4.4	-4.2
$C(A_E, A_Z)$ t. e.	11.8	26.6	10.3	35.6
$C(A_E, A_Z)$ s. e.	13.4	11.8	15.3	14.1
A_Z	10.9	26.4	5.9	18.2
A_E*	.46	1.7	3.1	2.4

* Values A_E are probably too small due to an approximation in their calculation.

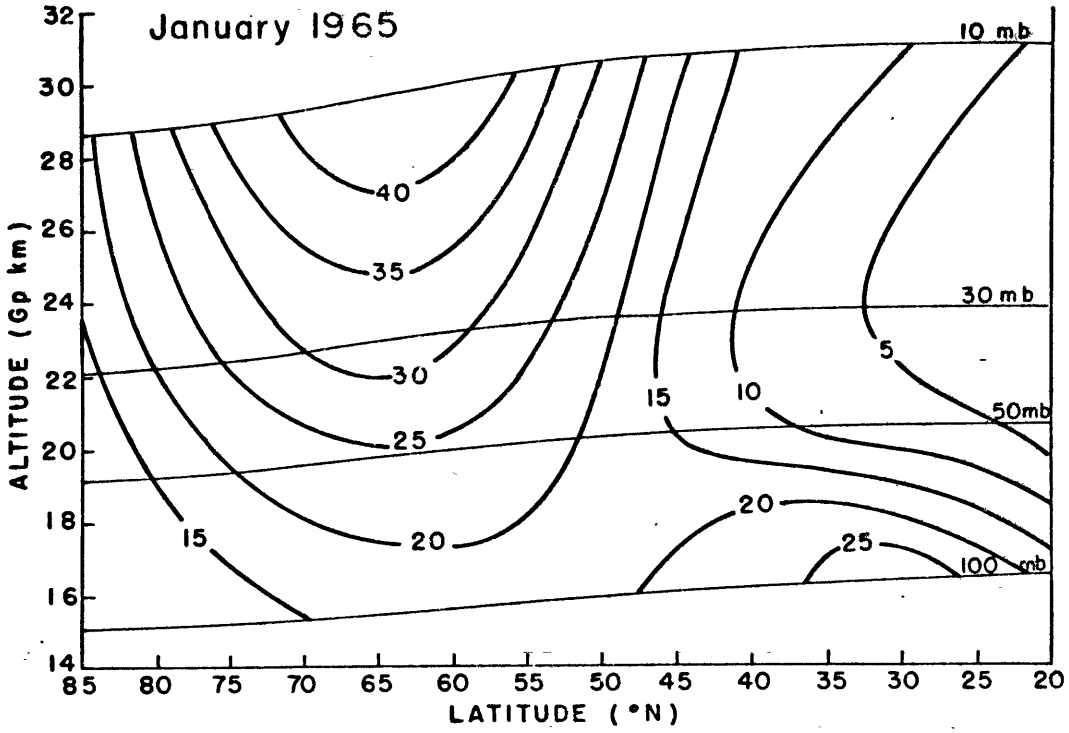

Figure 2a: Meridional distribution of mean zonal winds, $[\bar{u}]$. Units: m sec^{-1}.

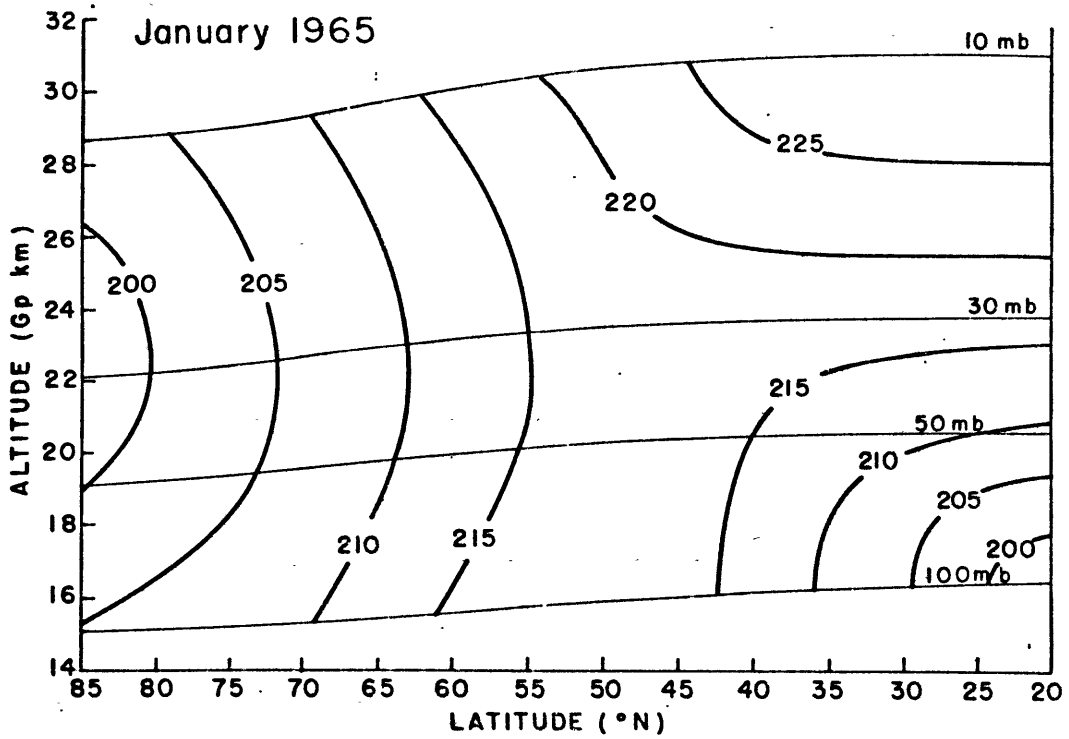

Figure 3a: Meridional distribution of mean zonal temperature, $[\bar{T}]$. Units: ^{o}K.

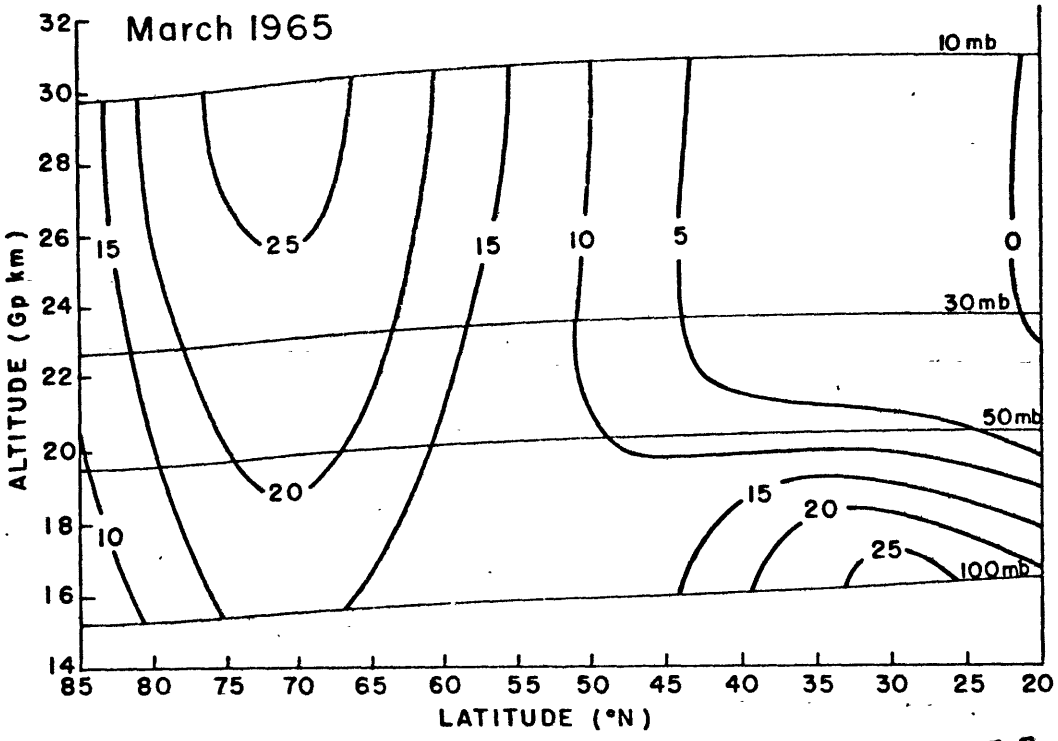

Figure 2b: Meridional distribution of mean zonal winds, $[\bar{u}]$. Units: m sec^{-1}.

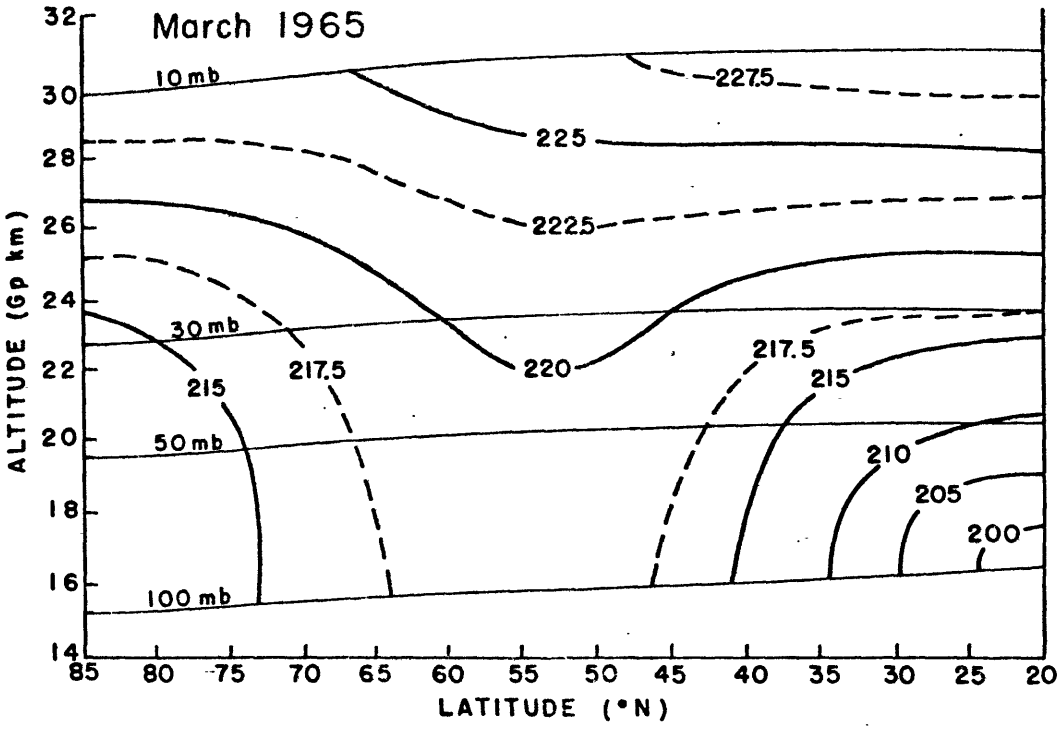

Figure 3b: Meridional distribution of mean zonal temperature, $[\bar{T}]$. Units: ^{o}K.

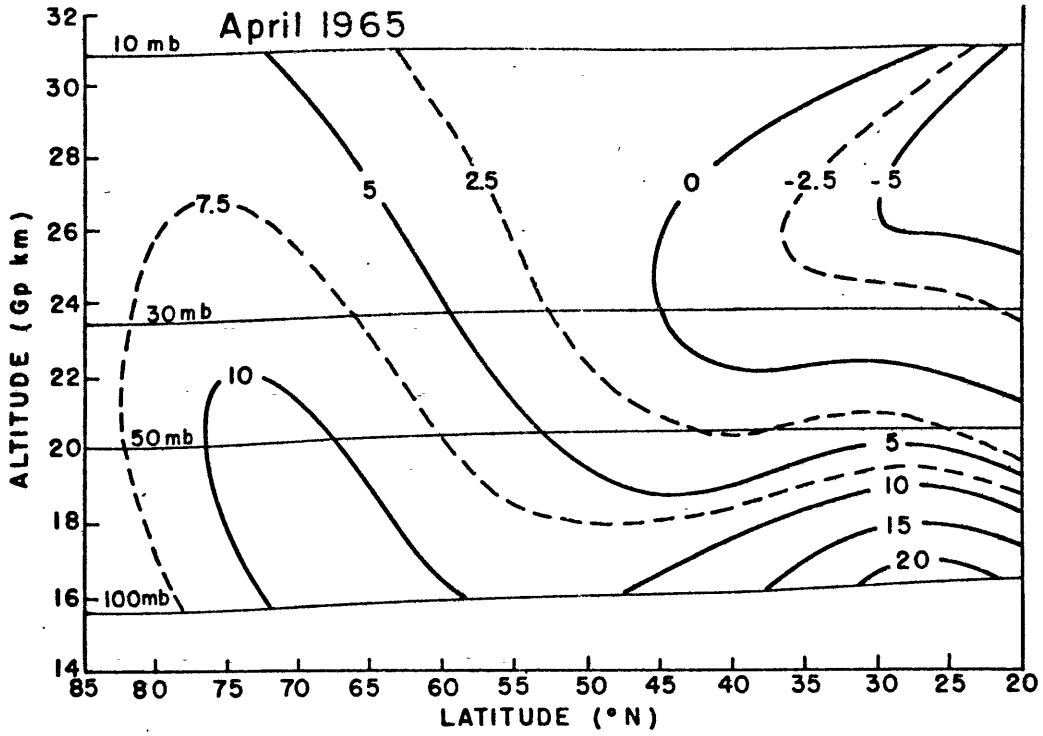

Figure 2c: Meridional distribution of mean zonal winds, $[\bar{u}]$. Units: m sec^{-1}.

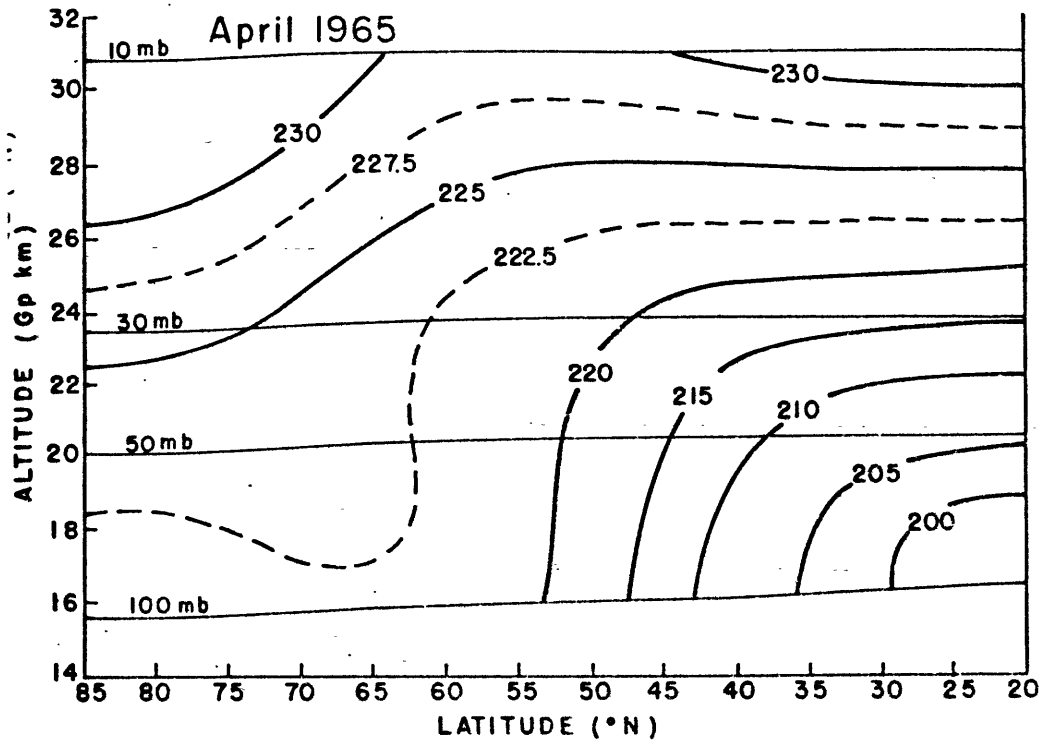

Figure 3c: Meridional distribution of mean zonal temperature, $[\bar{T}]$. Units: ^{o}K.

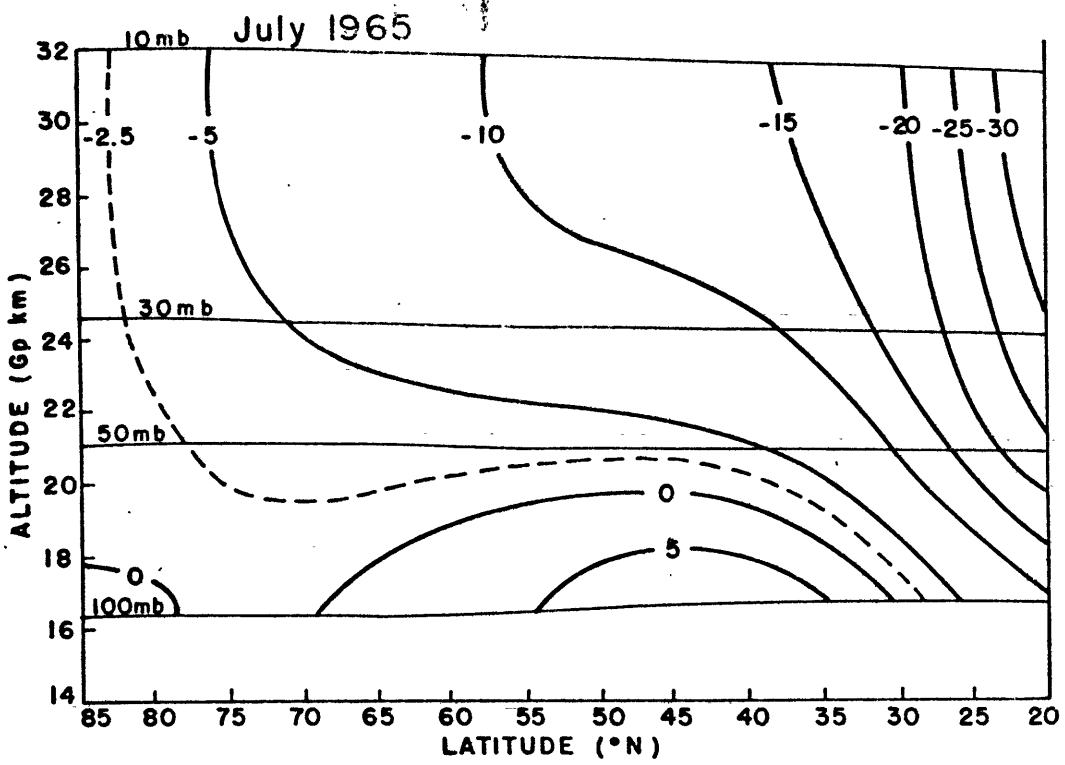

Figure 2d: Meridional distribution of mean zonal winds, $[\bar{u}]$. Units: m sec^{-1}.

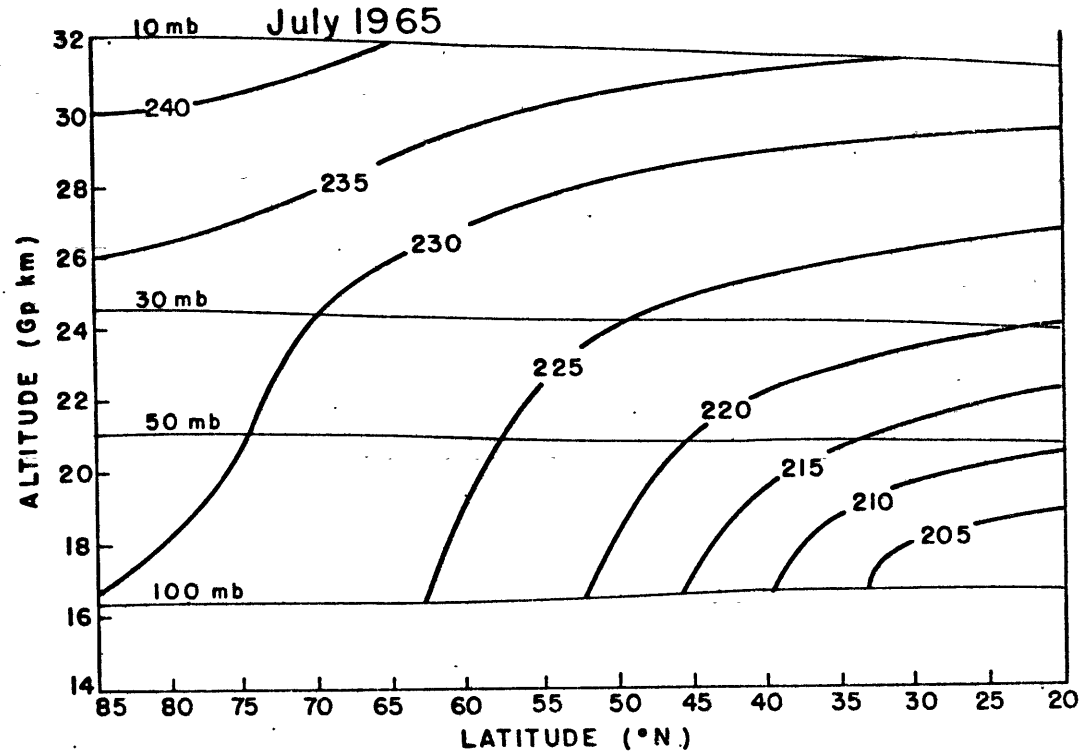

Figure 3d: Meridional distribution of mean zonal temperature, $[\bar{T}]$. Units: ^{o}K.

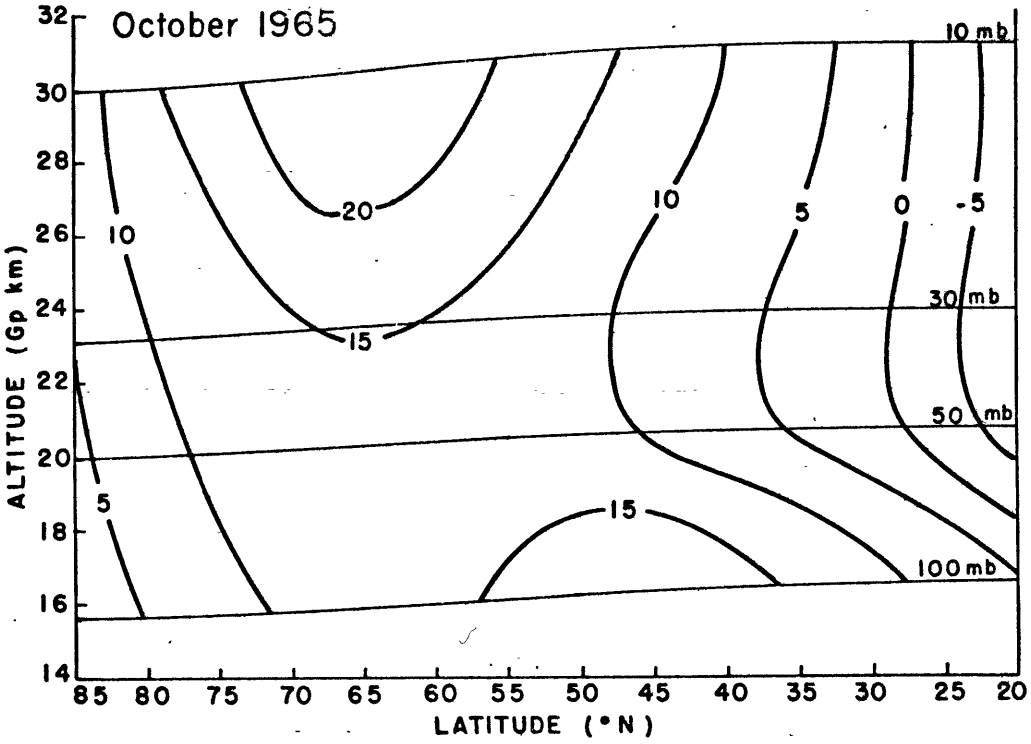

Figure 2e: Meridional distribution of mean zonal winds, $[\bar{u}]$. Units: m sec^{-1}.

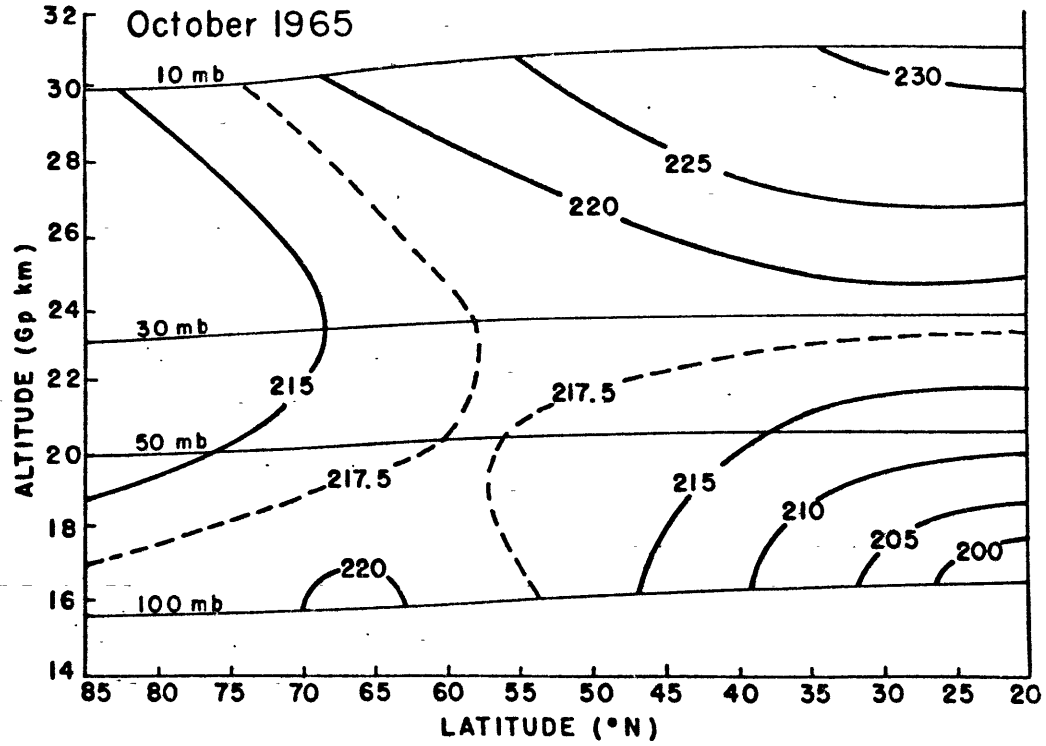

Figure 3e: Meridional distribution of mean zonal temperature, $[\bar{T}]$. Units: ^{o}K.

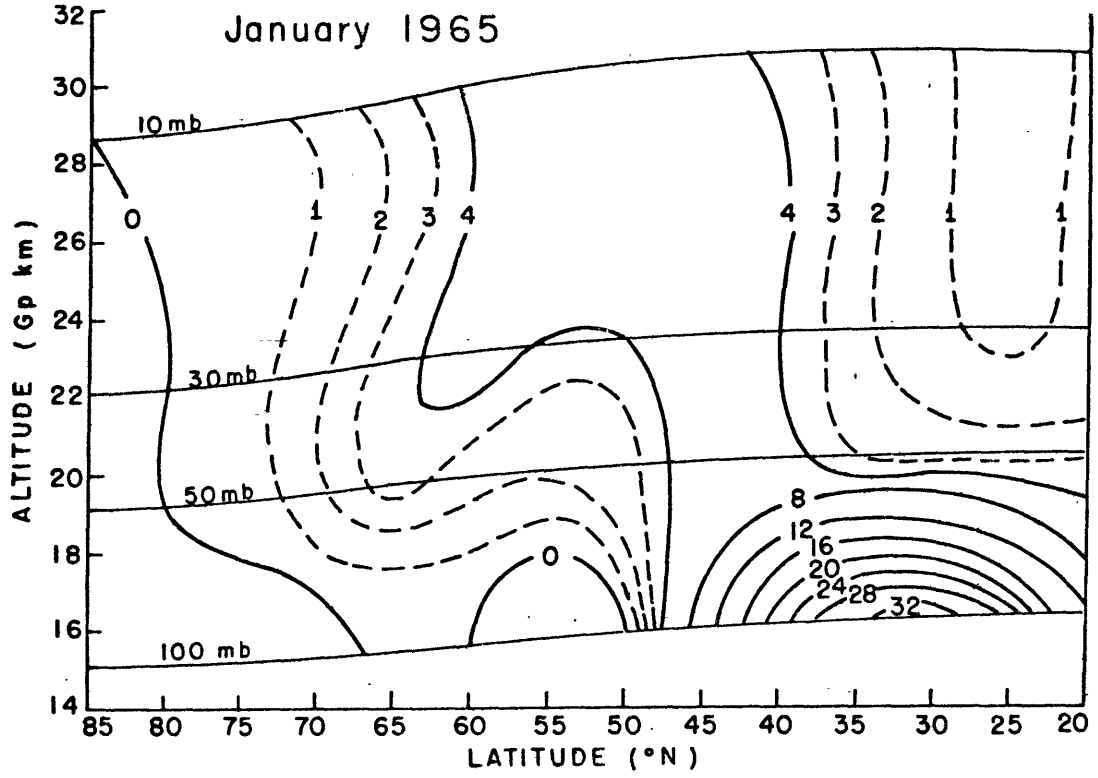

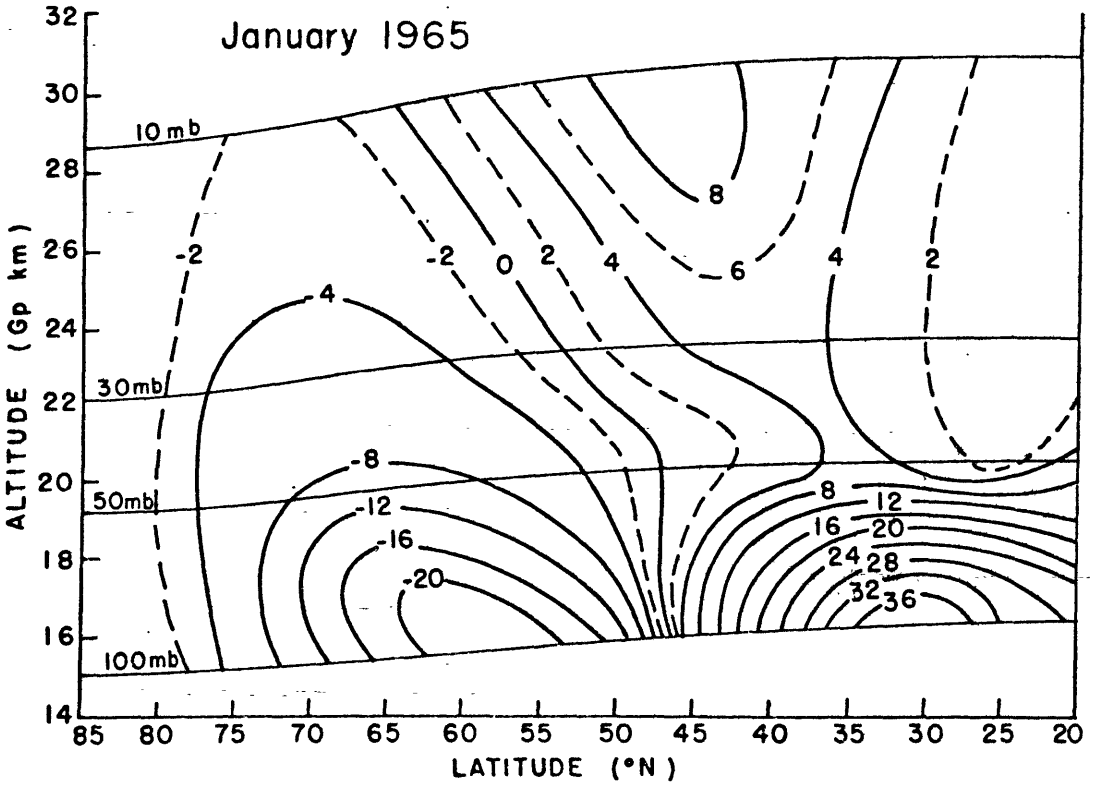

Figure 4a: Meridional distribution of relative angular momentum transport by transient eddies (upper diagram), $\iint \overline{u'v'}\, a^2 \cos^2\phi \, d\lambda \frac{dp}{g}$, and by standing eddies (lower diagram), $\iint \overline{u^*v^*}\, a^2 \cos^2\phi \, d\lambda \frac{dp}{g}$. Units: 10^{18} gm cm sec^{-2}.

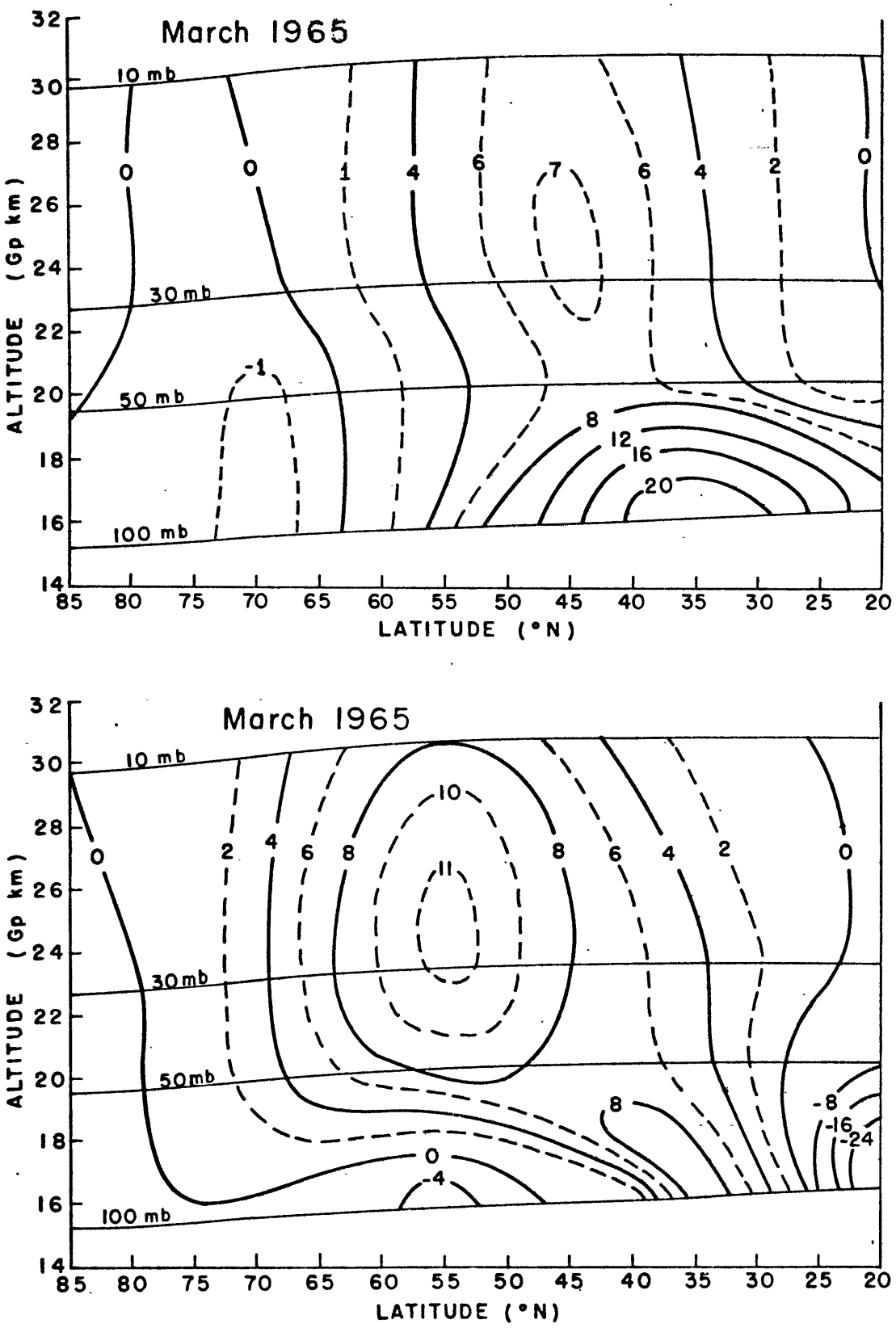

Figure 4b: Meridional distribution of relative angular momentum transport by transient eddies (upper diagram), $\iint \overline{u'v'} a^2 \cos^2\varphi \, d\lambda \frac{dp}{g}$, and by standing eddies (lower diagram), $\iint \bar{u}^* \bar{v}^* a^2 \cos^2\varphi \, d\lambda \frac{dp}{g}$. Units: 10^{18} gm cm sec^{-2}.

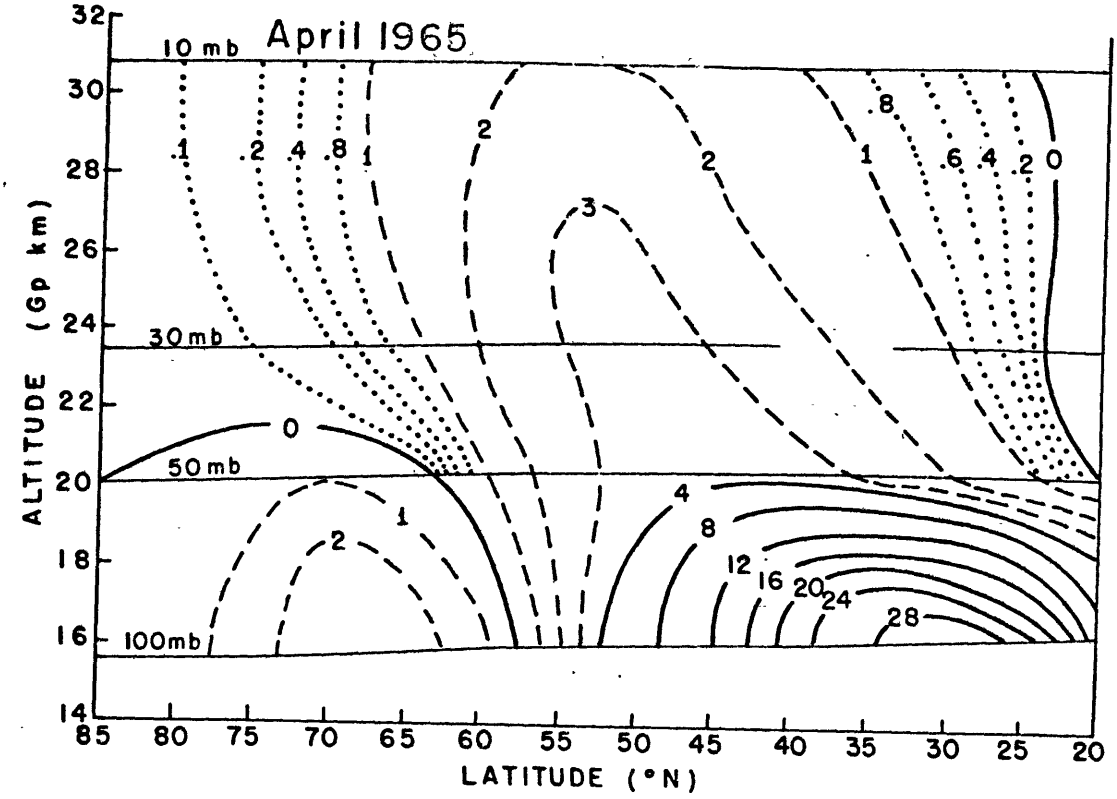

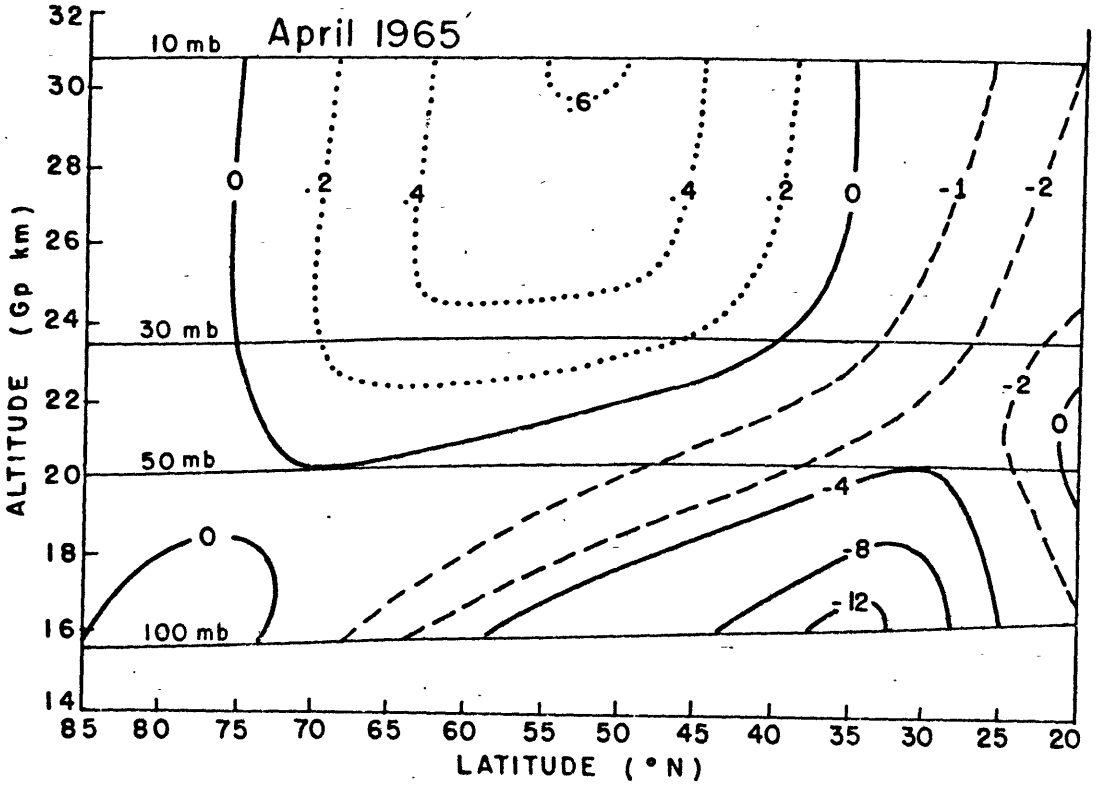

Figure 4c: Meridional distribution of relative angular momentum transport by transient eddies (upper diagram), $\iint \bar{u}^* \bar{v}^* a^2 \cos^2\phi \, d\lambda \frac{dp}{g}$, and by standing eddies (lower diagram), $\iint \bar{u}^* \bar{v}^* a^2 \cos^2\phi \, d\lambda \frac{dp}{g}$. Units: 10^{18} gm cm sec^{-2}.

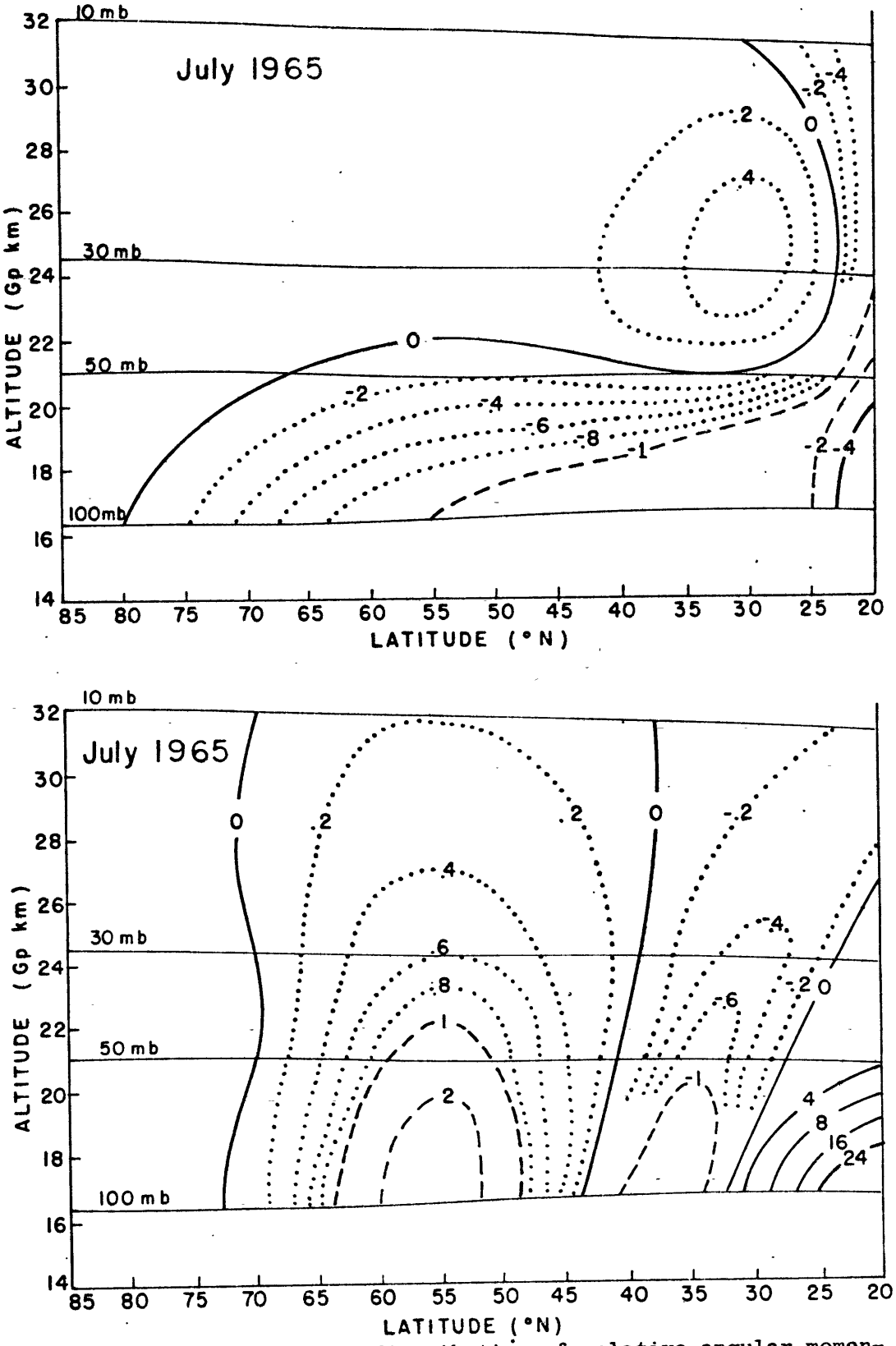

Figure 4d: Meridional distribution of relative angular momentum transport by transient eddies (upper diagram), $\iint \overline{u'v'} a^2 \cos^2\varphi \, d\lambda \frac{dp}{g}$, and by standing eddies (lower diagram), $\iint \overline{u}^* \overline{v}^* a^2 \cos^2\varphi \, d\lambda \frac{dp}{g}$. Units: 10^{18} gm cm sec^{-2}.

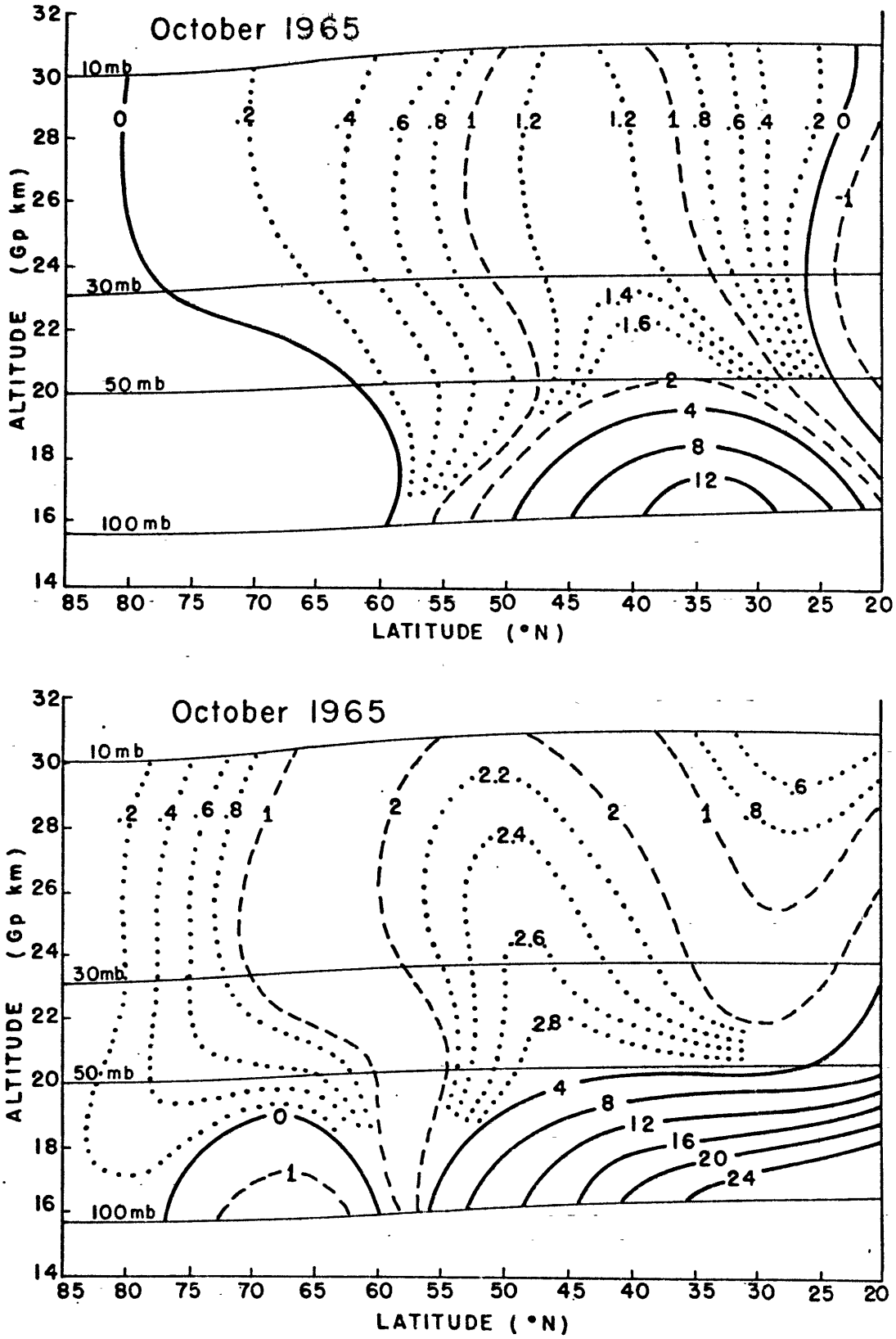

Figure 4e: Meridional distribution of relative angular momentum transport by transient eddies (upper diagram), $\iint \overline{u'v'}\, a^2 \cos^2\phi \, d\lambda \, \frac{dp}{g}$, and by standing eddies (lower diagram), $\iint \bar{u}^* \bar{v}^* \, a^2 \cos^2\phi \, d\lambda \frac{dp}{g}$. Units: 10^{18}gm cm sec^{-2}.

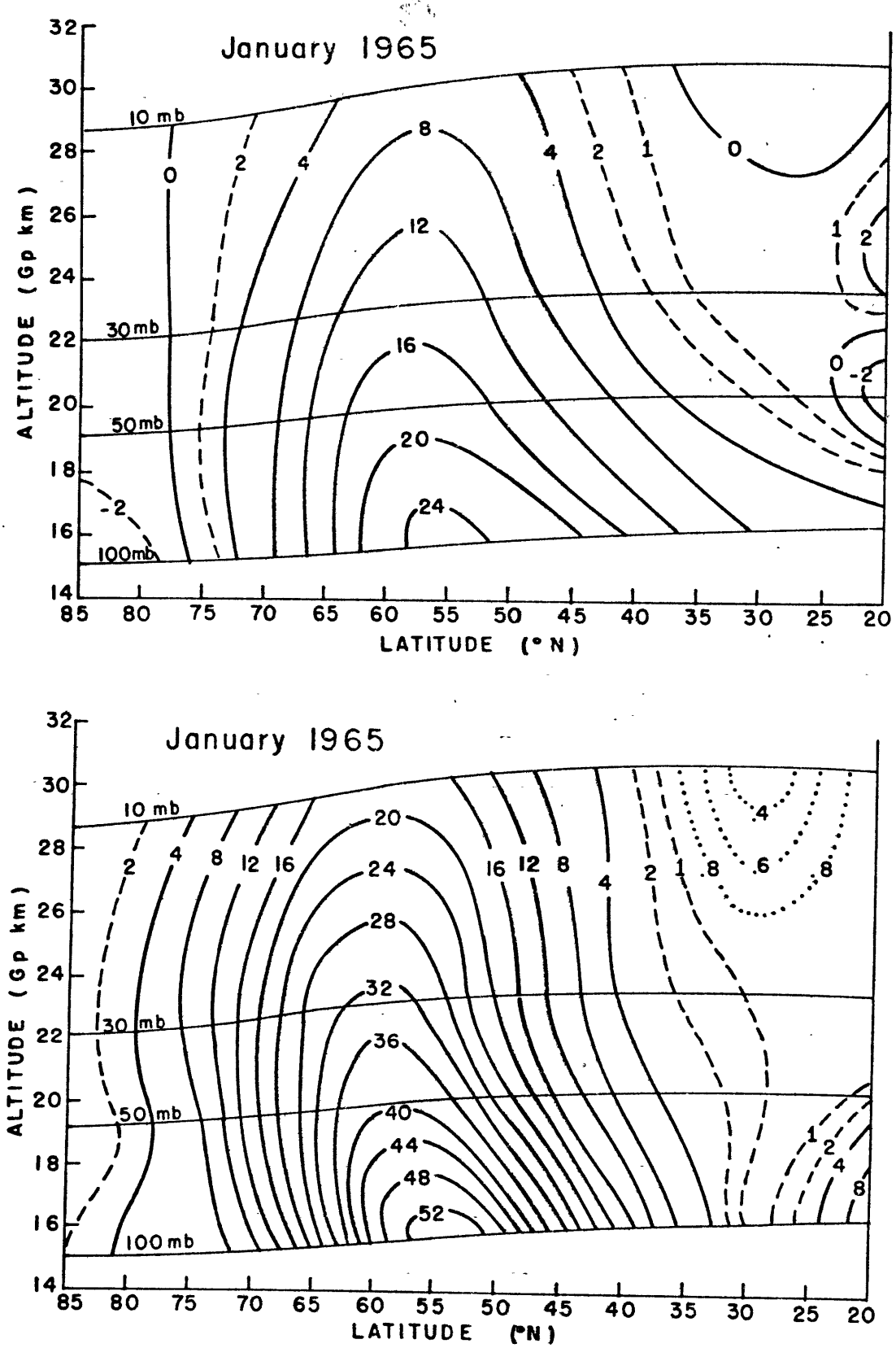

Figure 5a; Meridional distribution of sensible heat transport by transient eddies $c_p \iint \overline{v'T'} a \cos\phi \, d\lambda \frac{dp}{g}$, (upper diagram) and by standing eddies, $c_p \iint \overline{v}^* \overline{T}^* a \cos\phi \, d\lambda \frac{dp}{g}$, (lower diagram). Units: 10^{14}ergs cm^{-1} sec^{-1}.

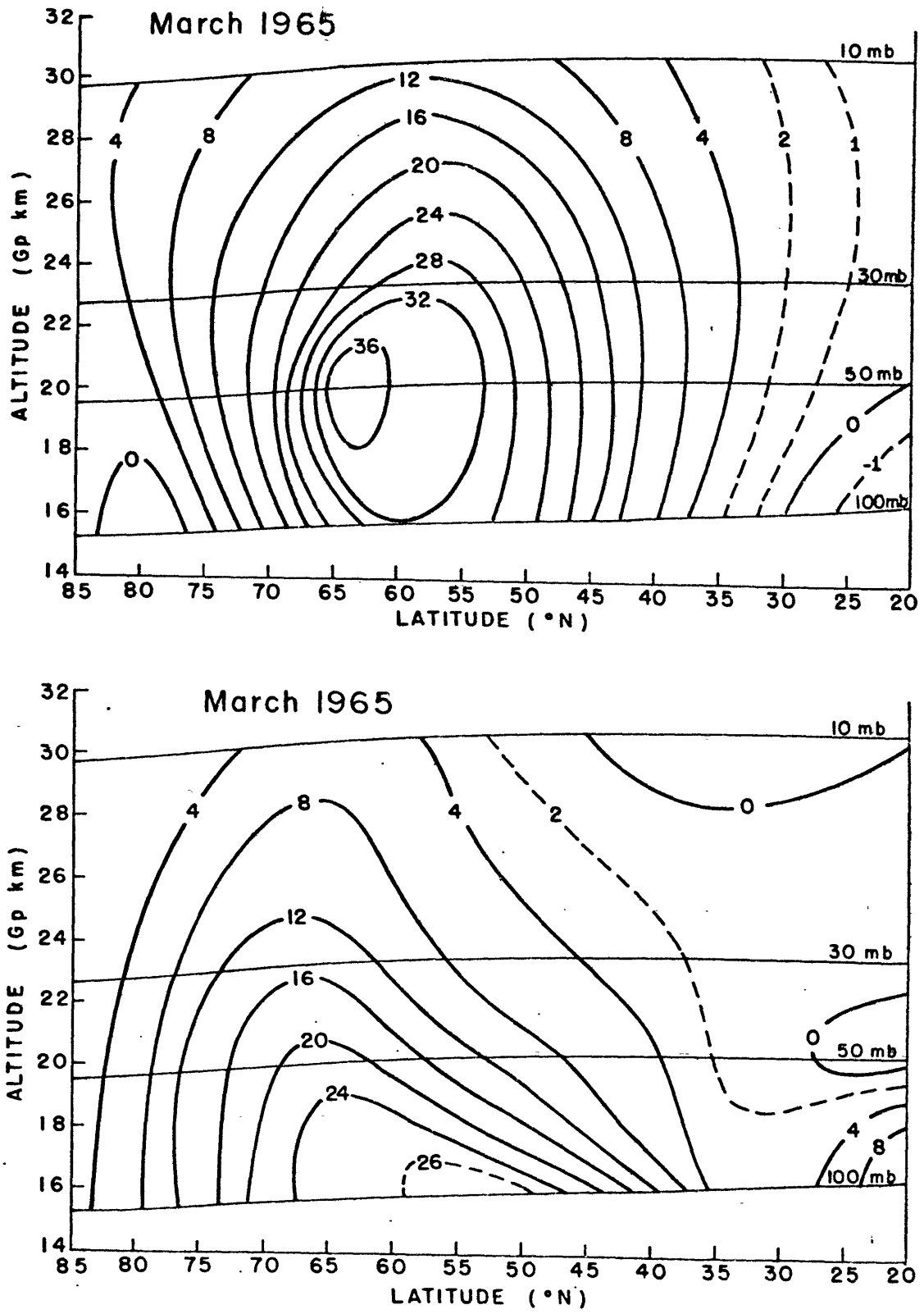

Figure 5b: Meridional distribution of sensible heat transport by transient eddies, $c_p \iint \overline{v'T'} \, a \cos\phi \, d\lambda \, \frac{dp}{g}$, (upper diagram) and by standing eddies, $c_p \iint \overline{v}^* \overline{T}^* \, a \cos\phi \, d\lambda \, \frac{dp}{g}$, (lower diagram). Units: 10^{14}ergs cm^{-1} sec^{-1}.

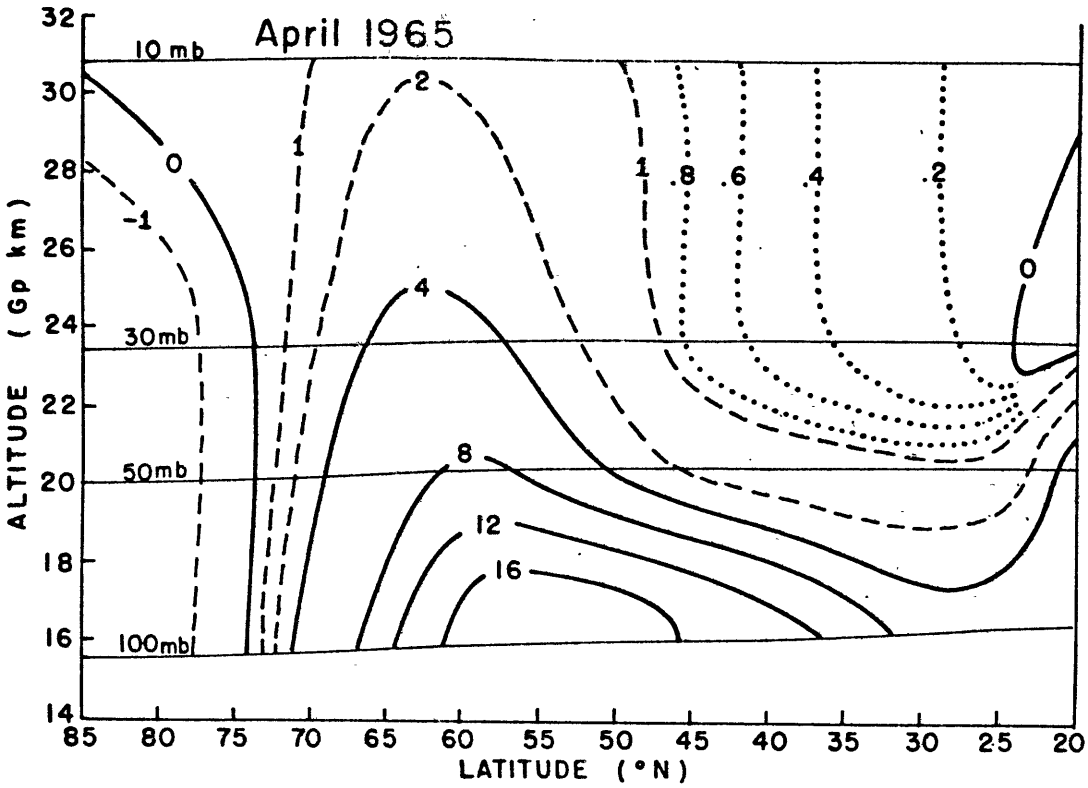

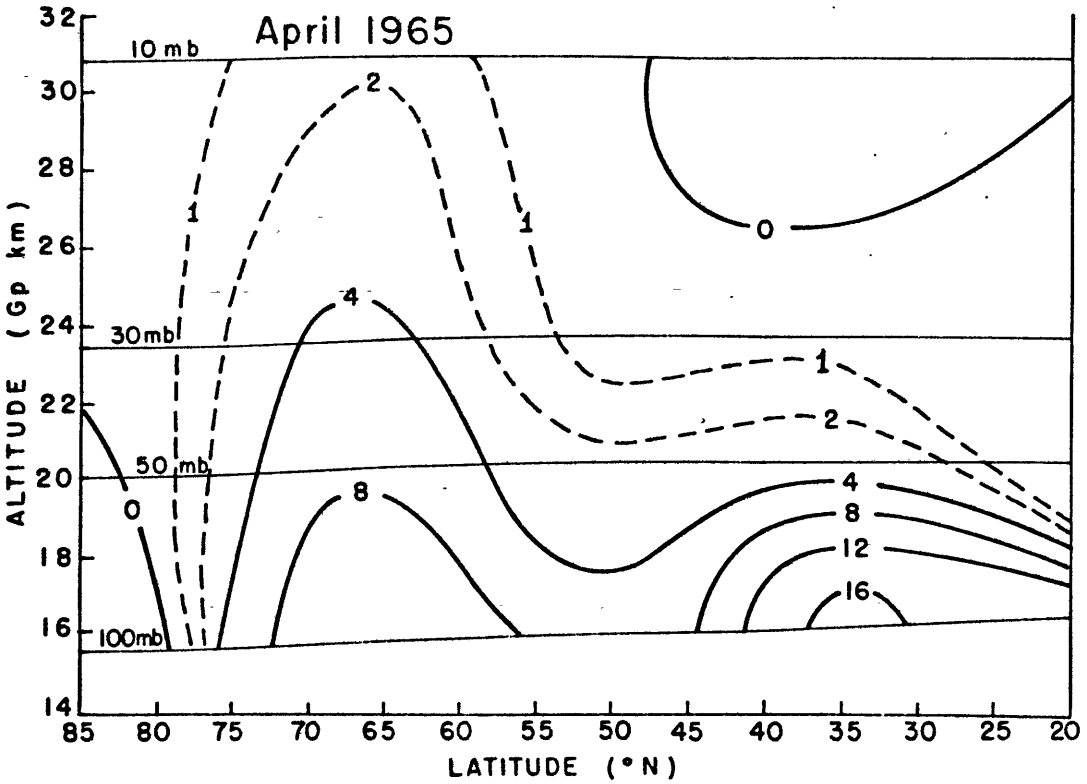

Figure 5c: Meridional distribution of sensible heat transport by transient eddies, $c_p \iint \overline{v'T'} \, a \cos\phi \, d\lambda \frac{dp}{g}$, (upper diagram) and by standing eddies, $c_p \iint \overline{v}^* \overline{T}^* a \cos\phi \, d\lambda \frac{dp}{g}$, (lower diagram). Units: 10^{14} ergs cm^{-1} sec^{-1}.

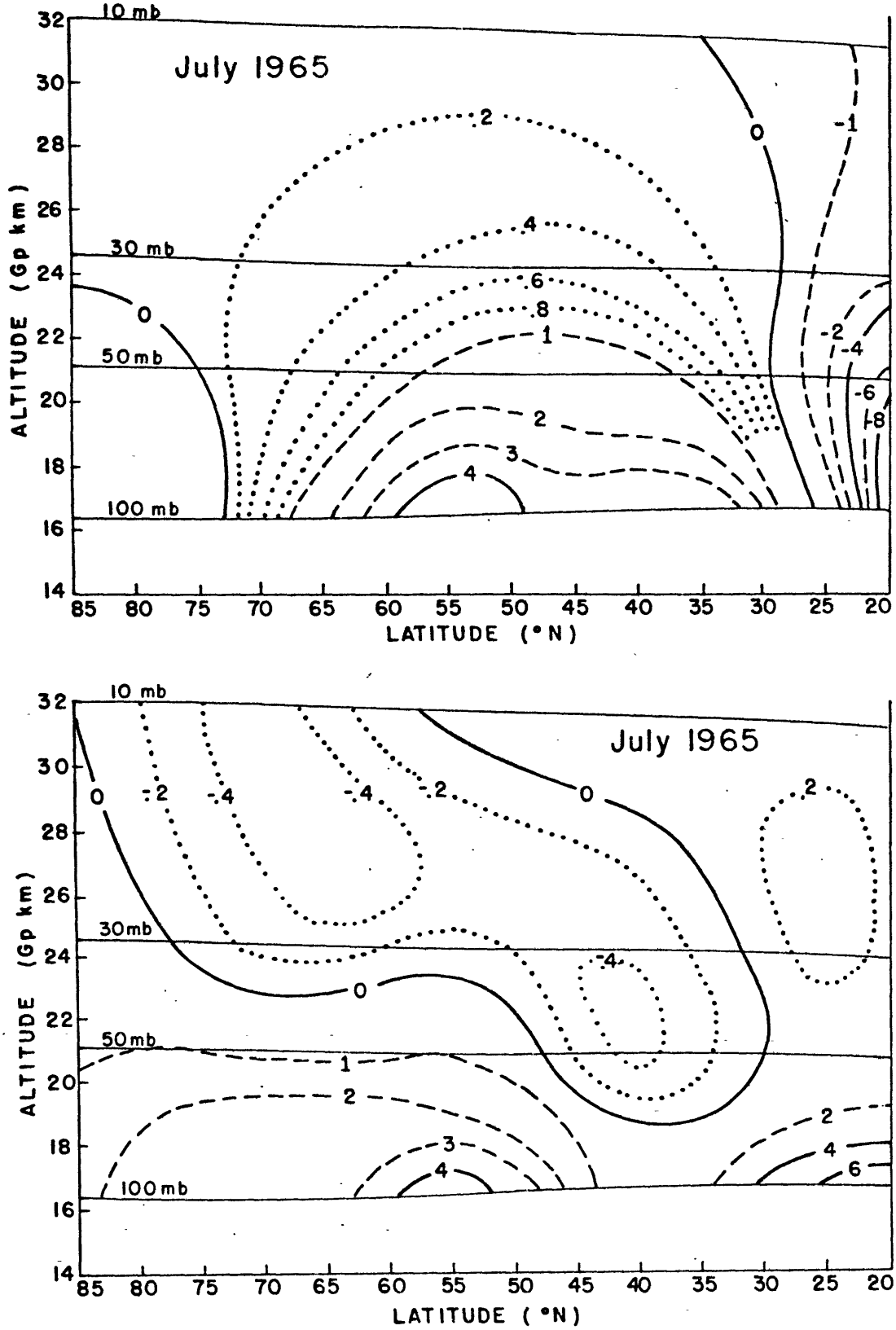

Figure 5d: Meridional distribution of sensible heat transport by transient eddies, $c_p \iint \overline{v'T'} a \cos\phi \, d\lambda \, d\frac{p}{g}$, (upper diagram) and by standing eddies $c_p \iint \overline{v^*T^*} a \cos\phi \, d\lambda \, d\frac{p}{g}$, (lower diagram). Units: 10^{14} ergs cm^{-1} sec^{-1}.

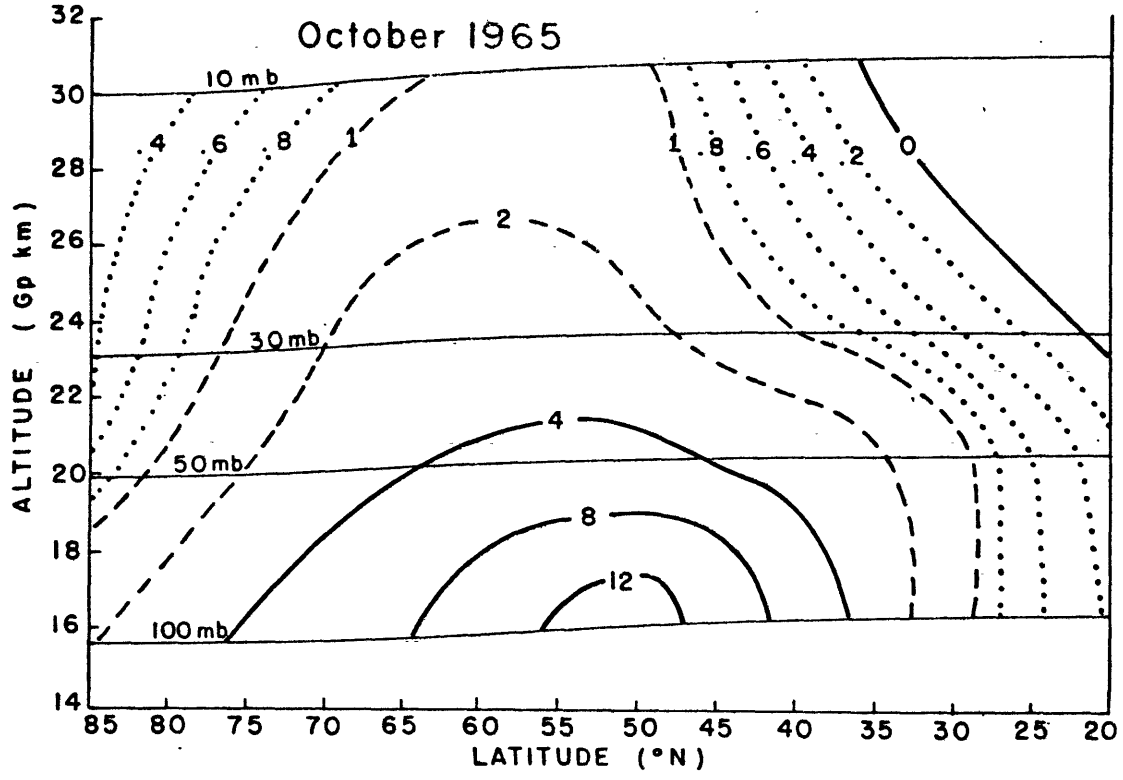

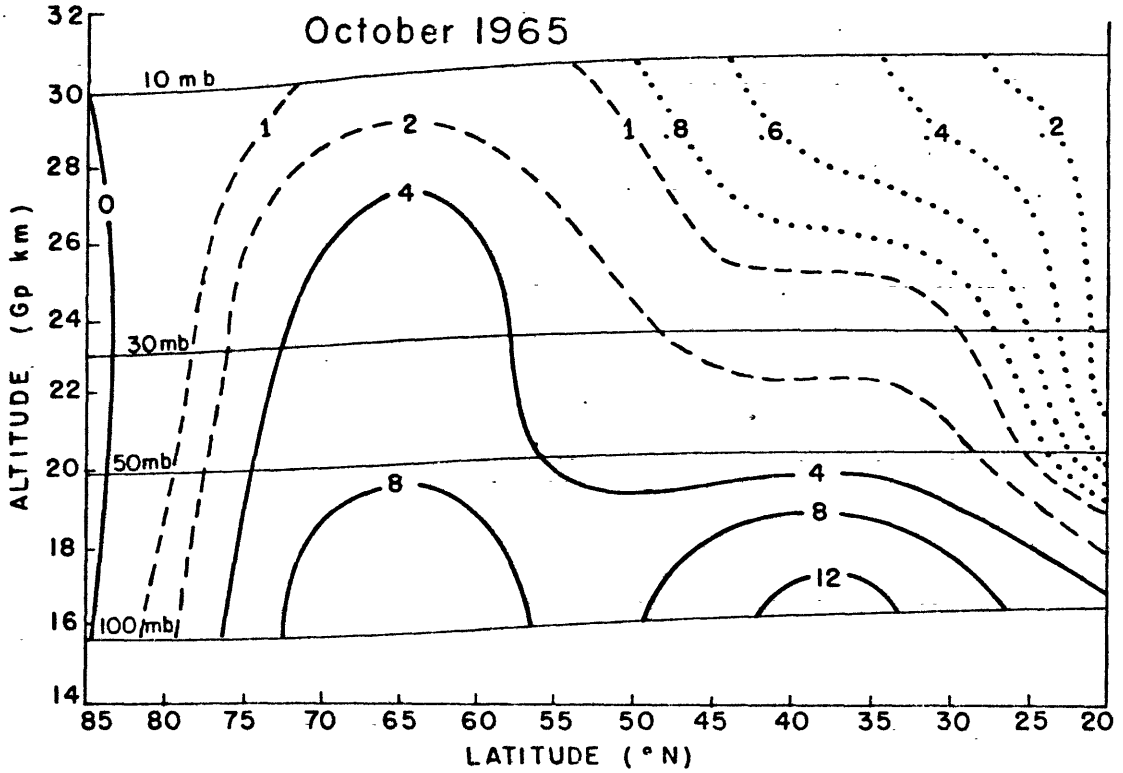

Figure 5e: Meridional distribution of sensible heat transport by transient eddies, $2\pi\int\int \overline{v'T'}\, a\cos\phi\, d\lambda \frac{dp}{g}$, (upper diagram) and by standing eddies, $2\pi\int\int \overline{v^*T^*}\, a\cos\phi\, d\lambda \frac{dp}{g}$, (lower diagram). Units: 10^{14} ergs cm^{-1} sec^{-1}.

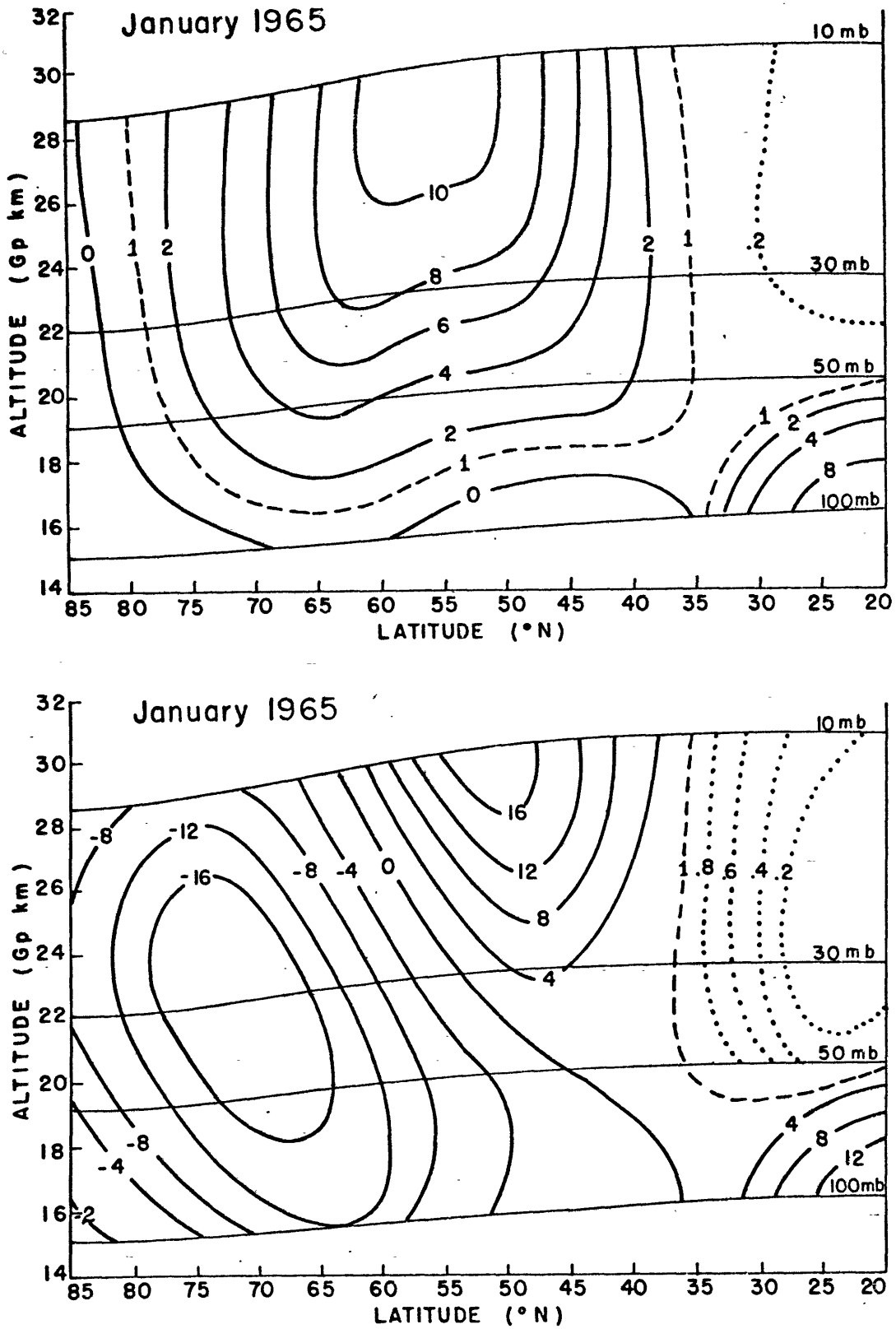

Figure 6a: Meridional distribution of the conversion from transient eddy kinetic energy, $\int [\overline{u'v'}] \cos\phi \frac{\partial [\overline{u}]}{\partial \phi a \cos\phi} \frac{dp}{g}$, (upper diagram) and standing eddy kinetic energy, $\int [\overline{u}^* \overline{v}^*] \cos\phi \frac{\partial [\overline{u}]}{\partial \phi a \cos\phi} \frac{dp}{g}$ (lower diagram) to zonal kinetic energy. Units: 10^{-5} ergs cm^{-3} sec^{-1}.

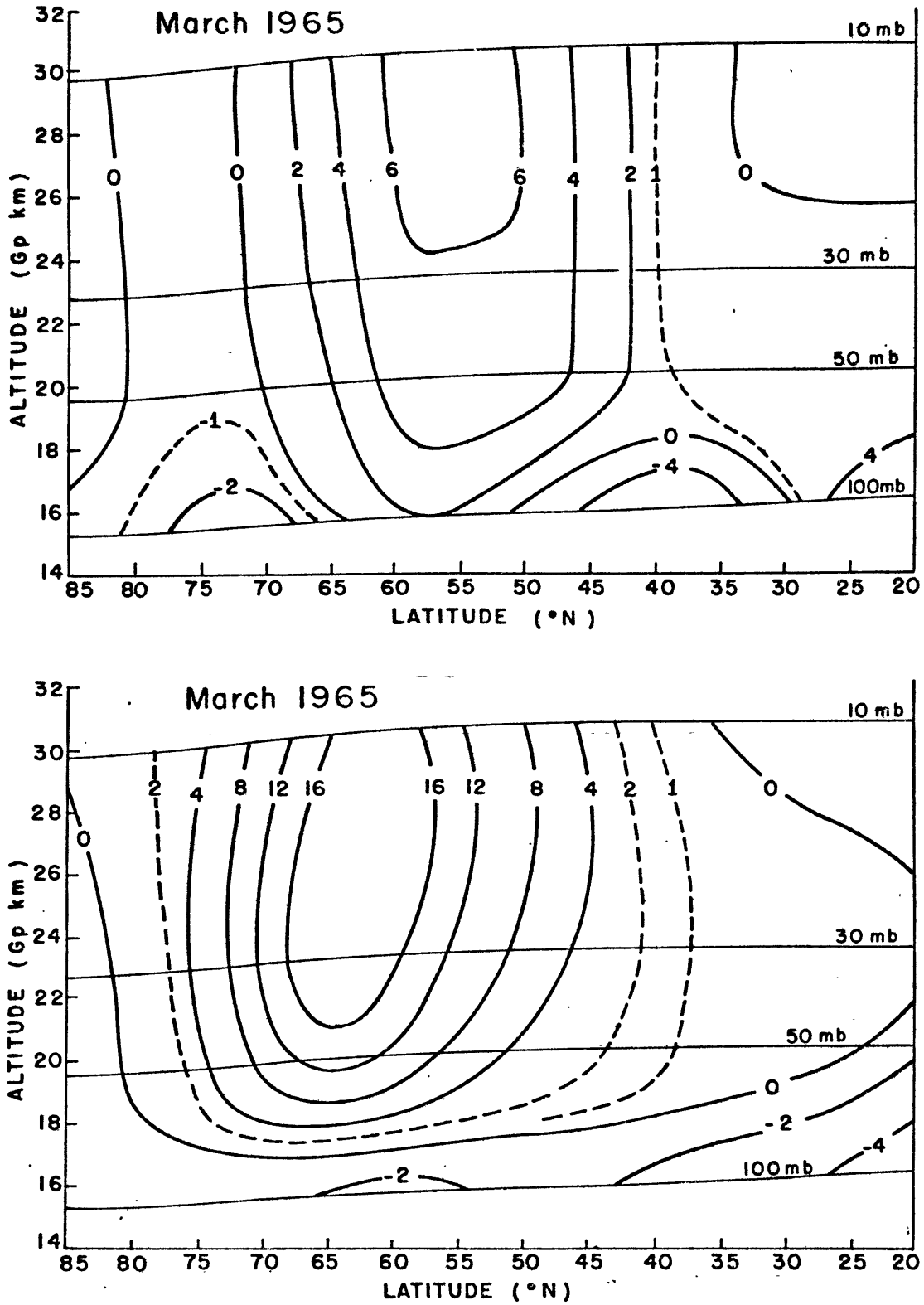

Figure 6b: Meridional distribution of the conversion from transient eddy kinetic energy, $\int [\overline{u'v'}] \cos\phi \frac{\partial [\bar{u}]}{\partial \phi a \cos\phi} \frac{dp}{g}$, (upper diagram) and standing eddy kinetic energy, $\int [\bar{u}^* \bar{v}^*] \cos\phi \frac{\partial [\bar{u}]}{\partial \phi a \cos\phi} \frac{dp}{g}$ (lower diagram) to zonal kinetic energy. Units: 10^{-5} ergs cm^{-3} sec^{-1}.

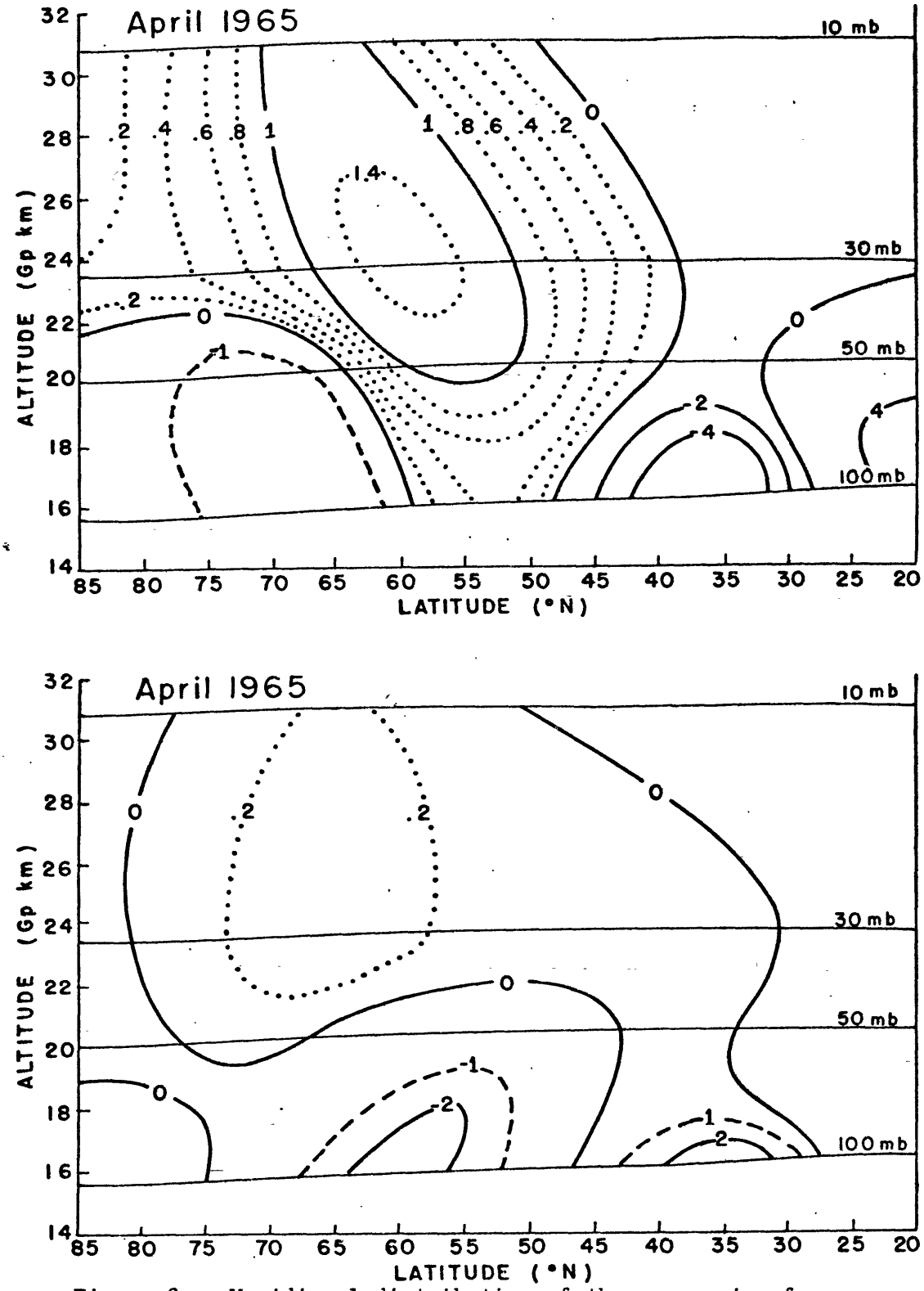

Figure 6c: Meridional distribution of the conversion from transient eddy kinetic energy, $\int [\overline{u'v'}] \cos\phi \frac{\partial [\bar{u}]}{\partial \phi a \cos\phi} \frac{dp}{g}$, (upper diagram) and standing eddy kinetic energy, $\int [\bar{u}^* \bar{v}^*] \cos\phi \frac{\partial [\bar{u}]}{\partial \phi a \cos\phi} \frac{dp}{g}$ (lower diagram) to zonal kinetic energy. Units: 10^{-5} ergs $cm^{-3} sec^{-1}$.

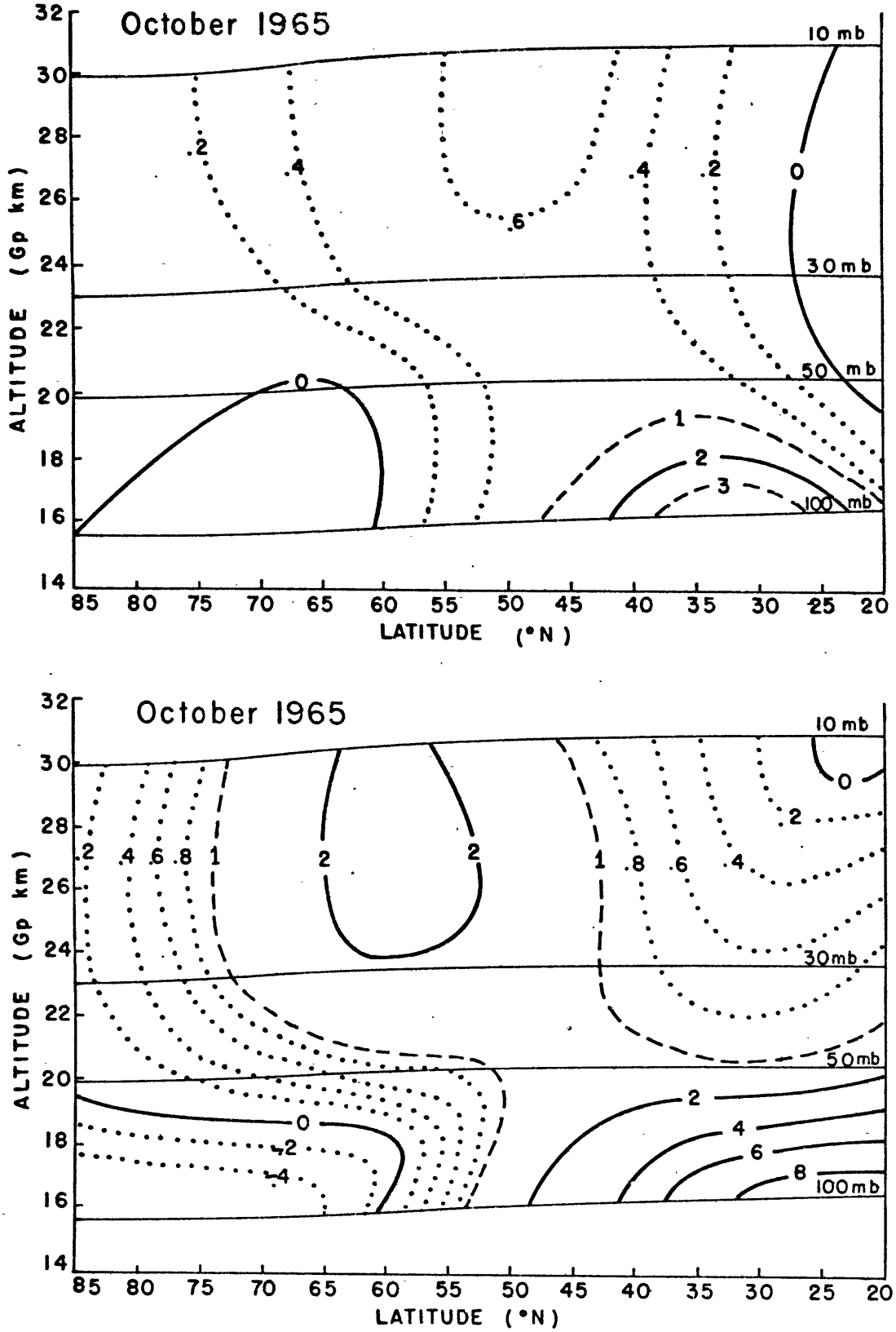

Figure 6d: Meridional distribution of the conversion from transient eddy kinetic energy, $\int [\overline{u'v'}] \cos\phi \frac{\partial [\bar{u}]}{\partial \phi} a \cos\phi \frac{dp}{g}$, (upper diagram) and standing eddy kinetic energy, $\int [\bar{u}^* \bar{v}^*] \cos\phi \frac{\partial [\bar{u}]}{\partial \phi} a \cos\phi \frac{dp}{g}$ (lower diagram) to zonal kinetic energy. Units: 10^{-5} ergs cm^{-3} sec^{-1}.

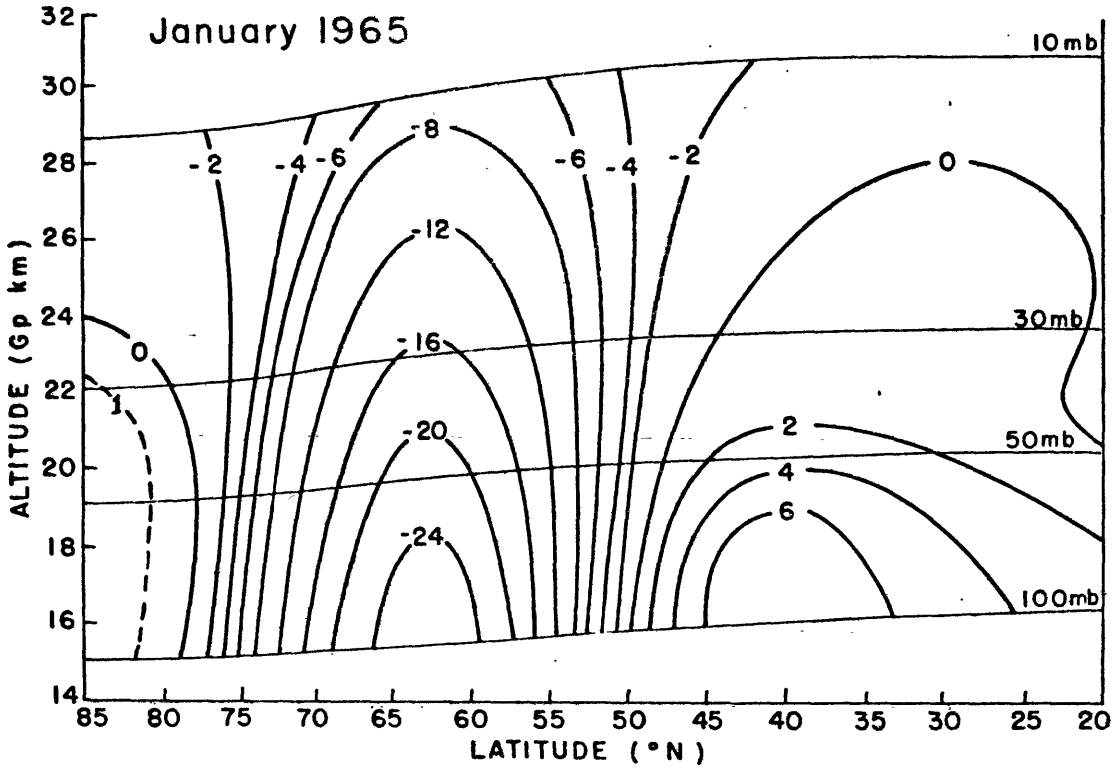

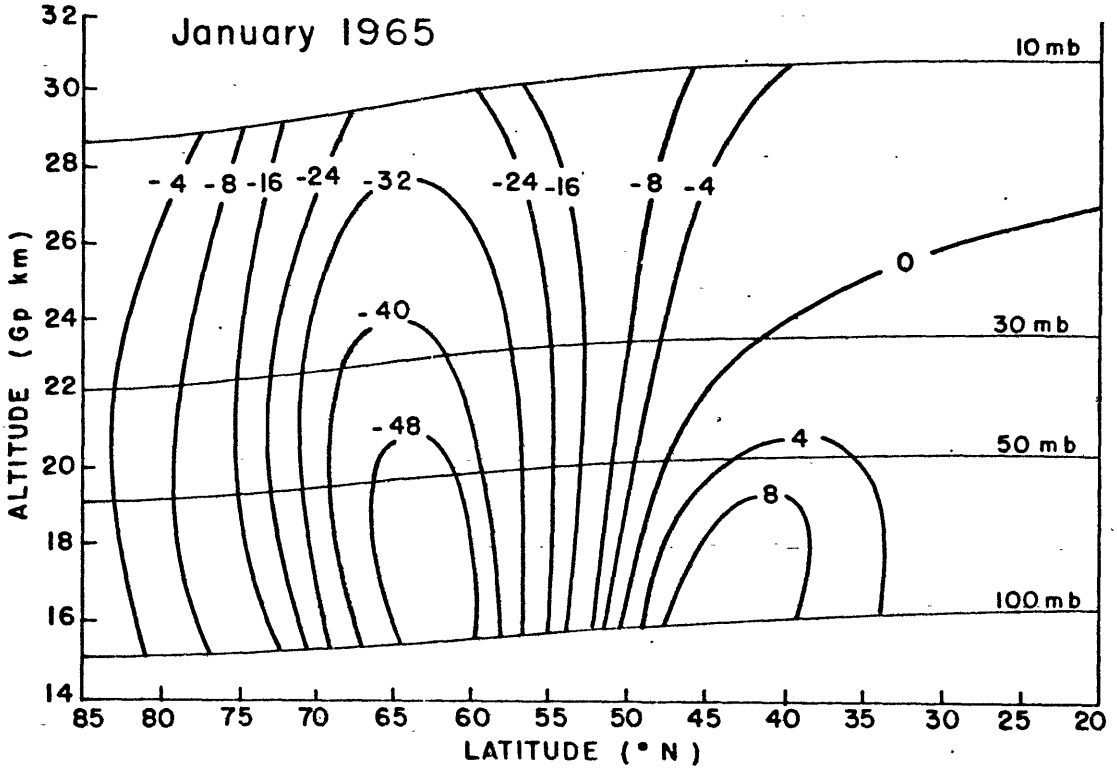

Figure 7a: Meridional distribution of the conversion from eddy available potential energy to zonal available potential energy by transient eddies, $c_p \int r \left[\overline{v'T'}\right] \frac{1}{a} \frac{\partial[\bar{T}]}{\partial\phi} \frac{dp}{g}$, (upper diagram) and by standing eddies, $c_p \int r \left[\overline{v^*T^*}\right] \frac{1}{a} \frac{\partial[\bar{T}]}{\partial\phi} \frac{dp}{g}$, (lower diagram). Units: 10^{-5} ergs cm^{-3} sec^{-1}.

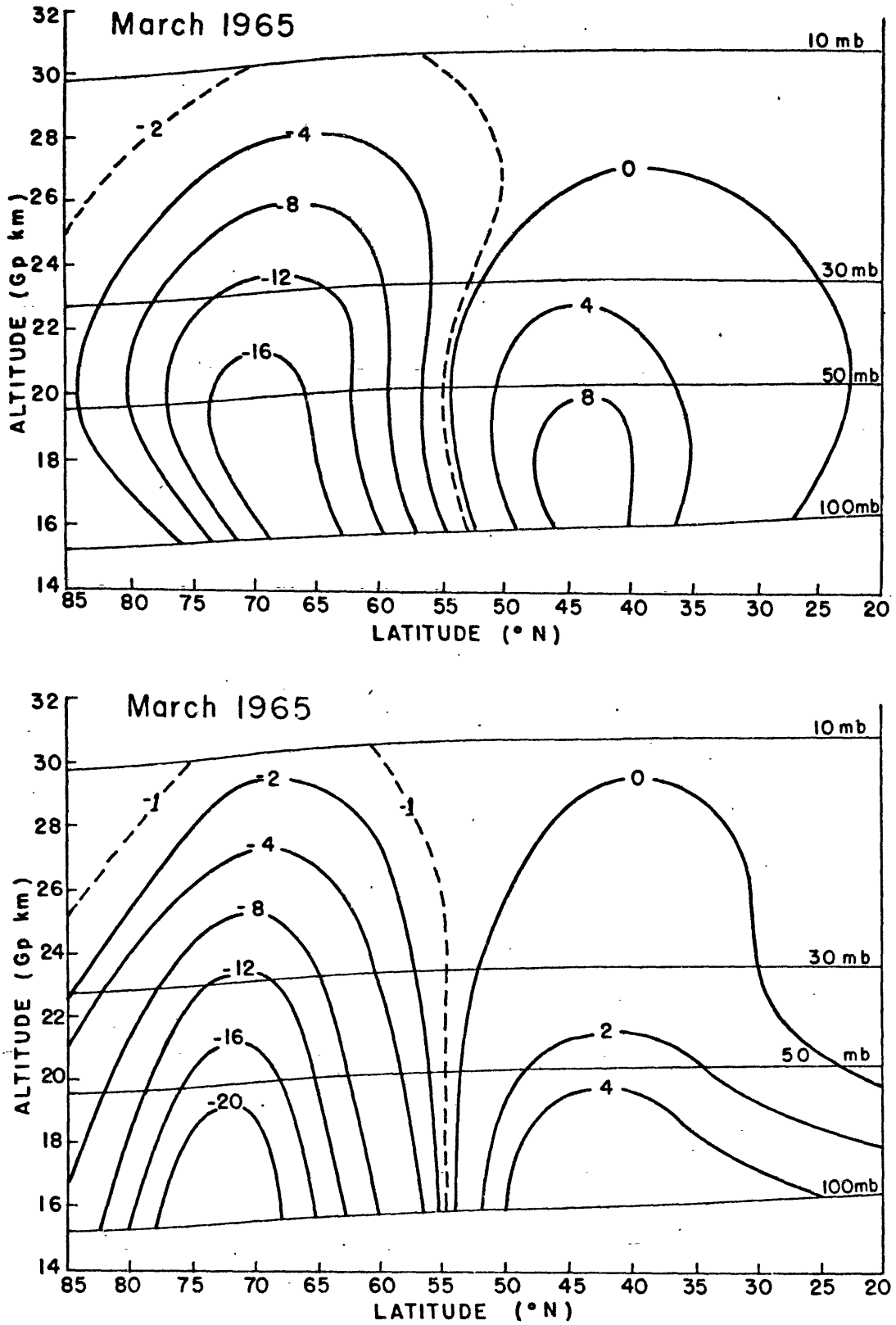

Figure 7b: Meridional distribution of the conversion from eddy available potential energy to zonal available potential energy by transient eddies, $c_p \int r \left[\overline{v'T'}\right] \frac{1}{a} \frac{\partial [\overline{T}]}{\partial \varphi} \frac{dp}{g}$, (upper diagram) and by standing eddies, $c_p \int r \left[\overline{v^*T^*}\right] \frac{1}{a} \frac{\partial [\overline{T}]}{\partial \varphi} \frac{dp}{g}$, (lower diagram). Units: 10^{-5} ergs cm^{-3} sec^{-1}.

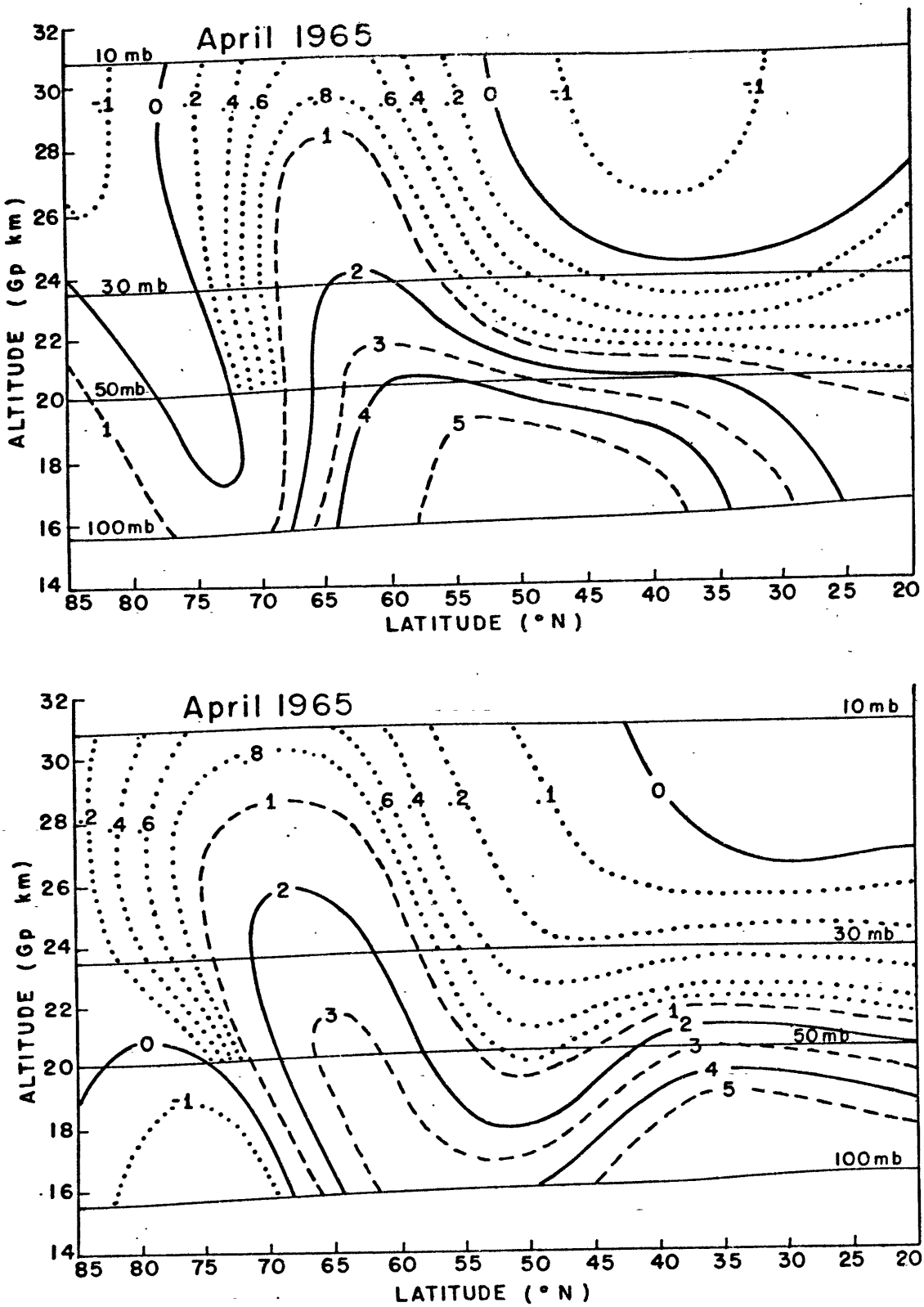

Figure 7c: Meridional distribution of the conversion from eddy available potential energy to zonal available potential energy by transient eddies, $C_p \int \gamma \left[\overline{v'T'}\right] \frac{1}{a} \frac{\partial [\overline{T}]}{\partial \phi} \frac{dp}{g}$, (upper diagram) and by standing eddies, $C_p \int \gamma \left[\overline{v^*T^*}\right] \frac{1}{a} \frac{\partial [\overline{T}]}{\partial \phi} \frac{dp}{g}$, (lower diagram). Units: 10^{-5} ergs cm^{-3} sec^{-1}.

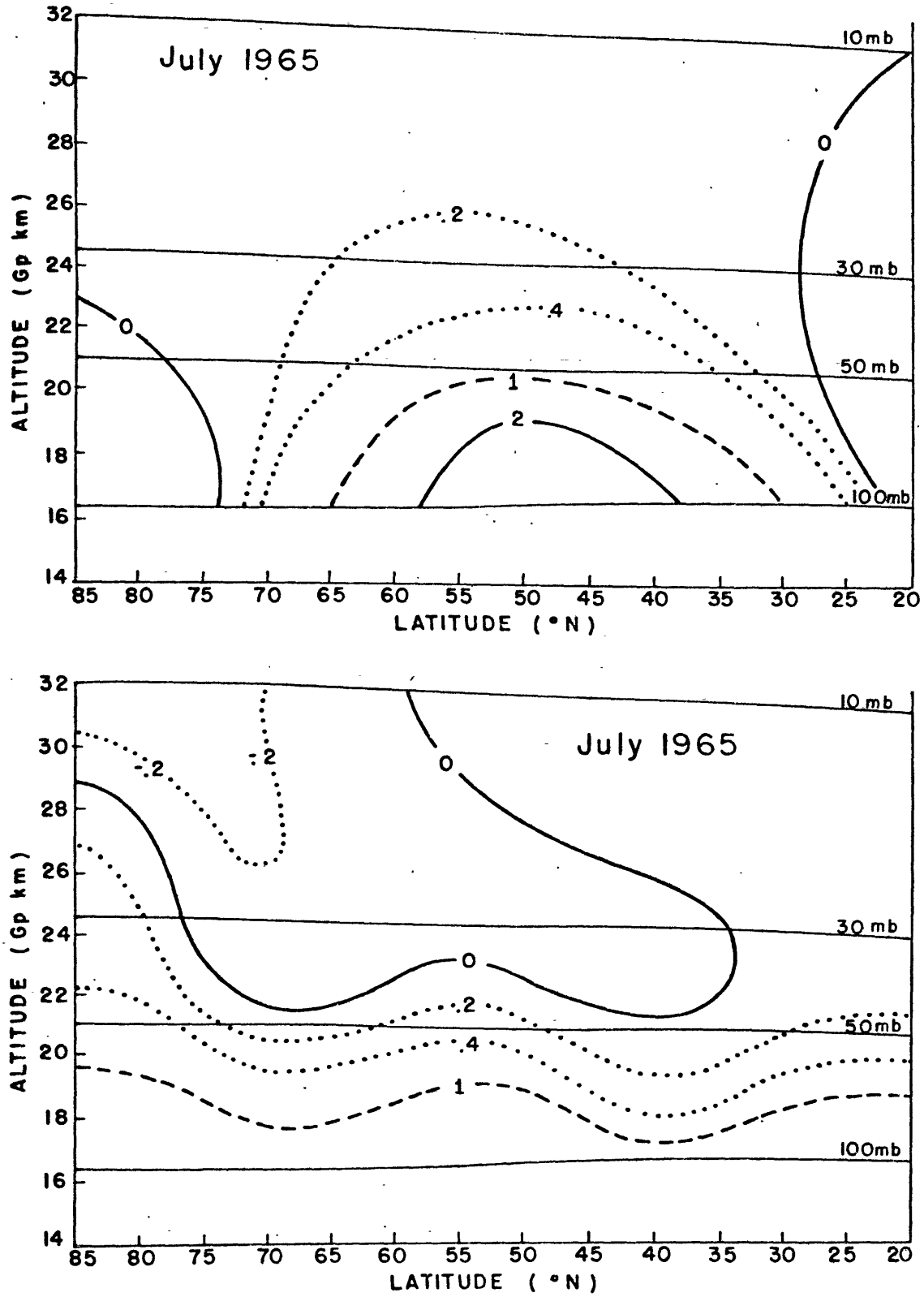

Figure 7d: Meridional distribution of the conversion from eddy available potential energy to zonal available potential energy by transient eddies, $C_p \int \gamma \left[\overline{v'T'}\right] \frac{1}{a} \frac{\partial [\bar{T}]}{\partial \varphi} \frac{dp}{g}$, (upper diagram) and by standing eddies, $C_p \int \gamma \left[\bar{v}^* \bar{T}^*\right] \frac{1}{a} \frac{\partial [\bar{T}]}{\partial \varphi} \frac{dp}{g}$, (lower diagram). Units: 10^{-5} ergs cm^{-3} sec^{-1}.

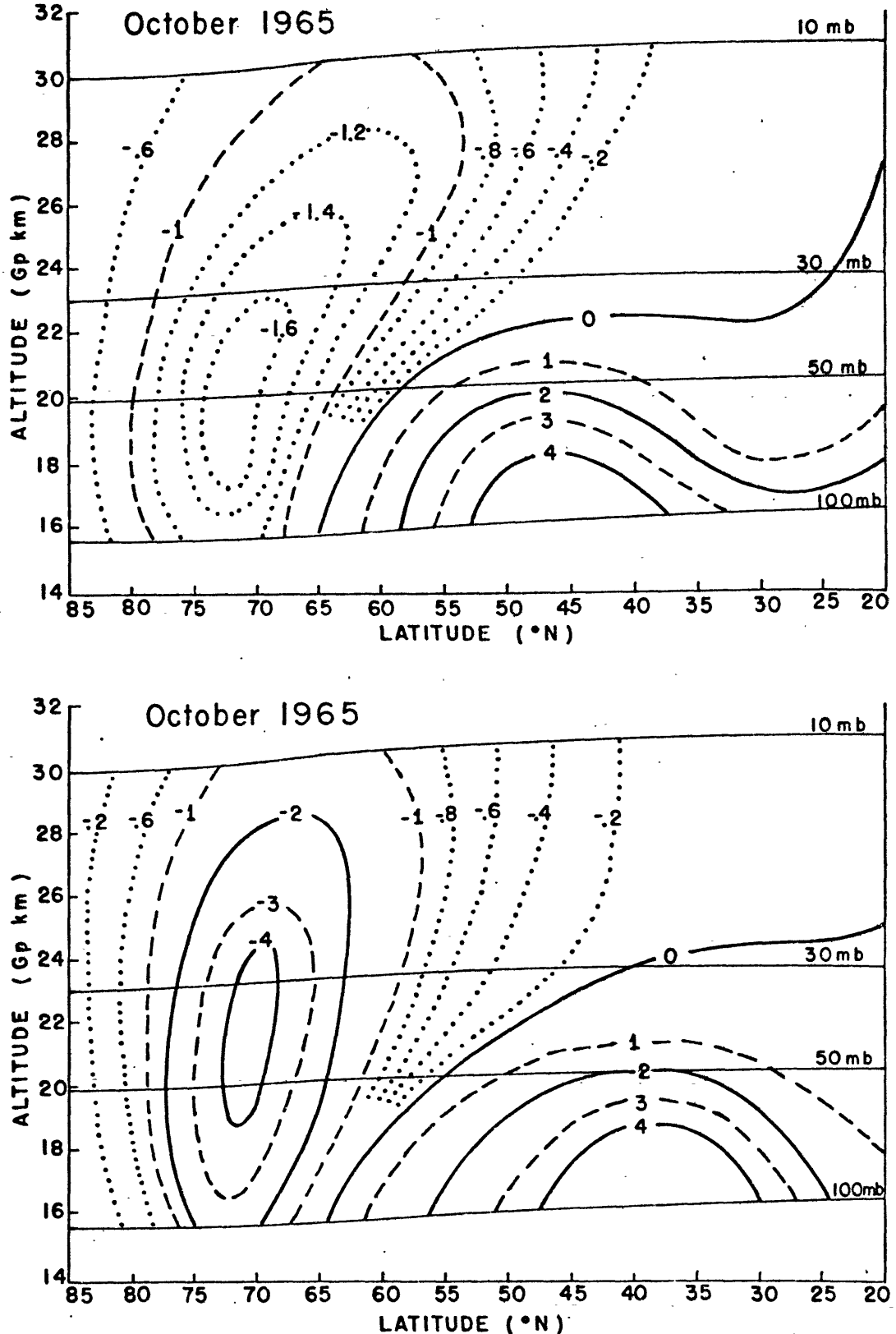

Figure 7e: Meridional distribution of the conversion from eddy available potential energy to zonal available potential energy by transient eddies, $c_p \int \gamma \left[\overline{v'T'}\right] \frac{1}{a} \frac{\partial [\bar{T}]}{\partial \varphi} \frac{dp}{g}$, (upper diagram) and by standing eddies, $c_p \int \gamma \left[\bar{v}^* \bar{T}^*\right] \frac{1}{a} \frac{\partial [\bar{T}]}{\partial \varphi} \frac{dp}{g}$, (lower diagram). Units: 10^{-5} ergs cm^{-3} sec^{-1}.

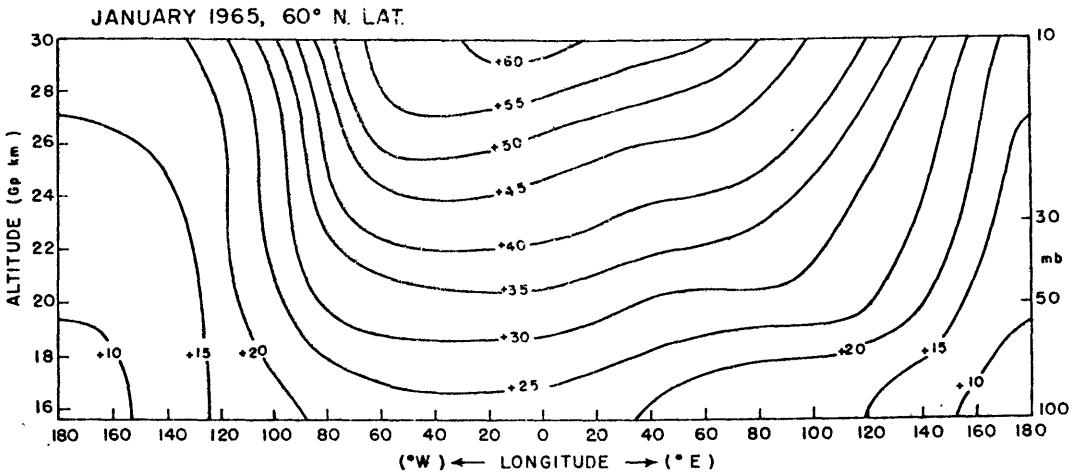

Figure 8: Zonal distribution of the monthly time averaged zonal wind, $\bar{u}$. Units: m sec^{-1}.

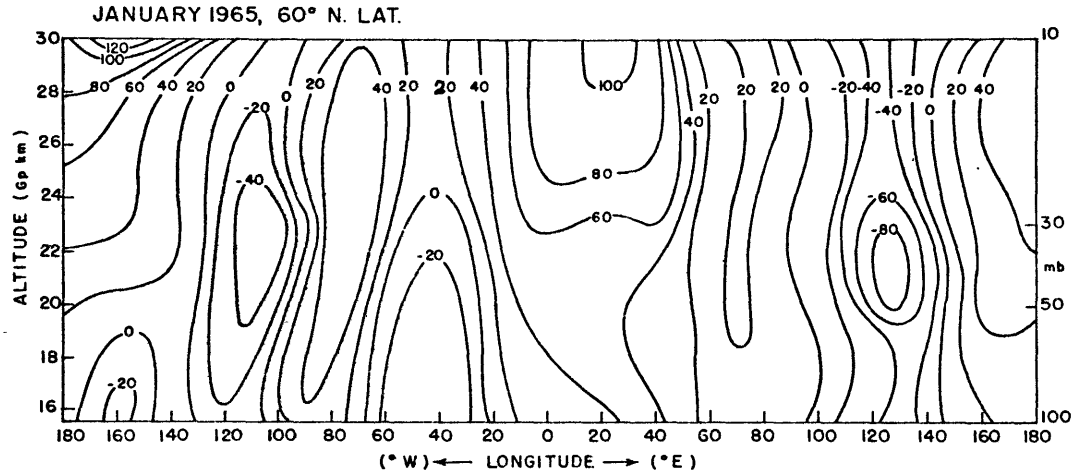

Figure 9: Zonal distribution of the monthly time averaged temporal covariance of u and v, $\overline{u'v'}$. Units: m^2sec^{-2}.

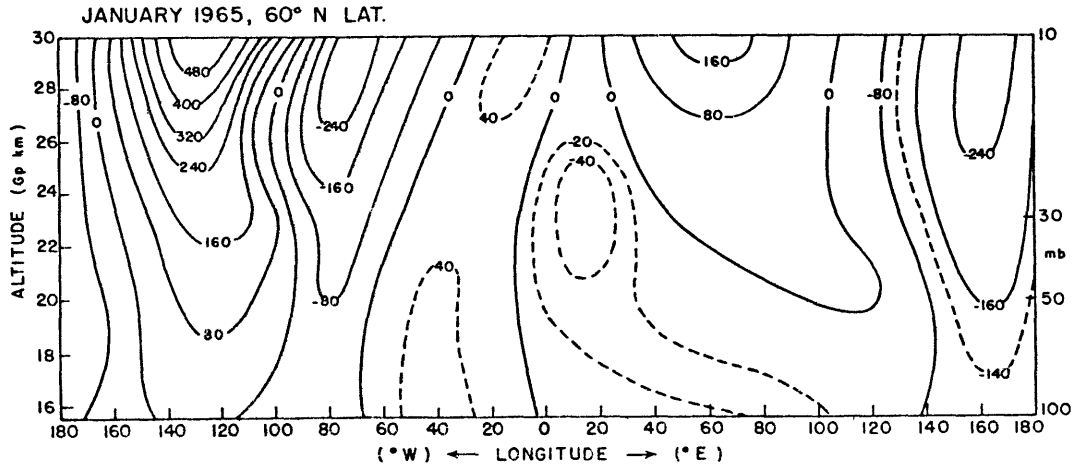

Figure: 10: Zonal distribution of the spatial covariance of $\bar{u}$ and $\bar{v}$, $\bar{u}^*\bar{v}^*$. Units: $m^2 sec^{-2}$.

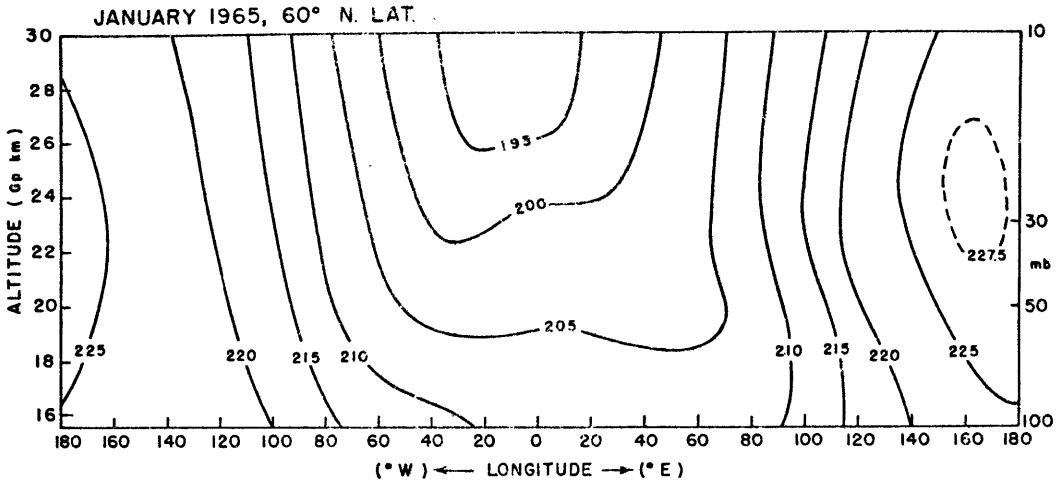

Figure 11: Zonal distribution of the monthly time averaged temperature, $\overline{T}$. Units: ^{o}K.

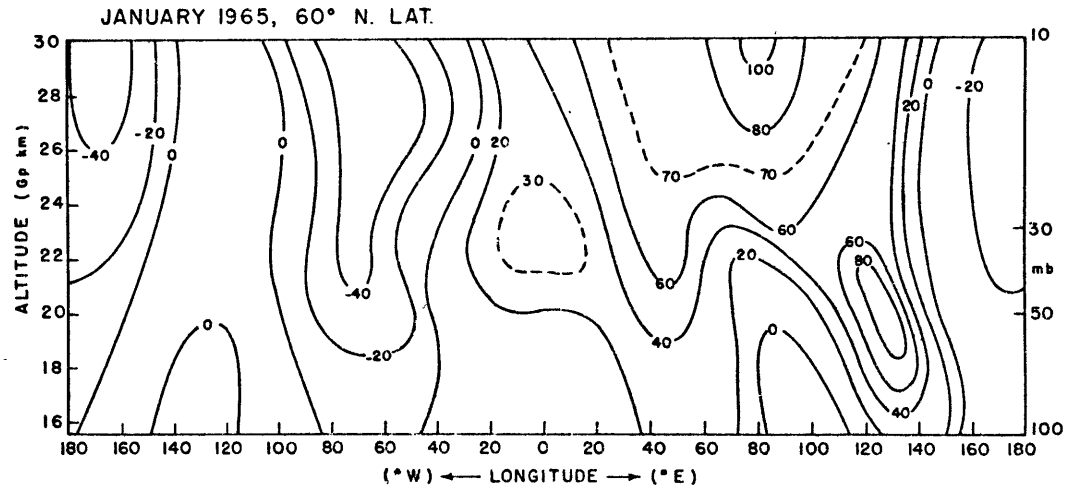

Figure 12: Zonal distribution of the monthly time averaged temporal covariance of v and T, $\overline{v't'}$. Units: $m\,^{o}C\ sec^{-1}$.

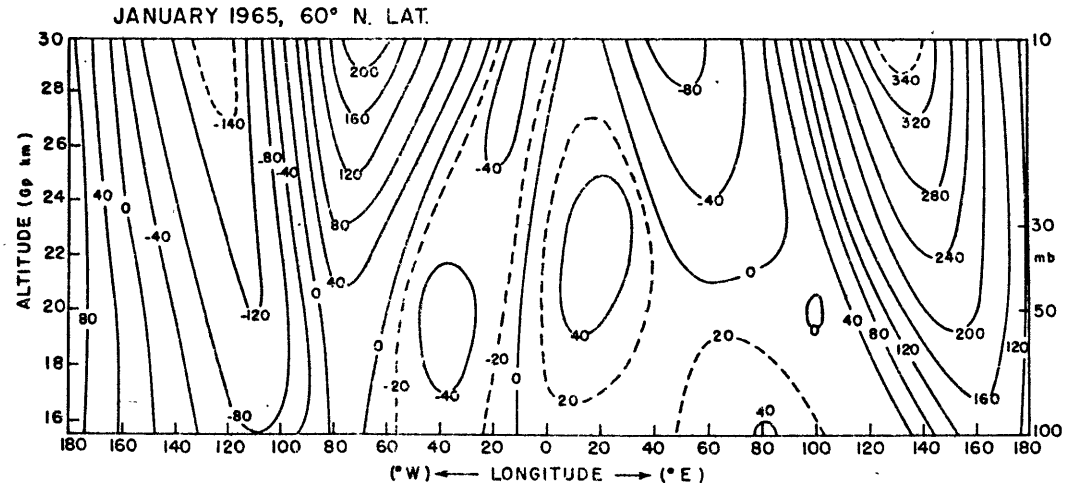

Figure 13: Zonal distribution of the spatial covariance of $\overline{v}$ and $\overline{T}$, $\overline{v}^{*}\overline{T}^{*}$. Units: $m\,^{o}C\ sec^{-1}$.

BIBLIOGRAPHY

Barnes, A.A. Jr., 1962: Kinetic and potential energy between 100 mb 10 mb during the first six months of the IGY. Final Rept., Planetary Circulations Project, Dept. of Meteor., Mass. Inst. of Tech., p. 8.

Boville, B.W., 1960: The Aleutian stratospheric anticyclone. J. of Meteor., 17, p. 329.

Boville, B.W., 1961: A dynamical study of the 1958-59 stratospheric polar vortex. Report No. 9, Arctic Meteor. Research Group, Mc Gill University, 134 pp.

Cole, A.E., A. Courtand A.J. Kantor, 1965: Model atmospheres. Handbook of Geophysics and Space Environments, S.L. Valley, Editor, AFCRL, Cambridge, Mass.

Dickinson, R.E., 1962: The momentum balance of the stratosphere during the IGY. Final Report, Planetary Circulations Project, Dept. of Meteor., Mass. Inst. of Tech., p. 132.

Finger, F.G., H.M. Woolf and C.E. Anderson, 1965: A method for objection analysis of stratospheric constant-pressure charts. Monthly Weather Review, 93, p. 619.

Gilman, P.A., 1963: On the mean meridional circulation in the presence of a steady state, symmetric, circumpolar vortex. Tellus, 16, p. 160.

Gilman, P.A., 1965: The mean meridional circulation of the sourthern hemisphere inferred from momentum and mass balance. Tellus, 17, p. 277.

Hare, F.K., 1960: The disturbed circulation of the arctic stratosphere. J. of Meteor., 17, p. 36.

Jensen, C.E., 1961: Energy transformation and vertical flux processes over the northern hemisphere. J. Geophysical Research, 66, p. 1145.

Kennedy, J.S., 1964: Energy generation through radiative processes in the lower stratosphere. Report No. 11, Planetary Circulations Project, Dept. of Meteor., Mass. Inst. of Tech., 116 pp.

Kuo, H.L., 1951: A note on the kinetic energy balance of the zonal wind systems. Tellus, 3, p. 205.

Lorenz, E.N., 1955: Available potential energy and the maintenance of the general circulation. Tellus, 7, p. 157.

Martin, D.W., 1956: Contribution to the study of atmospheric ozone. Report No. 6, Planetary Circulations Project, Mass. Inst. of Tech., 49 pp.

Miller, A.J., 1966: Vertical motion atlas for the lower stratosphere during the IGY. Report No. 16, Planetary Circulations Project, Mass. Inst. of Tech., 35 pp.

Molla, A.C. and C.J. Loisel, 1962: On the hemispheric correlations of vertical and meridional wind components. Geofisica pura e applicata, 51, p. 166.

Murakami, T., 1962: Stratospheric wind, temperatures and isobaric height conditions during the IGY period. Part I, Report No. 5, Planetary Circulations Project, Dept. of Meteor., Mass. Inst. of Tech., 213 pp.

Newell, R.E., 1961: The transport of trace substances in the atmosphere and their implications for the general circulation of the stratosphere. Geofisica pura e applicata, 49, p. 137.

Newell, R.E., 1963a: Preliminary study of quasi-horizontal eddy fluxes from meteorological rocket network data. J. Atmos. Sci., 20, p. 213.

Newell, R.E., 1963b: The general circulation of the atmosphere and its effects on the movement of trace substances. J. Geophys. Res., 68, p. 3949.

Newell, R.E., 1965: A review of studies of eddy fluxes in the stratosphere and mesosphere. Report No. 12, Planetary Circulations Project, Dept. of Meteor., Mass. Inst. of Tech., 53 pp.

Newell, R.E., 1966: Thermospheric energetics and a possible explanation of some observations of geomagnetic disturbances and radio aurorae. Nature, Vol. 211, No. 5050, p. 700.

Newell, R.E. and A.J. Miller, 1964: Some aspects of the general circulation of the lower stratosphere. Proceedings of the Second AEC Conference on Radioactive Fallout from Nuclear Weapons Tests, Germantown, Md.

Oort, A.H., 1963: On the energy cycle in the lower stratosphere. Report No. 9, Planetary Circulations Project, Dept. of Meteor., Mass. Inst. of Tech., 122 pp.

Oort, A.H., 1964a: On the energetics of the mean and eddy circulations in the lower stratosphere. Tellus, 16, p. 309.

Oort, A.H., 1964b: On estimates of the atmospheric energy cycle. Monthly Weather Review, 92, p. 483.

Peixoto, J.P., 1960: Hemispheric temperature conditions during the year 1950. Sci. Report No. 4, Planetary Circulations Project, Dept. of Meteor., Mass. Inst. of Tech., 211 pp.

Peixoto, J.P., 1965: On the role of water vapor in the energetics of the general circulation of the atmosphere. Portugaliae Physica, 4, p. 135.

Peng, L., 1963: Stratospheric wind, temperature and isobaric height conditions during the IGY period. Part II, Report No. 10, Planetary Circulations Project, Dept. of Meteor., Mass. Inst. of Tech., 208 pp.

Peng, L., 1965a: A simple numerical experiment concerning the general circulation of the lower stratosphere. Pure and Applied Geophysics, 61, p. 191.

Peng, L., 1965b: Numerical experiments on planetary meridional temperature gradients contrary to radiational forcing. Pure and Applied Geophysics, 62, p. 173.

Peng, L., 1965c: Stratospheric wind, temperature and isobaric height conditions during the IGY period. Part III, Report No. 15, Planetary Circulations Project, Mass. Inst. of Tech., 201 pp.

Priestly, C.H.B., 1949: Heat transport and zonal stress between latitudes. Quart. J. R. Met. Soc., 75, p. 28.

Reed, R.J., J.L. Wolfe and H. Nishimoto, 1963: A spectral analysis of the energetics of the stratospheric sudden warming of early 1957. J. Atmos. Sci., 20, p. 256.

Reynolds, O., 1894: On the dynamical theory of incompressible viscous fluids and the determination of the criterion. Phil. Trans. Roy. Soc., London (A), 136, p. 123.

Saltzman, B., 1957: Equations governing the energetics of the large scales of atmospheric turbulence in the domain of wave number. J. Meteor., 14, p. 513.

Saltzman, B., 1961: Perturbation equations for the time average state of the atmosphere including the effects of transient disturbances. Geofisica Pura e Applicata, 48, p. 143.

Sawyer, J.S., 1964: Dynamical aspects of the bi-polar stratospheric circulation. Quart. J. Roy. Meteor. Soc., 90, p. 395.

Sheppard, P.A., 1963: Atmospheric tracers and the general circulation of the atmosphere. Reports on Progress in Physics, 26, p. 213.

Staff, Upper Air Branch NMC, 1967: Monthly Mean 100, 50, 30 and 10 millibar charts, January 1964 through December 1965 of the IQSY period. ESSA Tech. Report WB1, U.S. Dept. of Commerce, Silver Spring, Md.

Starr, V.P., 1951a: A note on the eddy transport of angular momentum. Quart. J. R. Met. Soc., 77, p. 215.

Starr, V.P., 1951b: Application of energy principles to the general circulation. Compendium of Meteorology, AMS, p. 568.

Starr, V.P., 1953: Note concerning the nature of the large-scale eddies in the atmosphere. Tellus, 5, p. 494.

Starr, V.P., 1954: Commentaries concerning research on the general circulation. Tellus, 5, p. 494.

Starr, V.P. and R.M. White, 1952: Schemes for the study of hemispheric exchange processes. Quart. J. R. Met. Soc., 78, p. 407.

Starr, V.P. and R.M. White, 1954: Balance requirements of the general circulation. Geophysical Research Papers, No. 35, 57 pp.

Teweles, S., 1963: Spectral aspects of the stratospheric circulation during the IGY. Report No. 8, Planetary Circulations Project, Dept. of Meteor., Mass. Inst. of Tech., 191 pp.

Wilson, C.V. and W.L. Godson, 1963: The structure of the arctic winter stratosphere over a 10-yr period. Quart. J. Roy. Meteor. Soc., 89, p. 205.

White, R.M., 1954: The counter-gradient flux of sensible heat in the lower stratosphere. Tellus, 6, p. 177.

White, R.M. and G.F. Nolan, 1960: A preliminary study of the potential to kinetic energy conversion process in the stratosphere. Tellus, 12, p. 145.

ACKNOWLEDGEMENTS

The author wishes to thank Professor Reginald E. Newell for his suggestion of the topic and for his enthusiasm and counsel during the course of the investigation. Thanks are due to Dr. Robert E. Dickinson and Mr. John W. Kidson for helpful discussions and suggestions. The author owes a debt of gratitude to the Department of the Air Force who, through the Air Force Institute of Technology, provided the author with this educational opportunity. Thanks are also due to Miss Judy A. Roxborough, who wrote the computer programs, Mr. Steven A. Ricci, who drafted the figures, Mrs. Cynthia A. Webster, who typed the tables and Mrs. Marie L. Gabbe, who typed the manuscript.